Frother Blends in Flotation: Polyglycols and Alcohols

Ahmed Mohamed Elmahdy Ahmed Mohamed

Department of Mining and Materials Engineering

McGill University

Montréal, Quebec, Canada

A thesis submitted to McGill University in partial fulfillment of the requirements of the degree of Doctor of Philosophy

July 2011

Abstract

Frothers are non ionic surfactants, commonly alcohols and polyglycols, used to provide two functions in flotation, namely to reduce bubble size and stabilize froth. Both functions imply an impact on the properties of the air-water interface (bubble surface) but there is no consensus on the mechanism, particularly with regard to bubble size reduction. Blending frothers is becoming common in flotation practice arguably enhancing performance by permitting independent control of the two frother functions. However, there have been no studies to determine this blend possible action. The blends used here focused on a small addition of polyglycol (F150 and DF250) to alcohols (1-pentanol and MIBC). The effect of blends on gas dispersion properties (bubble size and gas holdup) and froth properties (froth height and water overflow rate) was measured in three units, bubble column, 800 L and 5.5 L mechanical cells. Froth height and water overflow rate showed a strong blend effect, both increasing significantly compared to individual frothers. However, while the bubble size was decreased at blend concentration below the critical coalescence concentration (CCC) of the alcohol frother, bubble size was significantly larger above the alcohol CCC. Gas holdup data supported these effects on bubble size. This bubble size effect compromised testing the hypothesis of independent function control using blends. The thesis focussed on explaining the bubble size observations by designing coalescence and beak-up experiments.

Coalescence time of bubbles generated from two horizontal capillaries did not show a blend effect. Break-up tests for one-bubble-at-a-time and from an air stream conducted for F150 – pentanol blends showed that the blend reduced bubble break-up compared to single frothers. The increase in bubble size above the base CCC therefore appears to due to decreased break-up. A mechanism based on the Marangoni effect is introduced to explain this phenomenon.

Résumé

Les moussants sont des surfactants non ioniques. Ceux-ci sont communément des alcools et des polyglycols, utilisés en flottation pour assumer deux fonctions : réduire la taille de la bulle et stabiliser la mousse. Ces deux fonctions exercent une influence sur les propriétés de l'interface air-eau (surface des bulles). Cependant il n'existe pas de consensus sur le mécanisme, particulièrement en ce qui a trait à la réduction de la taille des bulles. Mélanger des moussants devient une pratique généralement acceptée en flottation, laquelle sans doute renforce la performance en permettant le contrôle indépendant des deux fonctions de moussants. Toutefois, aucune étude n'a été réalisée pour déterminer l'action possible du mélange des moussants. Le mélange utilisé dans ce travail est un ajout d'une petite quantité de polyglycol (F150 et DF250) aux alcools (1-pentanol et MIBC). L'effet des mélanges sur les propriétés de dispersion de gaz (taille des bulles, rétention de gaz) que sur celles de la mousse (hauteur de la mousse, vitesse du flux du trop plein d'eau) a été mesurée en trois unités, colonne à bulles, 800 L et 5.5 L cellules mécaniques. La hauteur de la mousse et la vitesse du flux du trop plein d'eau ont révélé un fort effet de mélange puisque les deux paramètres accusent dans le cas du mélange une augmentation significative en comparaison aux moussants individuels. Alors que la taille des bulles avait diminué lorsque la concentration du mélange avait atteint une valeur inferieure à la concentration critique de coalescence (CCC) de la mousse d'alcool, la taille de la bulle était devenue largement supérieure à celle d'alcool CCC,

contre toute attente. Les données sur la rétention de gaz ont aussi corroboré ces effets affectant la taille des bulles. Cet effet de taille de la bulle compromise tester l'hypothèse de la contrôle indépendante de fonction utilisant des mélanges. Le pivot de cette thèse est l'explication des observations de la taille des bulles par le biais des tests de coalescence et de rupture.

Le temps de coalescence de bulles générées à partir de deux capillaires horizontaux n'a pas démontré un effet du mélange. Les tests de rupture réalisés avec une seule bulle à la fois et à partir d'un courant d'air pour le mélange F150 – pentanol, démontre que le mélange a réduit la possibilité de rupture par rapport à un seul moussant. L'augmentation de la taille de la bulle au-delà de la base CCC pourrait être due à la diminution de l'effet de rupture. Afin d'expliquer ce phénomène, un mécanisme basé sur l'effet de Marangoni est introduit.

Acknowledgements

I would like to express my gratitude to Professor James A. Finch for his guidance, fruitful discussions, and constant support during my studies at McGill University.

Thanks to Dr. Cesar Gomez and Dr. Ramachandra Rao for their useful advice and help in the work. Also, I want to thank my friends and colleagues at McGill University for their help, especially Dr. Mitra Mirnezami, Frank Rosenblum and Ray Langlois. Also, I would like to thank Dr. Barnabe for translating the abstract into French and Roger Ren for doing experimental Metso cell tests.

Finally, I want to express my deep gratitude to my beloved wife, Marwa, for her unconditional love and support, and to my parents for their constant support and encouragement in all that I have done in my life.

I would like to thank the Egyptian ministry of higher education for funding my PhD scholarship.

This work was conducted under the Chair in Mineral Processing funded through an NSERC (Natural Sciences and Engineering Research Council of Canada) CRD (Collaborative Research and Development) grant now sponsored by Vale Inco, Xstrata Process Support, Teck Cominco, Agnico-Eagle, COREM, SGS Lakefield Research, Shell Canada and Flottec.

Table of Contents

Nomenclature

A	cm^2	Cell cross-sectional area
c	mmol/L	Frother concentration
CCC	mmol/L	Critical coalescence concentration
CF		Correction factor
C_{wf}	cm^3/s	Rate of water carried into the froth
d_{32}	mm	Sauter mean diameter
d_b	mm	Equivalent diameter
DFI		Dynamic frothability index
E_g	%	Gas holdup
FI:		Frothability index
g	cm/s^2	The gravitational acceleration
H_f	cm	Froth height
h_f	cm	Target froth height
H_{max}	cm	Total foam height
J_d	cm/s	Liquid superficial drainage from a foam
J_g	cm/s	Superficial gas velocity
J_{wf}:	cm/s	Superficial water velocity carried into the froth
J_{wo}	cm/s	Water overflow superficial velocity from flowing foam
k_1		Constant reflecting a balance of gravity and viscous forces
L	cm	Distance
n		Number of bubbles per unit time

Q_g	cm^3/s	Gas flow rate
Q_{wo}	cm^3/s	Water overflow rate from flowing foam
Re		Reynolds number
rt	s	Bubble retention time
S	cm^2	Surface area per bubble
S_b	s^{-1}	Bubble surface area flux
Sk		Stokes-type number expressing superficial drainage from a foam
t	s	Time
U_{sb}	cm/s	Bubble rise velocity
V_b	cm^3	Volume of a single bubble
V_f	cm^3	Foam volume
V_g	cm^3	Gas volume
Vol_w	cm^3	Wake volume
ΔP	Pa	Pressure difference between the two tapping points
R	J/K.mol	Gas constant

Greek Letters

ρ_f	kg/m^3	Froth density
ρ_l	kg/m^3	Liquid density
α		Fraction of air overflowing as unburst bubbles
δ	mm	Equivalent water layer thickness
ε	%	Liquid fraction

λ	cm	Length of Plateau borders per volume of foam
ν	m^2/s	Kinematic viscosity
$\sum$	s^{-1}	Unit of Foaminess
Γ	mol/cm^2	Surface excess per unit area
γ	mN/m	Surface tension

List of Figures

List of Tables

CHAPTER - 1: INTRODUCTION

1.1 General background

Froth flotation is a widely used process for particle separation introduced on large scale in the minerals industry over a century ago. Although well established the underlying mechanisms are still the subject of research. Striving to improve metallurgical performance (i.e., grade/recovery) drives the need to better understand the process. The mechanism(s) by which frothers play their role in the flotation process is the focus of this thesis.

Commercial frothers are mostly non-ionic surfactants, commonly alcohols and polyglycols, used in flotation to reduce bubble size and stabilize the froth. Both these functions imply an impact on the properties of the air-water interface (bubble surface) but, particularly with regard to bubble size reduction, there is no consensus on their action.

What is known is that the mean bubble size tends to decrease rapidly with increasing frother concentration until a certain concentration is reached, now referred to as the critical coalescence concentration (CCC), above which the bubble size is minimum and roughly constant (Cho and Laskowski, 2002). The decrease in bubble size is commonly attributed to increasing inhibition of coalescence (Harris, 1976), which is completely prevented at the CCC (Cho and Laskowski, 2002). A measure related to bubble size, gas holdup, will tend to increase as frother concentration increases reflecting the decrease in rise velocity as bubble size is reduced (Harris, 1976; Azgomi et al., 2007). Exactly how

coalescence prevention is achieved at the moment of formation (a process occurring over milliseconds) is not clear, although speculations have been offered (Finch et al., 2006; 2008).

Studying bubble swarms, as in determining CCC, does not permit coalescence prevention to be separated from the other possibility, namely that frothers may act on break-up of the air mass. The latter mechanism, while occasionally mentioned (Gupta et al., 2007; Grau and Laskowski, 2006), is only recently attracting study (Finch et al., 2006; 2008; Acuna et al., 2007; Kracht and Finch, 2010).

The second main frother function, froth stabilization, has received considerably more attention, possibly because the froth is highly visible in the flotation process compared to what goes on below the froth, for which measurement tools are only now becoming widely used. Parameters related to the froth stability include: bubble size and shape (Sadr-Kazemi and Cilliers, 1997; Xie et al., 2004), froth depth, film thickness (between bubbles) and water content (Xie et al., 2004) and water overflow rate (Zhang et al., 2010). Particles play an important role in froth stabilization even in the absence of surfactant. Particles present on the bubble surface provide both a physical barrier to bubbles coming together and retard water drainage leading to more stable froth compared to that in the absence of particles (Hunter et al., 2008). The flotation literature recognizes the importance of particles by reserving the term "froth" to distinguish from "foam" where particles are absent. The distinction will be kept here.

Various mechanisms have been proposed for the role of frothers in froth stabilization among them an increase of surface viscosity and surface tension gradient driven phenomena (surface elasticity, Marangoni effect) (Marangoni, 1871; Plateau, 1873; Pugh, 1996).

One way to enhance metallurgical performance in flotation is to minimize entrainment of undesired hydrophilic mineral particles. Entrainment recovery is the non-selective transfer of particles into the froth that are carried in the wake and in the film of slurry around the bubble as it rises through the pulp (Ross, 2001). Particle recovery by entrainment is directly related to water recovery (i.e., the fraction of the water entering the flotation cell that is recovered in the overflow (usually the concentrate)) (Trahar, 1981; Zheng et al., 2006). By changing frother type and concentration water recovery, and therefore entrainment recovery, is modified. The relationship between frother properties and water recovery is not fully understood.

Frothers not only affect bubble size and froth stability, but also bubble shape and movement in a liquid (Frumkin and Levich, 1947; Dukhin et al., 1998; Malysa et al., 2005; Finch et al., 2008). For example, bubbles larger than ca. 1 mm adopt an oblate shape in water but become more spherical in the presence of frothers. Bubble shape and motion (e.g., rise velocity) are related (Wu and Gharib, 2002; Kracht and Finch, 2010).

Blending frothers is becoming common in flotation practice apparently enhancing performance (Tan et al., 2005). Little research work has been conducted on frother blends and none suggest a mechanism for their joint action

(Laskowski et al., 2003; Tan et al., 2005). As a working hypothesis in this thesis it is suggested that using two frothers will give some control over the two functions, bubble size reduction and froth stability. Properties related to bubble size (e.g. Sauter mean size and gas holdup) are often referred to as “gas dispersion” properties to distinguish from froth-related properties (e.g. froth height, water overflow rate). For convenience the two (i.e., gas dispersion and froth-related properties) are here collectively referred to as "hydrodynamic” properties. In this thesis, the effect of frother blends in regard to hydrodynamic properties is investigated.

In determining frother properties, several characterization tools have been explored including: water carrying rate (Moyo et al., 2007), gas holdup (Azgomi et al., 2007), critical coalescence concentration (CCC), dynamic foamability index (DFI) and the relationship between CCC and DFI (Laskowski, 2003), and the relationship between froth height and gas holdup (Cappuccitti and Nesset, 2010).

Laskowski et al. (2003) measured bubble size and dynamic foamability index for blends of MIBC with a series of polyglycols (polyypropylene alkyl ethers). They suggested that the more powerful polyglycol frothers dominated the properties.

Tan et al. (2005) measured foam height, static and dynamic surface tension, and estimated surface elasticity of polyglycols (polypropylene glycol (PPG)) blended with MIBC. They found a synergistic action, froth height with the blend being larger than the sum of froth height formed by both frothers alone. They suggested a configuration of the mixed molecules at the air/water interface. From

the measurements of static and dynamic surface tension the high molecular weight component appeared to dominate the mixture but, nevertheless they concluded that the blend provided greater surface elasticity. No effect on bubble size was considered.

The limited research to date means the effect of frother blends on hydrodynamic properties cannot be predicted from our current understanding of the mechanism(s) involved.

The purpose of this thesis is to determine the hydrodynamic properties of frother blends consisting of alcohols, specifically 1-pentanol or MIBC, and polyglycols, namely the commercial products F150 and DF250. Basic studies on bubble coalescence and break-up are conducted to probe the mechanisms.

1.2. Thesis objectives

The general objective is to determine and interpret the effect of blended frothers on control of hydrodynamic properties compared to single frothers. To accomplish, the following is experimental effort is performed:

1. Measurements of bubble size, gas holdup, froth height and water overflow rate using a combination of bubble column and mechanical flotation machines;
2. Development of an experimental setup to measure bubble coalescence time;

3. Development of a setup to determine single bubble break-up by measurement of the resulting daughter bubble size distribution.

1.3. Thesis structure

The thesis is organized in six chapters: a general introduction (chapter 1), a literature review (chapter 2), materials and procedures used (chapter 3), results (chapter 4), discussion (chapter 5), and conclusions and original contributions to knowledge (chapter 6). The structure of the thesis may be summarized as follows:

Chapter 1 – Introduction: The importance of frothers and their role in flotation are introduced. The thesis objectives and thesis structure are presented.

Chapter 2 – Literature review: This covers frother classification, frother effects on hydrodynamic properties, bubble coalescence, and break-up.

Chapter 3 – Experimental: Description of apparatus, chemicals used and procedures.

Chapter 4 – Results: The measured hydrodynamic properties, coalescence time, and break-up.

Chapter 5 – Discussion: The results are integerated, and mechanisms offered. In particular, the effect of the blended frothers on bubble size is analyzed.

Chapter 6 – Conclusions, contributions, and future work: Overall conclusions and claims of original research are presented, along with suggestions for future work.

Following chapter 6, a complete listing of references and six appendices providing supporting material are included.

REFERENCES

Acuna, C., Nesset, J. E., and Finch, J. A., 2007, "impact of frother on bubble production and behaviour in the pulp zone", The 6th International Copper Conference, Aug 25-30, p. 197-210.

Azgomi, F, Gomez, C.O., Finch, J.A., 2007, "Characterizing frothers using gas hold-up", Canadian Metallurgical Quarterly, Vol. 46 (3), p. 237-242.

Cappuccitti, F., and Nesset, J., 2009, "Frother and collector effects of flotation cell hydrodynamics and their implication on circuit performance", In: Proceedings of the 7th UBC-McGill-UA International Symposium on Fundamentals of Mineral processing, Editors: Gomez, C. O., Nesset, J. E., and Rao, S. R., Sudbury, Ontario, p. 169-182.

Cho, Y. S, and Laskowski, J. S., 2002, "Effect of flotation frothers on bubble size and foam stability", International Journal of Mineral Processing, Vol. 64, p. 69-80.

Dukhin, S.S., Miller, R., Loglio, G., 1998, "Physico-chemical hydrodynamics of rising bubbles. In: Mubius, D., Miller, R. (Eds.), Studies in Interfacial Science, Drops and Bubbles in Interfacial Research, vol. 6. Elsevier Science, pp. 367–432.

Finch, J. A., Gelinas, S., and Moyo, P., 2006, "Frother related research at McGill university", Minerals Engineering, Vol. 19, p. 726 – 733.

Finch, J. A., J. E. Nesset, and Claudio Acuña, 2008, "Role of frother on bubble production and behaviour in flotation", Minerals Engineering Vol. 21**,** p. 949-957.

Frumkin, A.N., and Levich, V. G., 1947, " On the surfactants and interfacial motion", Zh. Fizicheskoi Khimii, Vol. 21, p. 1183–1204.

Grau, R. A., and Laskowski, J. S., 2006, "Role of frothers in bubble generation and coalescence in a mechanical flotation cell", The Canadian Journal of Chemical Engineering, Vol. 84, p. 170-182.

Gupta, A. K., Banerjee, P. K., Mishra, A., Satish, P., and Pradip, 2007, " Effect of alcohol and polyglycol ether frothers on foam stability, bubble size and coal flotation", nternational Journal of Mineral Processing, Vol. 82, p. 126-137.

Harris, C. C., 1976, "Flotation machines", in Flotation, A. M. Gaudin Memorial volume, Vol. 2, M.C. Fuerstenau, Ed., AIME, New York, p. 753 – 815.

Hunter, T. N., Pugh, R. J., Franks, G. V., Jameson, G. J., 2008, "The role of particles in stabilising foams and emulsions", Advances in Colloid and Interface Science, Vol. 137, No.2, p. 57-81.

Kracht, W., Finch, J. A., 2010, "Effect of frother on initial bubble shape and velocity", International Journal of Mineral Processing, Vol. 94, No. 3-4, p. 115-120.

Laskowski, J. S, 2003, "Fundamental properties of flotation frothers", in Proceedings of 22nd International Mineral Processing Congress, Vol. 2,

Lorenzen, L., Bradshaw, D. J., editors, South African Institute of Mining and Metallurgy, Cape Town, p. 788-797.

Laskowski, J. S, Tlhone, T., Williams, P., and Ding, K., 2003, “Fundamental properties of polyoxypropylene Alkyl ether flotation frothers”, International Journal of Mineral Processing, Vol. 72, p. 289-299.

Malysa, K, Krasowska, M and Krzan, M., 2005, "Influence of surface active substances on bubble motion and collision with various interfaces", Advances in Colloid and Interface Science., Vol. 114-115, p. 205-225.

Marangoni, C. G., 1871, Ann. Phys. Chem., Vol. 143, p. 337-354.

Moyo, P., Gomez, C.O. and Finch, J.A., 2007, “Characterizing frothers using water carrying rate”, Canadian Metallurgical Quarterly, Vol. 46, N. 3, p. 215-220.

Plateau, J.A.F., 1873, "Statique Experimentale et Teorique des Liquides Soumis aux Seules Forces Moleculaires", Gauthier-Villiard, Paris.

Pugh, R. J., 1996, “Foaming foam films, antifoaming and defoaming”, Advances in Colloid and Interface Science, Vol. 64, p. 67-142.

Ross, V. E., 2001, “Mechanisms operating in flotation froth”, Frothing in flotation II, Edited by Laskowski, J.S and Woodburn, E. T., 109-144.

Sadr-Kazemi, N., and Cilliers, J.J., 1997, " an image processing algorithm for measurement of flotation froth bubble size and shape distributions", Minerals Engineering, Vol. 10, No. 10, p. 1075-7083.

Tan, Su Nee, Pugh, R.J., Fornasiero, D., Sedev, R., and Ralston, J., 2005, "Foaming of polypropylene glycols and glycol/MIBC mixtures", Minerals Engineering, Vol. 18, p. 179–188.

Trahar, W.J., 1981, "A rational interpretation of the role of particle size in flotation", International Journal of Mineral Processing, Vol. 8, p. 289-327.

Wu, M., and Gharib, M., 2002, "Experimental studies on the shape and path of small air bubbles rising in clean water", Physics of Fluids, Vol. 14, No. 7, p. L45-L56.

Xie, W., Neethling, S.J., and Cilliers, J.J., 2004, " Anovel approach for estimating the average bubble size for foams flowing in vertical columns", Chemical Engineering Science, Vol. 59, p. 81-86.

Zhang, W., Nesset, J. E., and Finch, J. A., 2010, "Water Recovery and Bubble Surface Area Flux in Flotation", Canadian Metallurgical Quarterly, Vol 49, No 4, p. 353-362.

Zheng, X., Franzidis, J. P., and Johnson, N. W., 2006, "An evaluation of different models of water recovery in flotation", Minerals Engineering, Vol. 19, p. 871 – 882.

CHAPTER - 2: LITERATURE REVIEW

2.1. Frothers in flotation

Flotation is a physico-chemical method widely used in mineral processing to separate finely divided solids in a suspension. The process involves contacting hydrophobic solid particles and air bubbles. Although the majority of minerals are naturally hydrophilic, they can be selectively rendered hydrophobic by the use of surfactants called collectors.

Collectors are commonly heteropolar compounds that adsorb at the solid/water interface via their reactive polar head group such that their hydrocarbon chain is oriented towards the aqueous phase thus rendering the mineral surface hydrophobic. Upon introducing bubbles the hydrophobized particles are collected and buoyed to the top of the flotation machine (cell) to form a froth that overflows to yield the floated particle product (usually the valuable mineral product or concentrate). A high population of small bubbles, by providing a high surface area, favours rapid particle collection.

The addition of a second surfactant, a frother, aids in this process of producing small bubbles. In flotation systems small refers to bubbles typically in the range 0.5 to 2.5 mm (Gorain et al., 1995). A high population of small bubbles in the presence of frother also helps stabilize the froth that forms as the bubbles accumulate on the pulp surface. Most frothers comprise a molecule with a neutral hydrophilic polar head group (often OH) and a hydrophobic hydrocarbon chain. This heteropolar (amphipathic) nature promotes adsorption at the air/water

interface with the polar group oriented towards the aqueous phase and the hydrocarbon chain towards the gaseous phase. One manifestation of this adsorption is reduction in surface tension (Harris, 1982).

The two frother functions, to reduce bubble size and stabilize the froth, play a central role in flotation. By increasing frother concentration, the bubble size is reduced until a particular concentration is reached after which no further reduction in mean bubble size takes place (Klassen and Mokrousov, 1963; Finch and Dobby, 1990). One argument is that at this concentration bubble coalescence is completely prevented and as a consequence this concentration was referred to as the critical coalescence concentration (CCC) by Laskowski and coworkers (Cho and Laskowski, 2002a, b; Laskowski et al., 2003; Laskowski, 2003). They considered CCC to be a characteristic property of a frother, i.e., independent of method of determination (Cho and Laskowski, 2002a). Laskowski and co-workers use a graphical method to estimate CCC; Nesset et al. (2007) introduced a refinement based on fitting to a 3-parameter model. There have been attempts to estimate CCC using gas holdup as a surrogate for bubble size as gas holdup is easier to measure (at least in two phase air-water systems) (Azgomi et al., 2007a).

Bubble size, gas holdup and CCC refer to properties of the solution below the froth (the pulp or slurry zone in flotation systems). The action of frother on the froth is tracked in a variety of ways such as measuring froth height, bubble size through the froth, gas holdup (water content) and water overflow rate.

2.2. Frother classification

2.2.1. Chemical classification

Based on chemical structure, frothers are classified into three main groups (Rao and Leja, 2004). The first group is the alcohols (aliphatic, cyclic and aromatic) which have one OH group. Aliphatic alcohol frothers produce relatively weak, dry froth (Cytec 2003). A common industrial example of this group is methyl isobutyl carbinol (MIBC), which is one of the most widely used frothers. Aromatic alcohol frothers, derived from pine oil, have been used, but find reduced application due to environmental concerns (Rao and Leja, 2004).

The second group, which similar to pine oil has limited applications, is alkoxy-substituted paraffins such as triethoxy butane (TEB). The third group is the polyglycol frothers which are synthetic reagents consisting of polyethylene oxide (PEO), polypropylene oxide (PPO) and polybutylene oxide (PBO) types (Tan et al., 2005). They give more voluminous, wetter froths compared to the alcohols (Cytec 2003). Some frothers and their chemical structure are shown in Table 2.1.

Table 2.1. Common Frother types

Frother	Structure	Formula	Solubility in H_2O
2-ethyl hexanol	Aliphatic alcohol	$CH_3CH_2CH_2CH_2CHCH_2OH$ | CH_2CH_3	Low
MIBC	Aliphatic alcohol	$CH_3CHCH_2CHCH_3$ | | CH_3 OH	Low
1,1,3 triethoxybutane	Alkoxy	OC_2H_5 OC_2H_5 \ / CH_3-CH——CH_2-CH \\ OC_2H_5	Low
DF-250	Polyglycol	$CH_3(PO)_4OH^*$	Total
F-150	Polyglycol	$H(PO)_7OH^*$	Total

* PO = C_3H_6O

2.2.2. Bubble size and critical coalescence concentration (CCC)

Bubble size distribution reflects how well air is dispersed in a liquid (slurry). The Sauter mean diameter (d_{32}) is commonly used to provide a single size metric calculated using equation 2.1:

$$d_{32} = \frac{\sum_{i=1}^{i=n} d_i^3}{\sum_{i=1}^{i=n} d_i^2} \qquad (2.1)$$

where d_i is diameter of bubble i and n the total number of bubbles

The typical Sauter mean bubble size in flotation is 0.5-2.5mm (Gorain et al., 1995). Critical coalescence concentration is the concentration giving approximately the minimum d_{32}.

There is considerable literature to support that the d_{32} remains constant above some concentration (Finch and Dobby, 1990; Cho and Laskowski, 2003; Nesset et al., 2007). Bubble size, however, is not always readily measured. Hence the attraction of gas holdup as a possible surrogate because it is easier to measure, at least in a two phase (air-water system). Gas holdup (or voidage) is the volume fraction of gas phase in a gas-water or gas-slurry mixture. Gas holdup tends to increase as bubble size reduces (e.g. as a result of adding frother) because buoyancy decreases and thus bubble rise velocity decreases resulting in bubble retention time (i.e., holdup) increasing. The CCC, in principle therefore, could be determined from gas holdup measurements. Azgomi et al. (2007b), however, found that gas holdup continued to increase, albeit slowly, with increasing concentration above the CCC. On examination they found that the population of fine bubbles did continue to increase. Since the d_{32} is not sensitive to small changes in the finer bubbles, the constancy of the bubble size above the CCC should be qualified as referring to the mean size, d_{32}.

Cho and Laskowski (2002a) and Grau et al. (2005) suggested that CCC is a material constant, independent of generation mechanism (e.g. flotation machine type and geometry). More recently, Cappuccitti and Nesset (2009) showed that CCC increases with increasing gas flow rate which means it is not strictly a material constant. The CCC nevertheless remains a useful concept. It is now widely understood that below the CCC bubble size is a strong function of frother dosage, thus providing an argument to run at frother concentrations higher than the CCC to reduce fluctuations in bubble size. Many plants, however, appear to operate below the CCC (Nesset et al., 2007) and this may be to avoid problems due to excess frothing.

Although useful, the CCC is difficult to establish on the asymptotic plot using the graphical procedure of Laskowski (2003). To provide a more systematic determination Nesset et al. (2007) used a three-parameter model to fit the data and estimate the CCC95, i.e., the concentration giving 95% bubble size (d_{32}) reduction relative to water only. Provided sufficient bubble size vs. concentration data are collected to fit the model this gives a more objective measure than the graphical procedure.

2.2.3. Frothability

While the notion of frothability (in three-phase) and foamability (in two-phase) is generally understood there is no universal definition and various measurements have been proposed. One of the first used in flotation-related

studies was the frothability index (FI) introduced by Sun (1952). It was defined as the ratio of foam volume measured for the tested frother solution to the volume of foam generated in a solution of n-hexanol. Although useful for comparing frothers, the FI, it was argued, is not connected with any physicochemical properties of the system investigated and hence could lead to erroneous conclusions (Czarnecki et al., 1982).

Bikerman (1973) proposed the ratio of steady-state foam volume to gas rate as a unit of foaminess for dynamic foams, i.e., foams formed while gas (usually air) is still flowing. This ratio ($\sum$) is a measure of the average time that gas remains entrained in foam. To measure, a certain gas flowrate is passed through a column containing a known volume of frother solution. After an initial period the height becomes constant as steady-state is established. The dynamic foam stability ($\sum$) is expressed as:

$$\sum = \frac{V_f}{Q_g} = \frac{H_{max} A}{Q_g} \qquad (2.2)$$

where V_f is the foam volume, Q_g is the gas flowrate, H_{max} is the total foam height and A is cross-sectional area of the column.

The dynamic frothability index (DFI), introduced by Malysa and co-workers (1981, 1982), is defined as the limiting slope of the retention time (rt) vs. concentration (c) curve as $c \rightarrow 0$. Here the retention time is defined as the slope of the linear part of the dependence of the total gas volume in the system (V_g) on gas flow rate (Q_g). Physically, the retention time is the average lifetime of a bubble in the whole system (i.e., solution + froth).

$$rt = \Delta V_g / \Delta Q_g \quad (2.3)$$

$$DFI = rt_{\infty} * k \quad (2.4)$$

where rt_{∞} is the limiting rt volume for $c \rightarrow \infty$ and k is a constant.

The DFI is treated as a material property (i.e., it is considered constant and concentration independant) to provide for comparison of frothers. Measurement involves more than one step. Cappuccitti and Finch (2008) recently proposed a one-step characterization technique using froth height vs. gas holdup. The relationship is generated by operating a column at a given air rate and changing frother concentration. The froth height - gas holdup trends readily distinguish alcohol frothers that give little froth height but give a wide range of gas holdup from polyglycols which give greater froth height over the same gas holdup range. The technique has the dual advantage over the DFI of simplicity and clearly discriminating the two frother functions, frothing (measured as froth height) and bubble size reduction (measured by gas holdup as a surrogate). The technique was used to identify a replacement frother by searching for one that provided the same froth height - gas holdup relationship.

2.2.4. Water carrying rate and entrainment

The flow of water is an important component in flotation plant design and operation. It determines to a large extent the residence time in the individual

process units. Importantly, the amount of water reporting to the flotation cell overflow (concentrate) controls hydrophilic particle (often the gangue) entrainment recovery and thus influences concentrate grade (Trahar and Warren, 1976; Lynch et al., 1981; Warren, 1985; Neethling and Cilliers, 2002). Particle recovery by entrainment is strongly associated with water recovery (Trahar, 1981; Zheng et al., 2006).

Entrainment is a non-selective recovery of particles in water recovered to the float product mainly involving fine particles, approximately less than 50μm. Water could be carried over mechanically due to turbulence but most emphasis is on water transport by bubbles and the "crowding" effect of bubble swarms, which is called hydraulic entrainment (George et al., 2004).

2.2.4.1. Water transport in the pulp

Water recovery in a flotation cell is the result of a two-step mass transfer process; water transfers first from the pulp zone to the froth zone and then through the froth phase to the overflow (Zheng et al., 2006).

Two general mechanisms have been suggested to explain the presence of hydrophilic fine particles in the froth product (Smith and Warren, 1989): Transport of particles in the inter-bubble water (entrainment), and recovery via aggregates attached to air bubbles (entrapment).

The work of Ata and Jameson (2005) supports the second mechanism. They found that hydrophilic silica particles became entrapped in bubble clusters formed

by hydrophobic particles bridging between bubbles. Most researchers, however, have shown that entrainment is the major mechanism (Engelbrecht and Woodburn, 1975; Trahar, 1981; Warren, 1985; Smith and Warren, 1989; George et al., 2004). There are three mechanisms invoked to explain the transport of water into the froth:

(i) Water is carried upward in the water film surrounding the bubble (Figure 2.1) (Gaudin, 1957),

(ii) Water is transported in the wake of the ascending air bubble (Yianatos et al., 1986; George et al., 2004), and

(iii) Water is mechanically pushed into the froth by ascending swarms of bubbles (the "crowding" effect) (Smith and Warren, 1989). All three mechanisms seem plausible and may occur simultaneously.

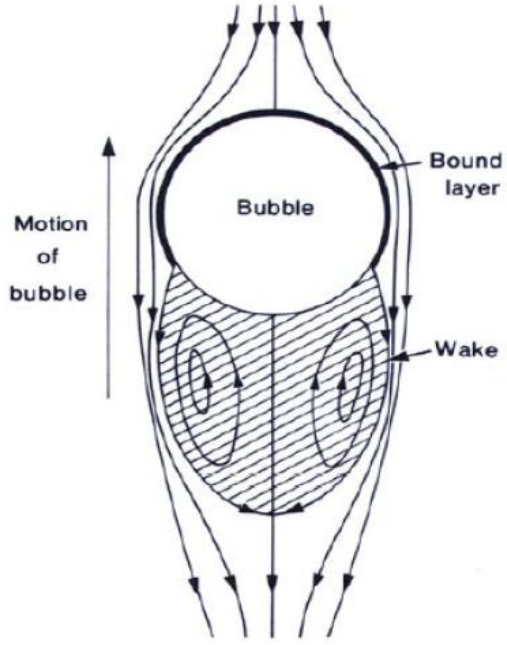

Figure 2.1: Ascending bubble with bound water layer and an attached wake (Smith and Warren, 1989. Reprinted with permission from Taylor & Francis)

One way to estimate the rate of water carried into the froth (i.e., arriving at the liquid/froth interface) (C_{wf}) is to assume it is a function of rate of bubble surface area passing through the cell multiplied by an equivalent water layer thickness (δ) (Bascur and Herbst, 1982),

$$C_{wf} = n*S*\delta \qquad (2.5)$$

where n is the number of bubbles per unit time ($=\frac{Q_g}{V_b}$, Q_g being the volumetric flowrate of air (e.g., m^3/s) and V_b the volume of a single bubble ($=\frac{\pi d_b^3}{6}$)), and S is the surface area per bubble ($=\pi d_b^2$). Equation 5 simplifies to (assuming spherical bubbles of mean size d_{32}):

$$C_{wf} = \frac{6Q_g * \delta}{d_{32}} \qquad (2.6)$$

Dividing equation 6 by the cross sectional area of the flotation cell (A, m^2) and introducing the superficial gas velocity J_g (= Q_g/A) gives

$$J_{wf} = 6\frac{J_g}{d_{32}} * \delta \qquad (2.7)$$

$$J_{wf} = S_b * \delta \qquad (2.8)$$

where S_b is the bubble surface area flux ($=\frac{6J_g}{d_{32}}$) . Xu et al. (1991) showed that the volume of water transported to the froth did vary with S_b. Bascur and Herbst (1982) used Levich's (1962) boundary layer thickness correlations to estimate δ, namely:

$$\delta = \left(\frac{\nu * \left[\frac{d_b}{2} \right]}{U_{sb}} \right)^{\frac{1}{2}} \qquad (2.9)$$

where ν is the kinematic viscosity and U_{sb} is the bubble rise velocity. For Re >> 1 (Re = Reynolds number), the thickness of the boundary layer is small compared to the bubble radius (Levich, 1962). Hydration effects at the bubble-water interface and agitation conditions in the slurry were considered to control the magnitude of the boundary layer (Bascur and Herbst, 1982). Equation (2.8) has been fitted to rate of water overflow from the froth (i.e., after passing through the froth) to obtain an empirical δ which shows a strong dependence on frother type (Zhang et al., 2010).

An alternative estimation route for C_{wf} is based on the wake volume. From numerical analysis, George et al. (2004) correlated the wake volume (Vol_w) with the bubble volume (V_b) and the Reynolds number (Re)

$Vol_w = V_b (0.045\ Re^{0.649} - 0.314)$ for $20 < Re < 400$ (2.10)

2.2.4.2. Water transport in the froth

In the froth, water is transported through Plateau borders and the bubble lamellae (Neethling et al., 2003). Stevenson (2006) proposed an expression for the liquid superficial drainage from a foam $J_{d,}$ expressed by a Stokes-type number, Sk, as a function of liquid fraction, ε:

$Sk = m\ \varepsilon^n$, (2.11)

where m and n are dimensionless adjustable constants dependent on surfactant type and concentration. Ireland and Jameson (2007) compared Stevenson's model and subsequently, a model derived from drift flux analysis and found good agreement for both with their experimental results. Dickinson et al. (2010) using drift flux analysis reached the same expression as Stevenson.

Cilliers and coworkers (Neethling et al., 2000; Neethling and Cilliers, 2002; Neethling et al., 2003) have proposed fundamental models to predict water overflow from flowing foam. Their analysis takes into account foam drainage and the fraction of air overflowing as unburst bubbles, i.e., air recovery (α) They found two solutions depending on α:

$$\alpha < \frac{1}{2} : J_{wo} = \frac{Q_{wo}}{A} = \frac{J_g^2 \lambda}{k_1}(1-\alpha)\alpha \qquad (2.12)$$

$$\alpha \geq \frac{1}{2} : J_{wo} = \frac{J_g^2 \lambda}{4k_1} \qquad (2.13)$$

where k_1 is a constant, reflecting a balance of gravity and viscous forces, λ is the length of Plateau borders per volume of foam, A is the column cross sectional area and J_g is the superficial gas velocity. Unlike Stevenson's model, there are no parameters related to surfactant (frother) type or concentration, these effects being incorporated through their impact on bubble size.

2.3. Frother blending

It is observed that frother blends can be more effective than single frothers in achieving the best technical (and economic) advantage (Tan et al., 2005).

Despite this, limited research has been undertaken to understand the action of frother blends. Alone in offering a mechanism, Tan et al. (2005) found that mixtures of low and high molecular weight polypropylene glycols showed better foaming properties compared to single frothers and suggested it might be due to the formation of close packed cohesive film at the interface (Figure 2.2).

Figure 2.3 shows some results of blending frothers in a continuously operating lab-scale mechanical cell (Shockley, 2007). It is evident that at low concentration the blends of F150 ($H(PO^{*})_7$ OH) with 1-pentanol caused a significant increase in water overflow rate, far greater than the sum of the two frothers when alone. At high concentration this effect appears to reverse: e.g. at F150 concentrations higher than 15 ppm in presence of 20 ppm pentanol the water recovery became slightly lower than the corresponding concentrations of F150 alone. Knuutila (2007) arrived at the same conclusion regarding the increase in overflow rate of blends of F150 and 1- pentanol using a 50-cm diameter bubble column (Figure 2.4). The mechanism behind this behaviour was part of the motivation for this work.

[*] PO is propylene oxide (propoxy) [-O-CH_2-CH_2-CH_2-]

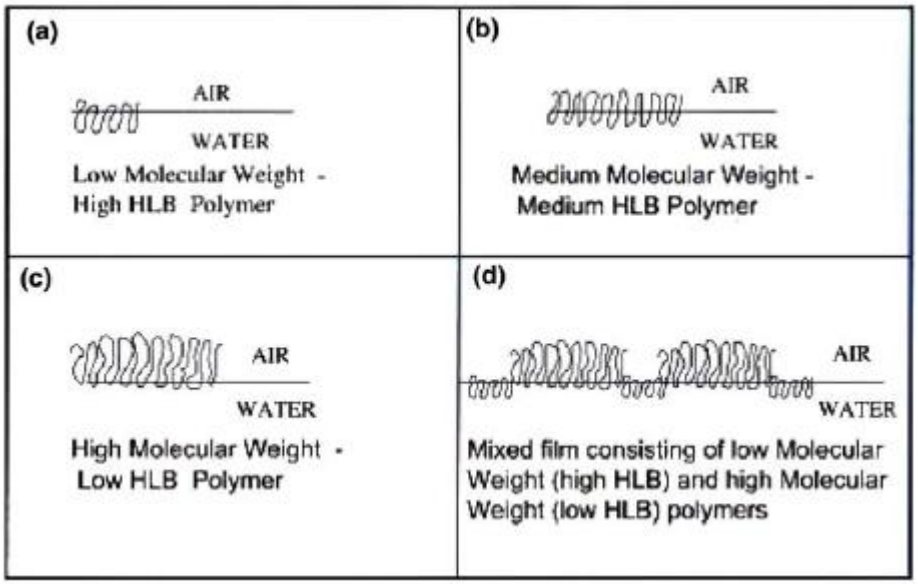

Figure 2.2: Suggested structures of PPG polymers and mixtures at the air/solution interface (Tan et al., 2005. Reprinted with permission from Elsevier).

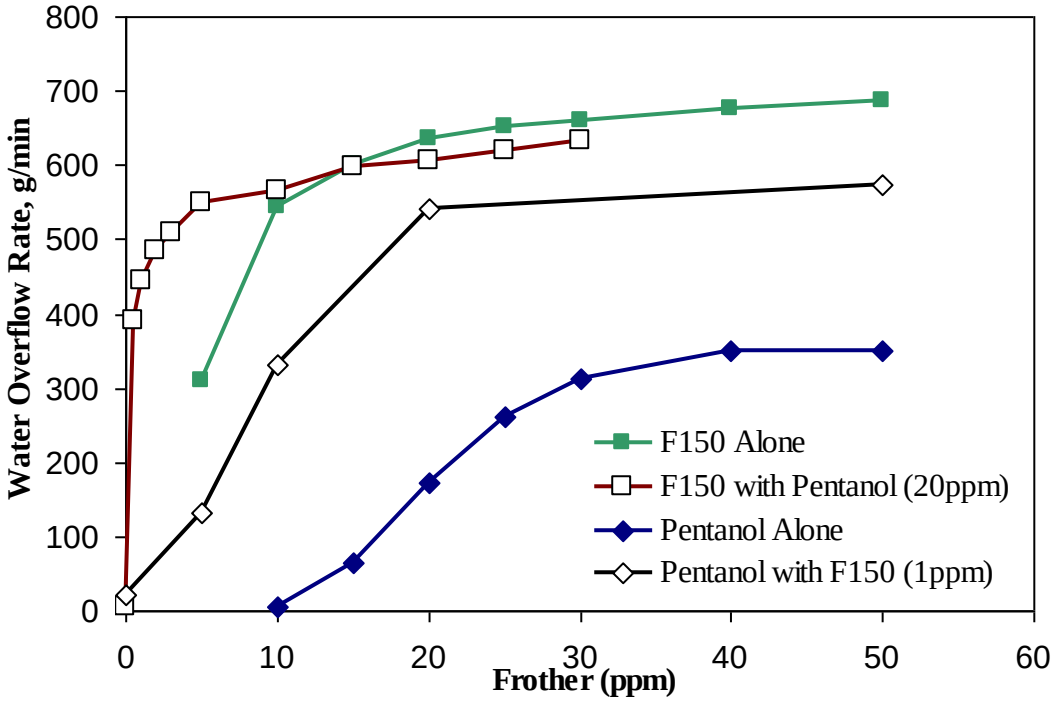

Fig. 2.3: Water overflow rate as a function of single and blended frother concentration (Adapted from Shockley, 2007)

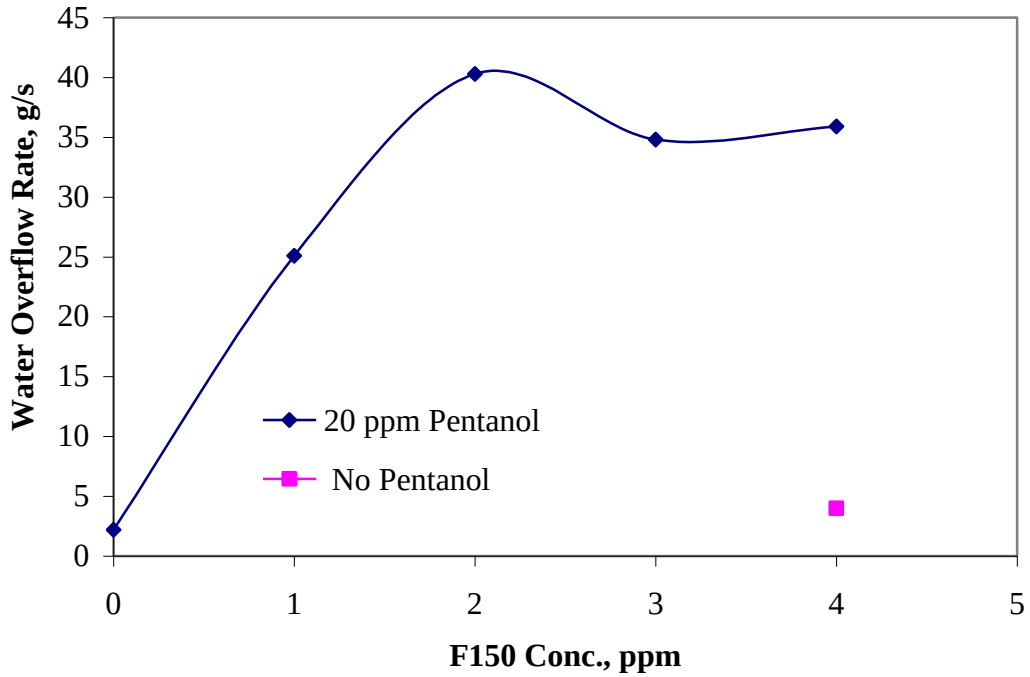

Figure 2.4: Water overflow rate of F150-pentanol blends (Adapted from Knuutila, 2007)

Laskowski et al. (2003) measured bubble size and dynamic foamability index of binary blends consisting of MIBC (methyl iso butyl carbinol) with each of three polyglycol frothers (Dowfrothers) DF-200 [$CH_3(PO^*)_3OH$], DF-250 [$CH_3(PO)_4OH$], and DF-1012 [$CH_3(PO)_{6.3}OH$]. They prepared the blends by mixing MIBC with each polyglycol in the same molar ratio as their CCC, which means that they tested a constant alcohol – polyglycol mass ratio, e.g. 9:1 in case of DF1012, for each blend at all concentrations. They found that the CCC value for each blend lay between the CCC values for the blend constituents. For a blend of interest in this thesis MIBC with DF1012 (since DF1012 molecular weight (ca.

* (PO) is abbreviation for ($-OC_3H_6-$)

400 g/mol) is close to that of F150), they concluded that for the 9:1 mass ratio blend the frothing properties were similar to DF-1012 alone.

2.4. Bubble coalescence

2.4.1. General concepts

Bubble coalescence is the event in which two or more bubbles merge (coalesce) to form a new, larger bubble. When two bubbles are in contact, a liquid film is formed between them. Coalescence occurs when the intervening film drains to a critical thickness at which it ruptures. The time required for the liquid film to rupture will be called here the 'coalescence time' although the term 'induction time' is also used (Albijanic et al., 2010). If the contact time is not long enough for the film to drain (i.e., does not exceed the coalescence time), the bubbles will rebound without coalescing.

There is a thermodynamic drive in favor of coalescence, namely to reduce the interfacial area and thus decrease the surface free energy component of the system free energy. Frothers provide a chemical energy that opposes the tendency for coalescence. Attached particles at the bubble surface provide mechanical energy (Hunter et al., 2008).

Kracht and Finch (2009a) captured coalescence events in the vicinity of an impeller and demonstrated the impact of frother. Figure 2.5a shows two bubbles colliding in the absence of frother: between images 4 and 5 they merge (coalesce), a time interval of ca. 1 ms. In Figure 2.5b a two-bubble collision also occurs but

now frother is present: in this case, the two bubbles remain in contact for some 20 ms without merging then separate.

The probability of coalescence as a result of a collision, i.e., number of coalescence events relative to number of collision events, is denoted as coalescence efficiency (Lehr et al., 2002). Coalescence at bubble formation mainly occurs due to the following: non-uniform bubble size (where small bubbles are captured by large bubbles due to air diffusion from small to large bubbles because of internal pressure differences), and energy dissipation in the generation volume (especially in mechanical machines) (Rao and Leja, 2004).

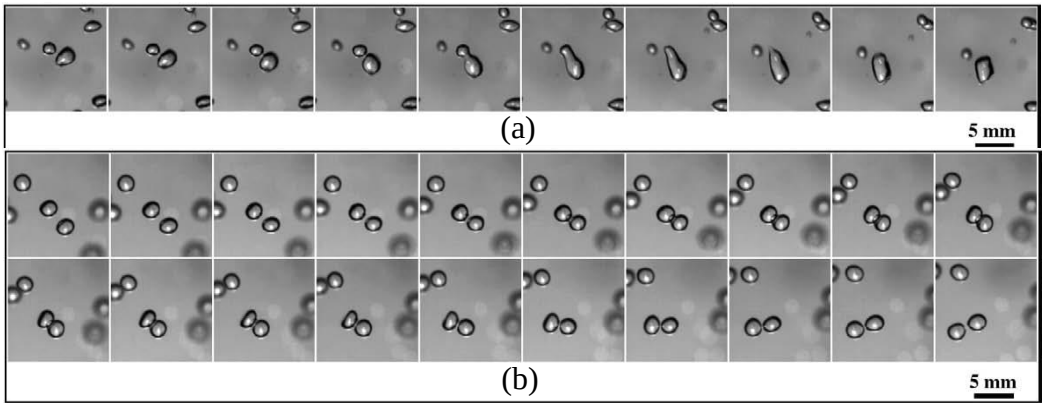

Figure. 2.5: a) Sequence of images (1 ms apart) showing two bubbles colliding (frames 4 & 5) then merging. No frother, 420 rpm; b) Sequence of images (2 ms apart) showing two bubbles colliding (frame 5), remaining in contact then bouncing apart (frame 20). Dowfroth 250, 0.038 mmol/L, 420 rpm. (Kracht and Finch, 2009a. Reprinted with permission from Elsevier)

Coalescence reduces bubble surface area available to collect and transport hydrophobic particles, which has a negative impact on recovery kinetics. At the

same time coalescence, by making larger bubbles with lower surface to volume ratio, reduces the amount of water that reports to overflow and, consequently, reduces recovery of entrained hydrophilic particles; i.e. some coalescence may benefit concentrate grade (Finch and Dobby, 1990; Patwardhan and Honaker, 2000). Eliminating coalescence in the pulp zone would seem the target to maximize kinetics with controlled coalescence in the froth zone perhaps to enhance grade.

Bubbles tend to coalesce in pure liquids regardless of the nature of the liquid (polar or non-polar (organic)). Pure liquids do not foam and do not promote the formation of small bubbles (Marrucci 1969). In aqueous systems bubble coalescence is reduced (inhibited) in presence of surfactants like frothers (Cho and Laskowski, 2002a) and also by high concentration of some salts (Craig, 2004; Quinn et al., 2007).

In the pulp zone in flotation systems, coalescence is arguably fully prevented at concentrations greater than the CCC of the frother. In the froth zone bubbles coalesce as they are transported up and liquid drains to the critical film thickness and this cannot be prevented only delayed dependent on frother type and concentration, and critically now on the presence of particles (Hunter et al., 2008). Most literature on mechanisms focuses on conditions related to coalescence in the froth (foam) zone.

2.4.2. Some factors governing bubble coalescence

2.4.2.1. Approach velocity

The relative velocity of the colliding bubbles affects coalescence efficiency (Thomas, 1981). Bubbles colliding at low relative velocity form small contact film areas which encourage coalescence because the distance for drainage is correspondingly small. In contrast, at high relative velocities the bubbles distort and the contact region flattens increasing the area of contact. In this case the distance to drain is larger and the time to drain correspondingly larger and thus coalescence is less likely.

Other studies have supported this approach velocity effect. Kirkpatrick and Lockett (1974) investigating collisions as bubbles freely rose found that they coalesced in the case of low approach velocity and bounced in the case of high velocity. Chesters and Hofman (1982) made the same observation and suggested the reason is a significant increase in the thin liquid film pressure. Lehr et al. (2002) reached a similar conclusion and added that approach perpendicular to the contact (film) surface favours coalescence. A decrease in bubble rise velocity (by about 20%) during and after coalescence was reported (Sanada et al., 2009) despite the size increase of the new formed bubble. This decrease was attributed to the bubble shape oscillations after coalescence (Sanada et al., 2009).

In flotation systems velocity of approach is a factor in coalescence in the turbulent region around the impeller, less in the pulp zone where bubbles are more-or-less freely rising and relevant again at the pulp-froth interface. In the

latter, rising bubbles collide with the bubbles at the froth base, encouraging coalescence and particle loss (Ata, 2009).

2.4.2.2. Film elasticity

Elasticity is defined as the ratio of stress to strain and measures the ability of a system to restore the original state after deformation. In the presence of surfactants and some salts variations in the surface concentration (e.g. due to mechanical deformation) can occur which induce surface tension gradients and elasticity in the air-water interface (bubble surface) (Tan et al, 2005). Surface elasticity tends to restore the surface to its equilibrium status before deformation, as depicted in Figure 2.6. According to Hofmeier et al. (1995) foam stabilizes because of this elastic response of the liquid-air interface. In the case of equilibrium with the bulk, surface elasticity is called Gibbs elasticity. It can be measured using isothermal equilibrium methods such as the spreading pressure – area method and it is considered a thermodynamic property (Schramm and Green, 1995; Pugh, 1996). Gibbs elasticity is more manifest at low bulk surfactant (frother) concentration as equilibrium surface concentration after deformation is otherwise restored quickly by transport from the bulk (Schramm and Green, 1995). In the case of dynamic non-equilibrium conditions (by applying stress to the system), it is termed Marangoni elasticity (Pugh, 1996; Tan et al., 2005). It is usually detected using dynamic surface tension methods (e.g., maximum bubble pressure vs. bubble age). The Marangoni elasticity represents resistance to

changes in local surface tension and the rate at which it is restored after deformation (Schramm and Green, 1995).

Gibbs elasticity can be expressed as in equation 2.14 (Hofmeier et al., 1995):

$$E = 2\,\frac{d\gamma}{d\ln A} = 2A\,\frac{d\gamma}{dc}\frac{dc}{dA} \qquad (2.14)$$

where γ is the surface tension, A the surface area, c the bulk concentration, and the factor 2 denotes that the film is between two bubbles; i.e., there are two liquid-air interfaces.

The Marangoni elasticity can expressed as in equation 2.15 (Huang et al., 1986) or equation 2.16 (Schramm and Green, 1995).

$$|E_M| = \left|1.5\,\frac{d\gamma}{d\ln t}\right| \qquad (2.15)$$

$$|E_M| = \left|2\,\frac{d\gamma}{d\ln t}\right| \qquad (2.16)$$

where t is time. The use of absolute values reflects measurement at a capillary where surface tension not only changes with time but with area as the bubble grows (Schramm and Green, 1995).

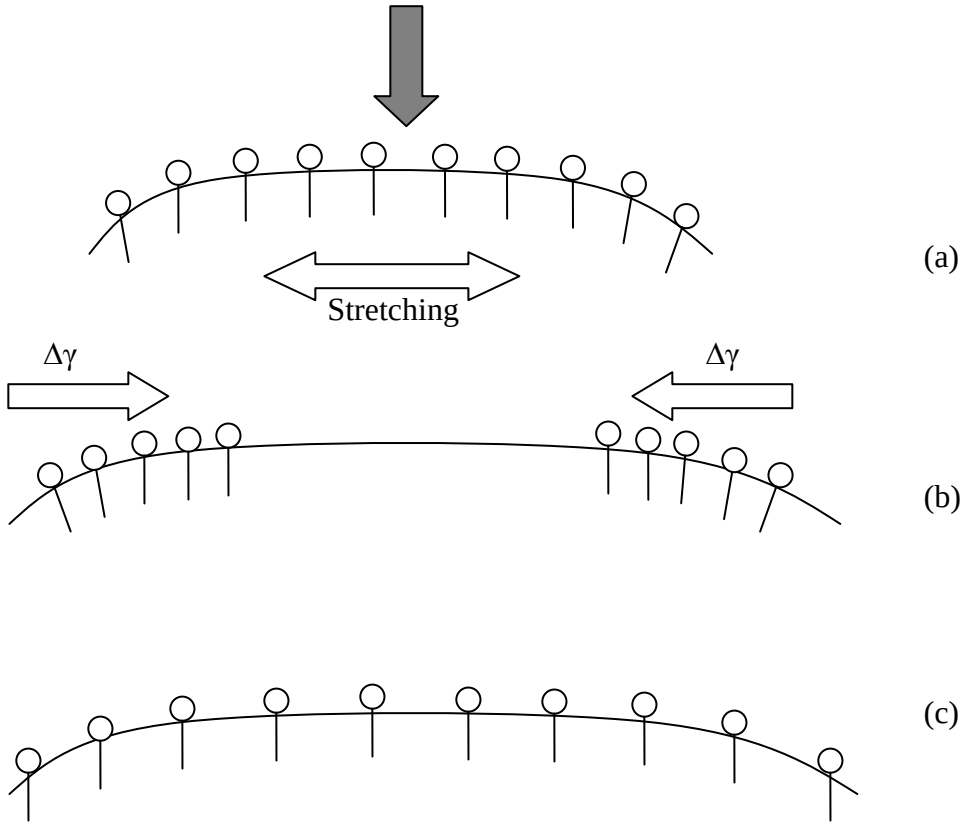

Figure 2.6: Schematic showing (a) surface initially in equilibrium subjected to stretching (e.g. due to mechanical strock) leading to (b) non uniform distribution of surfactant molecules, and associated surface tension gradient that generates a force opposing deformation and thus (c) restores surface to equilibrium

The force associated with the surface tension gradient also induces movement of liquid along the interface in the opposite direction to drainage (Marangoni effect) further stabilizing the froth (Tan et al., 2004; Schramm and Green, 1995). These flows can be visualized (Acuna et al., 2008).

Increasing surfactant surface activity, for example by increasing hydrocarbon chain length, increases surface elasticity (Malysa et al., 1981; Huang et al., 1986). This means that more stable foam will be formed in the presence of

long chain surfactants, and in flotation systems this is generally found (Cytec, 2003)

2.4.2.3. Surface viscosity

Fruhner et al. (1999) suggested that surface elasticity alone is not enough to explain foam stability and that surface viscosity has to be considered. Surface viscosity can be generated by any mechanism (e.g. surfactant diffusion from or adsorption at a surface) that restores the dynamic surface tension to its equilibrium value (Lucassen-Reynders and Lucassen, 1994); or, in other words, resists the interfacial motion and reduces the magnitude of bubble deformation (Pozrikidis, 1994). Surface viscosity is given by the ratio of surface tension gradient to rate of deformation. Surface dilational viscosity η_d^s (dilation refers to the frother molecules moving apart or together) can then be expressed as follows (Pugh, 1996):

$$\eta_d^s = \frac{\gamma_d - \gamma_0}{d \ln A / dt} \qquad (2.17)$$

where γ_0 and γ_d are the original and 'after deformation' static surface tensions, respectively, A is surface area, and t is time.

Increase in surface viscosity and elasticity decrease foam drainage and consequently, increase foam stability (Pugh, 1996). Surface viscosity can be increased by packing a high concentration of surfactant into the surface of the liquid film (between bubbles) leading to high inter-molecule cohesion. Using a blend of ionic and non-ionic surfactants may lead to higher cohesion force in the

liquid film surface as indicated in Figure 2.7 due to the formation of highly condensed film (Pugh, 1996). The presence of particles, especially recent evidence using nano-particles, may also introduce surface elasticity and viscosity effects (Hunter et al., 2008).

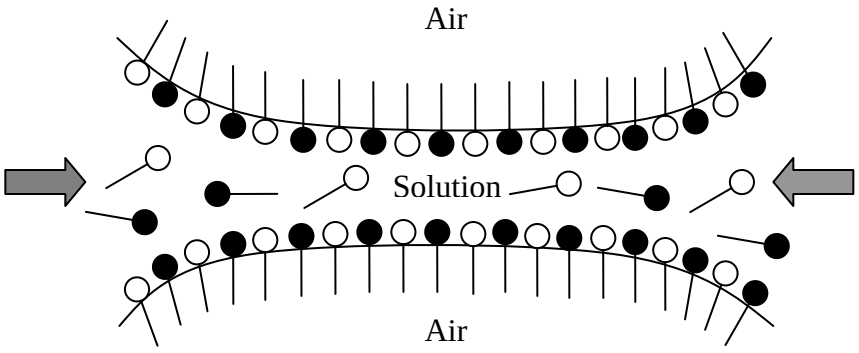

Figure 2.7: Schematic showing cohesion forces (indicated by arrows) which increase surface viscosity in blended surfactants system (adapted from Pugh, 1996)

2.5. Bubble break-up

Formation of bubbles by break-up is the process of dividing (dispersing) an air mass into smaller (daughter) bubbles. Bubble break-up depends on hydrodynamic conditions, particularly, wake shear effects and bubble perturbations (Tse et al., 2003).

In laminar flow systems shear causes bubble elongation which leads to break-up (Walter and Blanch, 1986). In turbulent flow regimes (as in flotation machines), oscillating eddies strike the bubble surface to cause break-up. Break-up results from the energy associated with eddies having sizes close to those of the bubble; eddies much larger than the bubble will transport rather than break bubbles (Hinze, 1955).

Some researchers (Walter and Blanch, 1986; Hesketh et al., 1991; Wilkinson et al., 1993) suggest that break-up in turblent flow fields occurs due to bubbles being streched leading to necking and breakage. Tsuchiya et al. (1989) suggested break-up for rising bubbles may be due to exposure to the preceding bubble wake, the trailing bubble being elongated and split.

Tse et al. (2003) introduced the concept of coalescence-mediated-break-up. Their images showed that coalescence of two bubbles resulted in an annular wave which distorted the newly formed (coalesced) bubble. Consequenly, this elongated bubble often led to ejection of a small bubble. Finch et al (2008) noted the phenomenon with bubbles coalescing at an orifice and offered the mechanism as an explanation for the population of small bubbles often identified in the absence of surfactant (i.e., conditions favouring coalescence) leading to a bi-modal size distribution.

Prince and Blanch (1990) found a significant increase in bubble break-up on increasing gas rate. They suggested the reason is an increase in the number of eddies with sufficient energy to break bubbles. Several researchers (Walter and Blanch, 1986; Hesketh et al., 1991; Wilkinson et al., 1993) have proposed the

same mechanism, namely bubble deformation due to eddies causing stretching resulting in a dumbbell shape with necking that leads to breakage.

Nesset et al. (2007) argued that the bubble size at formation is frother concentration dependent. One can extend that point to speculate that it also depends on the type of frother (surfactant). Studies have shown that frother prevents coalescence (Cho and Laskowski, 2002; Laskowski, 2003; Kracht and Finch, 2009b) but the evidence is growing that bubble size reduction in the presence of frothers is due to both coalescence prevention and break-up (Grau and Laskowski, 2006; Gupta et al., 2007; Finch et al., 2008).

Kracht and Finch (2009a) examined the combination of break-up and coalescence prevention by launching a stream of mono-sized bubbles (~ 2.5 mm diameter) into the path of a rotating impeller, recording the daughter bubble size distribution using a high-speed digital camera. They observed daughter bubbles both smaller and larger than the original (mother) 2.5 mm bubble. They interpreted the results in terms of the two mechanisms, noting that bubbles smaller than the mother bubble were the result of break-up and bubbles larger than the mother bubble indicated coalescence. Addition of frother largely suppressed coalescence (few daughter bubbles larger than 2.5 mm) and altered the distribution of bubbles smaller than 2.5 mm; i.e., frother influenced break-up. They found that the bubbles smaller than the mother bubble were concentrated close to the original size, especially in the presence of frother; i.e., break-up was strongly asymmetric. From analysis of the surface tension force involved they explained this asymmetry by noting that break-up in the presence of frothers

favours a high split ratio, 90:10 by volume or higher (i.e., over 90% of volume remains in the larger of the two daughter bubbles).

This work represents one of the first to address the two mechanisms under flotation-related conditions (i.e., presence of frothers). However, objections can be raised whether the break-up component is fairly examined by the experiment. Some of the objections are:

a) By using a stream of bubbles it is possible that the same bubble is imaged more than once due to circulation inside the vessel;

b) By allowing both coalescence and break-up the procedure tends to reduce the extent of break-up obscuring this possible role of frother;

c) The turbulence resulting from the impeller may cause some bubbles to pass without being subjected to the impeller.

These three features may lead to underestimation of the role of frother in bubble break-up.

One purpose of this thesis is to refine the procedure of Kracht and Finch (2009a) to isolate the effect of frother on the break-up event. This is approached by introducing one bubble at a time into a rotating impeller and by generating bubbles from an air vortex.

REFERENCES

Acuña, C. A., Radman, J., and Finch, J. A., 2008, "Measurement of flow visualized on surface of bubble blown in air", Colloids and Surfaces A: Physicochemical and Engineering Aspects, Vol. 330, No. 2-3, p. 112-115.

Albijanic, B., Ozdemir, O., Nguyen, A. V., and Bradshaw D., 2010, "A review of induction and attachment times of wetting thin films between air bubbles and particles and its relevance in the separation of particles by flotation", Advances in Colloid and Interface Science, Vol. 159, No. 1, p. 1-21.

Ata, S., 2009, "The detachment of particles from coalescing bubble pairs", Journal of Colloid and Interface Science, Vol. 338, No. 2, p. 558-565.

Ata, s., and Jameson, G.J., 2005, "The formation of bubble clusters in flotation cells", International Journal of Mineral Processing, Vol. 76, No. 1-2, p. 123-139.

Azgomi, F, Gomez, C.O., Finch, J.A., 2007a, "Characterizing frothers using gas hold-up", Canadian Metallurgical Quarterly, Vol. 46 (3), p. 237-242.

Azgomi, F., Gomez, C.O., and Finch, J.A., 2007b, “Correspondence of gas holdup and bubble size in presence of different frothers”, International Journal of Mineral Processing, Vol. 83, pp. 1-11.

Bascur, O.A., and Herbst, J.A., 1982, “Dynamic modeling of a flotation cell with a view toward automatic control”, 14th International mineral Processing Congress. Toronto, Canada, October 17-23, pp. 1-21.

Bikerman, J. J., 1973, “Foams”, Springer Verlag, New York.

Cappuccitti, F., and Finch, J. A., 2007, “Developing new frothers from 2-phase characterization tests”, Cape Town, Nov 6-9.

Cappuccitti, F., and Finch, J.A., 2008, "Development of new frothers through hydrodynamic characterization", Minerals Engineering, vol. 21, pp. 944–948.

Cappuccitti, F., and Nesset, J., 2009, "Frother and collector effects of flotation cell hydrodynamics and their implication on circuit performance", In: Proceedings of the 7th UBC-McGill-UA International Symposium on Fundamentals of Mineral processing, Editors: Gomez, C. O., Nesset, J. E., and Rao, S. R., Sudbury, Ontario, p. 169-182.

Chesters, A. K., and Hofman, G., 1982, "Bubble coalescence in pure liquids", Applied Scientific Research, Vol. 38, p. 353-361.

Cho, Y. S, and Laskowski, J. S., 2002 a, “Effect of flotation frothers on bubble size and foam stability”, International Journal of Mineral Processing, Vol. 64, p. 69-80.

Cho, Y. S, and Laskowski, J. S., 2002 b, “Bubble coalescence and its effect on dynamic foam stability”, Canadian Journal of Chemical Engineering, Vol. 80, p. 299- 305.

Craig, V. S. J., 2004, "Bubble coalescence and specific-ion effects", Current Opinion in Colloid & Interface Science, Vol. 9, No. 1-2, pp. 178-184.

Cytec Mining Chemicals Handbook, Revised Edition 2003.

Czarnecki, J., Malysa, K., and Pomianowski, A., 1982, “Dynamic frothability index”, Journal of Colloid and Interface Science, Vol. 86, No. 2, p. 570-572.

Dickinson, J. E., Laskovski, D., Stevenson, P., and Galvin, K. P., 2010, "Enhanced foam drainage using parallel inclined channels in a single-stage foam fractionation column", Chemical Engineering Science, Vol. 65, No., 8, p. 2481-2490.

Engelbrecht, J.A. and Woodburn, E.T., 1975, “The effect of froth height, aeration rate and gas precipitation on flotation”, Journal of South African. Institute of Mining and Metallurgy, Vol. 10, p. 125–132.

Finch, J. A., Gelinas, S., and Moyo, P., 2006, "Frother related research at McGill University", Minerals Engineering, Vol. 19, No. 6-8, p. 726-733.

Finch, J. A., Nesset, J. E., and Acuna, C., 2008, "Role of frother on bubble production and behavior in flotation", Minerals Engineering, Vol. 21, p. 949-957.

Finch, J. A., and Dobby, G.S., 1990, “Column flotation”, Pergamon Press, Elmsford, NY.

Fruhner, H., Wantke, K. -D., and Lunkenheimer, K., 1999, “Relationship between surface dilational properties and foam stability”, Colloids and Surfaces A: Physicochemical and Engineering Aspects, Vol. 162, p. 193–202.

Gaudin, A.M., 1957. “Flotation”, Chapter 11, p. 327-368.

George, P., Nguyen, A.V., and Jameson, G.J., 2004, “Assessment of true flotation and entrainment in the flotation of submicron particles by fine bubbles”, Minerals Engineering, Vol. 17, p. 847-853.

Gorain, B.K., Franzidis, J.-P., Mainlapig, E.V., 1995, « Studies on impeller type, impeller speed and air flow rate in an industrial scale flotation cell-Part 1: Effect on bubble size distribution”, Minerals Engineering, Vol. 8, p. 615-635.

Grau, R. A., and Laskowski, J. S., 2006, “Role of frothers in bubble generation and coalescence in a mechanical flotation cell”, The Canadian Journal of Chemical Engineering, Vol. 84, p. 170-182.

Grau, R. A., Laskowski, J. S., and Heiskanen, K., 2005, “Effect of frothers on bubble size”, International Journal of Mineral Processing, Vol. 76, p. 225-233.

Gupta, A. K., Banerjee, P. K., Mishra, A., Satish, P., and Pradip, 2007, " Effect of alcohol and polyglycol ether frothers on foam stability, bubble size and coal flotation", nternational Journal of Mineral Processing, Vol. 82, p. 126-137.

Harris, P. J., 1982, “Frothing phenomena and frothers”, In King, R. P. (Ed.), Principles of flotation, South African Institute of Mining and Metallurgy Monograph series, p. 237-263.

Hesketh, R. P., Etchells, A. W., and Russell, T. W. F., 1991, "Bubble breakage in pipeline flow", Chemical Engineering Science**,** Vol. 46, No. 1, p. 1-9.

Hinze, J. O., 1955, "Fundamentals of the hydrodynamic mechanism of splitting in dispersion processes", AIChE Journal, Vol. 1, No. 3, p. 289-295.

Hofmeier, U., Yaminsky, V. V., and Christenson, H.K., 1995, " Observations of solute effects on bubble formation", Journal of Colloid and Interface Science, Vol. 174, No. 1, p. 199-210.

Huang, D. D. W., Nikolov, A., and Wasan, D. T., 1986, "Foams: Basic properties with application to porous media", Langmuir, Vol. 2, p. 672-677.

Hunter, T. N., Pugh, R. J., Franks, G. V., Jameson, G. J., 2008, "The role of particles in stabilising foams and emulsions", Advances in Colloid and Interface Science, Vol. 137, No.2, p. 57-81.

Ireland, P. M. and Jameson, G. J. 2007, "Liquid transport in a multi-layer froth", Journal of Colloid and Interface Science, Vol. 314, No. 1, p. 207-213.

Kirkpatrick, R. D., and Lockett, M. J., 1974, "The influence of approach velocity on bubble coalescence", Chemical Engineering Science, Vol. 29, p. 2363-2373.

Klassen, V. and Mokrousov, V., 1963, "An Introduction to the Theory of Flotation", Butterworths, London, Chapter 5, p. 378-381.

Knuutila, D., 2007, Master Thesis, McGill University.

Kracht, W., Finch, J. A., 2009a, "Bubble break-up and the role of frother and salt", International Journal of Mineral Processing, Vol. 92, p. 153-161.

Kracht, W., Finch, J. A., 2009b, "Using sound to study bubble coalescence", Journal of Colloid and Interface Science, Vol. 332, No. 1, p. 237-245.

Laskowski, J. S, 2003, "Fundamental properties of flotation frothers", in Proceedings of 22nd International Mineral Processing Congress, Vol. 2,

Lorenzen, L., Bradshaw, D. J., editors, South African Institute of Mining and Metallurgy, Cape Town, p. 788-797.

Laskowski, J. S, Tlhone, T., Williams, P., and Ding, K., 2003, “Fundamental properties of polyoxypropylene Alkyl ether flotation frothers”, International Journal of Mineral Processing, Vol. 72, p. 289-299.

Lehr, F., Millies, M., and Mewes, D., 2002, "Bubble-Size distributions and flow fields in bubble columns", AIChE Journal, Vol. 48, No. 11, p. 2426-2443.

Levich, V.G., 1962, “Physicochemical hydrodynamics”, Chapter8, p. 395-471.

Lucassen-Reynders, E. H., and Lucassen, J., 1994, "Surface dilational viscosity and energy dissipation", Colloids and Surfaces: A, Vol. 85, p. 211-219.

Lynch A.J., Johnson N.W., Mainlapig, E.V., Thorne, C.G., 1981, “Mineral and coal flotation circuits and their simulation and control”, Elsevier Scientific Publishing.

Malysa, K., Lunkenheimer, K., Miller, R., and Hartenstein, C., 1981, “Surface elasticity and frothability of n-octanol and n-octanoic acid solutions”, Colloids and Surfaces, Vol. 3, N. 4, p. 329-338.

Marrucci, G., 1969, "A theory of coalescence", Chemical Engineering Science, Vol. 24, N. 6, p. 975-985.

Neethling, S.J., and Cilliers, J.J., 2002, “The entrainment of gangue into a flotation froth”, International Journal Mineral Processing, Vol. 64, p.123-134.

Neethling, S.J., Cilliers, J.J., and Woodburn E.T., 2000, “Prediction of water distribution in flowing foam”, Chemical Engineering Science, Vol. 55, p. 4021-4028.

Neethling, S.J., Lee, H.T., and Cilliers J.J., 2003, “Simple relationships for predicting the recovery of liquid from flowing foams and froths”, Minerals Engineering, Vol. 16, p. 1123-1130.

Nesset, J.E., Finch, J.A., Gomez, C.O., 2007, "Operating variables affecting the bubble size in forced-air mechanical flotation machines", In: Proceedings AusIMM 9th Mill Operators Conference, Fremantle, Australia, p. 66–75.

Patwardhan, A., and Honaker, R. Q., 2000, "Development of a carrying-capacity model for column froth flotation." International Journal of Mineral Processing, Vol. 59, No. 4, p. 275-293.

Pozrikidis, C., 1994, "Effects of surface viscosity on the finite deformation of a liquid drop and the rheology of dilute emulsions in simple shearing flow", Journal of Non-Newtonian Fluid Mechanics, Vol. 51, No. 2, p. 161-178.

Prince, M. J., and Blanch, H. W., 1990, "Bubble coalescence and break-up in air-sparged bubble columns", AIChE Journal, Vol. 36, No. 10, p. 1485-1499.

Pugh, R. J., 1996, “Foaming foam films, antifoaming and defoaming”, Advances in Colloid and Interface Science, Vol. 64, p. 67-142.

Quinn, J.J., Kracht, W., Gomez, C.O., Gagnon, C., and Finch, J.A., 2007, "Comparing the effect of salts and frother (MIBC) on gas dispersion and froth properties", Minerals Engineering, Vol. 20, No. 14, p. 1296-1302.

Rao, S. R., and Leja, J., 2004, “Surface chemistry of froth flotation”, Second edition, Kluwer Academic, New York.

Sanada, T., Sato, A., Shirota, M., and, Watanabe, M., 2009, "Motion and coalescence of a pair of bubbles rising side by side", Chemical Engineering Science, Vol. 64, No. 11, p. 2659-2671.

Schramm, L. L., and W. H. F., Green, 1995, "The influence of Marangoni surface elasticity on gas mobility reduction by foams in porous media", Colloids and Surfaces: A, Vol. 94, p. 13-28.

Shockley, J., 2007, Summer student.

Smith, P.G. and Warren, L.J., 1989, “Entrainment of particles into flotation froths”, Frothing in flotation I: Edited by Laskowski, J.S., p. 123-145.

Stevenson, P., 2006, “Dimensional analysis of foam drainage”, Chemical Engineering Science, Vol. 61, N. 14, p. 4503-4510.

Sun, S.C., 1952, “Frothing characteristics of pine oil in flotation”, Min. Eng.4 (1), p. 65–71.

Tan, S. N., Fornasiero, D., Sedev, R., and Ralston, J., 2004, "The interfacial conformation of polypropylene glycols and foam behaviour", Colloids and Surfaces A: Physicochemical and Engineering Aspects, Vol. 250, No. 1-3, p. 307-315.

Tan, Su Nee, Pugh, R.J., Fornasiero, D., Sedev, R., and Ralston, J., 2005, “Foaming of polypropylene glycols and glycol/MIBC mixtures”, Minerals Engineering, Vol. 18, p. 179–188.

Thomas, R. M.,1981, "Bubble coalescence in turbulent flows." International Journal of Multiphase Flow**,** Vol. 7, No. 6, p. 709-717.

Trahar, W. J., and Warren, L. J., 1976, “The flotability of very fine particles — A review”, International Journal of Mineral Processing, Vol. 3, p. 103-131.

Trahar, W.J., 1981, “A rational interpretation of the role of particle size in flotation”, International Journal of Mineral Processing, Vol. 8, p. 289-327.

Tse, K. L., Martin, T, McFarlane, C. M., and Nienow, A. W., 2003, "Small bubble formation via a coalescence dependent break-up mechanism", Chemical Engineering Science, Vol. 58, No. 2, p. 275-286.

Tsuchiya, K. ., Miyahara, T.., and Fan, L.-S., 1989, "Visualization of bubble-wake interactions for a stream of bubbles in a two-dimensional liquid-solid fluidized bed", International Journal of Multiphase Flow, Vol. 15, No. 1, p. 35-49.

Walter, J. F., and Blanch, H. W., 1986, "Bubble break-up in gas--liquid bioreactors: Break-up in turbulent flows", The Chemical Engineering Journal, Vol. 32, No. 1, p. 7-17.

Warren, L.J., 1985, “Determination of the contributions of true flotation and entrainment in batch flotation tests”, International Journal of Mineral Processing, Vol. 14, p. 33-44.

Wilkinson, P. M., Van Schayk, A., Spronken, J. P. M., and Van Dierendonck, L., 1993, "The influence of gas density and liquid properties on bubble breakup", Chemical Engineering Science, vol. 48, No. 7, p. 1213-1226.

Xu, M., Finch, J.A., and Uribe-Salas, A., 1991, "Maximum gas and bubble surface rates in flotation columns", International Journal of Mineral Processing, Vol. 32, p. 233-250.

Yianatos, J.B., Finch J.A., and Laplante, A.R.,1986, "Holdup profile and bubble size distribution of flotation froths", Canadian Metallurgical Quarterly, Vol. 25 , p. 23-29.

Zhang, W., Nesset, J. E., and Finch, J. A., 2010, "Water Recovery and Bubble Surface Area Flux in Flotation", Canadian Metallurgical Quarterly, Vol 49, No 4, p. 353-362.

Zheng, X., Franzidis, J. P., and Johnson, N. W., 2006, "An evaluation of different models of water recovery in flotation", Minerals Engineering, Vol. 19, p. 871 – 882.

CHAPTER 3 – EXPERIMENTAL

3.1. Introduction

Three test rigs were used to measure hydrodynamic properties. A bubble column provided the most complete data set: bubble size, gas holdup, froth height, and water overflow rate. A 0.8 m^3 mechanical cell provided a more realistic flotation machine (the column uses a porous sparger) but was only suited to batch operation and bubble size measurement. To complement, a 5.5 L (mini) mechanical flotation cell in closed loop continuous operation provided water overflow rate data.

3.2. Bubble column

A 3.5 m x 10 cm diameter Plexiglas bubble column was used (Figure 3.1) to run batch and continuous (closed loop) tests. Frother solutions were prepared, placed in the tank and then pumped to the column as indicated. The bubble generator was a porous, stainless steel plate sparger (nominal pore diameter 10 μm) and all the tests were carried out using superficial gas velocity (J_g) of 1 cm/s.

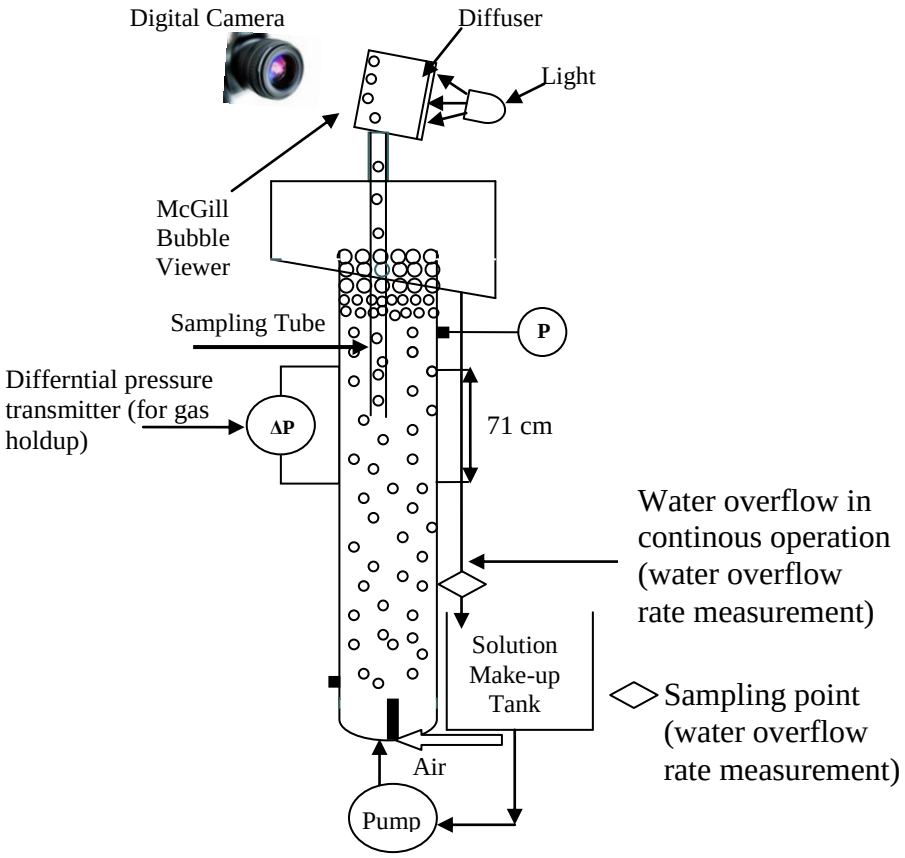

Figure 3.1: Column setup

3.2.1. Bubble size measurements

The bubble size measurements were made using the McGill bubble size analyzer or "bubble viewer" (Figure 3.2) (Gomez and Finch, 2007). The device consists of a sampling tube attached to a viewing chamber with a window inclined 15º from the vertical. The viewing chamber (31.7 cm × 22.1 cm × 13.0 cm) is made of PVC with two facing glass windows. To operate, the sampling tube is closed and the assembly filled with the same solution as present in the bulk (to counter bubble coalescence by preserving the bubble environment). The sampling

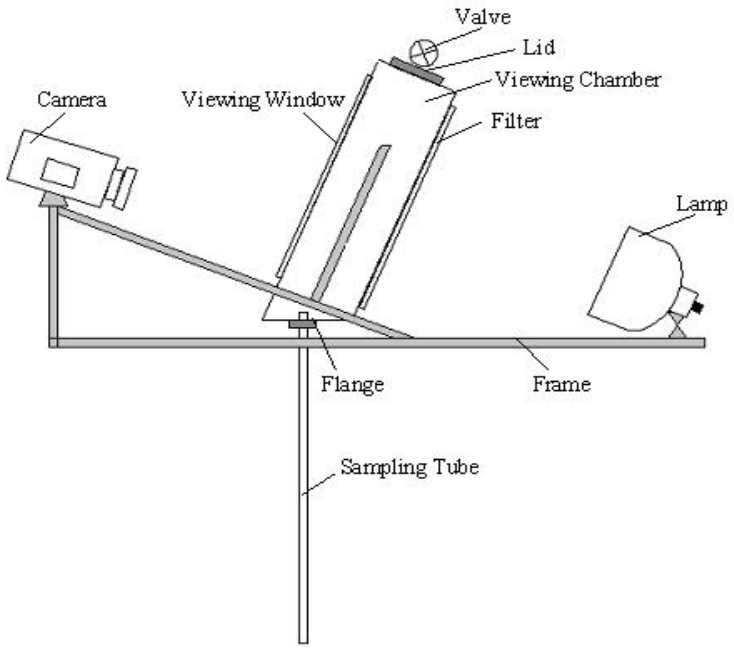

Figure 3.2: Schematic of McGill bubble viewer

tube, made of PVC with an inner diameter 2.54 cm and length 152 cm, was immersed below the froth to the middle of the section where gas holdup measurements were made. Upon opening the valve bubbles rise into the sampling tube and enter the viewing chamber where they spread into a near single plane after contact with the inclined window. This spreading offers the joint advantage of unambiguous definition of the focal plane and reduction in out of focus bubble images. Due to the use of diffused backlighting (note the ‘diffuser’), bubbles cast shadows, which are digitally imaged. The digital camera was Canon model "EOS 30D" 8.2 equipped with a macro lens of 100 mm able to take 99 images automatically (one image per second). Typically two hundred images were

collected per test, the exception being the water only tests where the fewer larger bubbles necessitated more images.

At least 3000 bubbles were processed for a given experiment to meet statistic requirements in determining reliable bubble size distribution (Hernandez-Aguilar and Finch, 2004; Hernandez-Aguilar et al., 2005).

Images were captured and analyzed using Empix Northern Eclipse v6.0 and in-house Empix BSD (bubble size distribution) processor software. Timing between frames was selected to avoid repeat counting of the same bubble.

3.2.2. Gas holdup

Readings from a differential pressure transmitter "Bailey model PTSDDD" with tapping points located between 224 cm and 295 cm above the sparger was used to calculate gas holdup, ε_g:

$$\varepsilon_g = \left(1 - \frac{\Delta P}{L} \right) \times 100 \qquad (3.1)$$

where ΔP is the pressure difference between the two tapping points set a distance L apart (71 cm in this case).

3.2.3. Froth height and water overflow rate

The equilibrium froth height was determined running the column batch and using a measuring tape (Figure 3.1). Frother solutions were prepared to a (total volume of 40 liters).

To measure water overflow rate a closed loop was employed, water overflow being returned to the make-up tank. A level (froth depth) was assigned,

and controlled using the PI control loop function in the software (iFix). The equation used to calculate froth depth is derived from static pressure measurements (Fernandez, 1995), as follows:

$$h_f = CF\left(\frac{P - \rho_l g h}{\rho_f g - \rho_l g}\right) \qquad (3.2)$$

where h_f is the target froth depth, CF is a correction factor (to allow for changes in froth density between conditions), g is the gravitational acceleration, and ρ_l and ρ_f are the liquid and froth densities, respectively. The pressure transmitter (*P*) sends signals to calculate level (i.e., using equation 3.2). As soon as the the desired level set point is entered through the computer, the control loop manipulates the speed of the feed pump (i.e., changes feed flow rate) so that the calculated level nears the set point. With froth depth at the set point timed water overflow samples were collected and then weighed.

3.3. The Metso 0.8 m^3 RCS^{TM} pilot-scale mechanical flotation cell

Figure 3.3 is a cut-away view of the unit (Metso brochure RCS flotation). While the nominal volume of the cell is 0.8m^3, the standard test volume is 700 liters. The cell was run batch with standard test conditions 1200 rpm impeller speed and 0.5 cm/s superficial gas velocity (J_g). Frother was mixed for 5 minutes at 1200 rpm prior to a test run. The bubble sampling tube of the McGill bubble viewer was 0.72 m long and was located 0.12 m above the shelf baffle (approximately 0.25 m above the stator/impeller assembly) in order to be well above the turbulent zone.

Figure 3.3: Cut-away view of Metso RCS^{TM} 0.8 m^3 mechanical flotation cell

3.4. Mini-mechanical cell

The set-up is based on the rig designed at the Noranda Technology Centre for continuous small-scale on-site flotation testing (Shink et al., 1992). The arrangement comprised the mini-cell, holding tank, conditioning tank and feed flow-regulator tank configured in a closed loop run to achieve steady state operation (Figure 3.4). The cell (Figure 3.5) volume is 5.5 L and volume of the entire set-up is 56 L. The cell has a decreasing cross-section with height, a design feature to more closely emulate the froth area to cell volume ratio of industrial cells. Water is held in the holding tank and pumped into the feed flow-regulator

tank, which allows a calibrated flow into the conditioning tank while the remainder returns to the holding tank. The conditioning tank is mixed (stirrer at 1000 rpm). Flow from the conditioning tank is fed to the cell. The position of an opening (4 cm x 4 cm) on the underflow (tailings) discharge pipe (Figure 3.5) regulates water rate to underflow and hence controls froth depth (level) in the cell, in this case 1 cm. Cell overflow and underflow were recombined and pumped to the holding tank to close the loop. The pump was used to ensure a flow above the minimum to maintain the target feed flow rate set at the regulator tank. Timed samples of cell overflow were taken to measure flow rate.

Frother was added to concentration and mixed by circulating between conditioning and holding tanks for 15 minutes prior to initiating a test. Operating conditions were adjusted as follows: feed flow 2300 g/min (i.e., retention time in cell ca. 2 min), impeller speed 1250 rpm, air flow rate 4200 cm^3/min and froth depth 1 cm. Based on the area of the cell at the froth depth used, 96.8 cm^2, the feed (water) velocity J_F = 0.396 cm/s and the air velocity J_g = 0.725 cm/s. The air velocity reported at the impeller region (area = 309.2 cm^2), which controls bubble size generated, is Jg = 0.227 cm/s, near the low end of the typical operating range for flotation cells (Gomez and Finch, 2002).

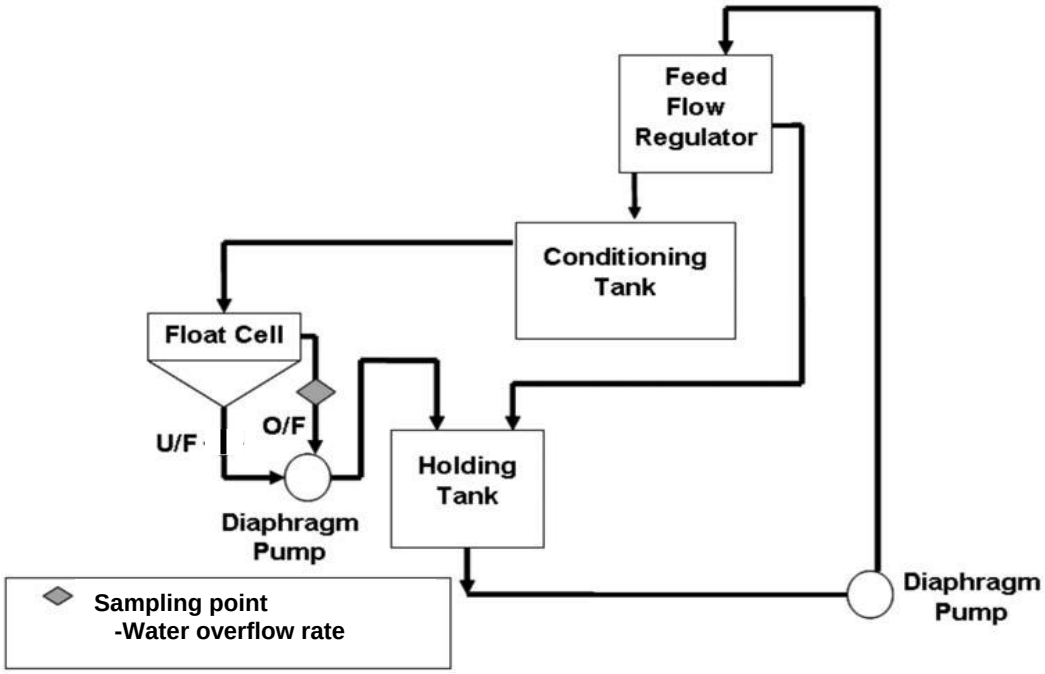

Figure 3.4: Set-up for continuous closed loop testing on a water-air system.

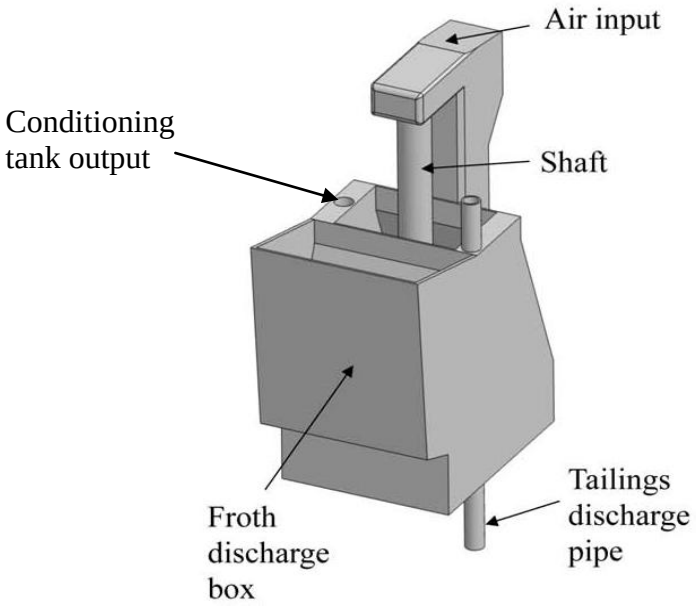

Figure 3.5: Schematic of the mini-flotation cell (Adapted from Zhang et al., 2010)

3.5. Frothers

The frothers examined are listed in Table 3.1 and correspond to those tested byAzgomi et al. (2007). They were used as supplied. Solutions (w/w) were made using Montreal tap water. After each test, the units were emptied and cleaned. Frother blends were prepared by adding the two frothers (F150, DF250, or octanol with pentanol or MIBC) separately to the solution make-up tank for the three test units. The concept is that the polyglycols give good frothing and the alcohols yield small bubble size, therefore the blends potentially offer a test of the the hypothesis of independent control over the frother two functions.

3.6. Surface tension

Static surface tension measurements were made for single and blended frother solutions using the Wilhelmy Plate Method (Kruss Processor Tensiometer K12). In this case samples were prepared using de-ionized water.

Table 3.1: Summary of frother chemical structure, molecular weight, and suppliers

Frother	**Formula**	**Molecular Weight g/gmol**	**Supplier**
1-Pentanol	$CH_3CH_2CH_2CH_2CH_2OH$	88.15	Arcos Organics
MIBC	$CH_3CH(CH_3)CH_2CH(OH)CH_3$	102.18	Dow Chemicals
1-Heptanol	$CH_3CH_2CH_2CH_2CH_2CH_2CH_2OH$	116.20	Arcos Organics
F150**	$H(PO)_7OH$ *	425	Flottec, USA
PPG425**	$H(PO)_7OH$ *	425	Aldrich
DF250	$H(PO)_4OH$ *	250	Flottec, USA
1- Octanol	$CH_3CH_2CH_2CH_2CH_2CH_2CH_2CH_2OH$	130.23	Fisher

* PO = C_3H_6O

** For some tests, F150 was replaced by PPG425

3.7. Bubble coalescence

A square cross section (15 cm x 15 cm) x 50 cm height Acrylic vessel held the test solution (Figure 3.6). Two stainless steel capillaries, 1.6 mm inner diameter and 3.1 mm outer diameter, were introduced from opposite sides of the

vessel at the same level 10 cm from the vessel bottom. Air was introduced using a plastic syringe connected to the capillaries. Bubbles were generated by manually applying pressure to both syringes simultaneously until the two bubbles came into contact. The same general setup was employed by Ata (2008) using two adjacent vertical capillaries and Duerr-Auster et al. (2009) using two vertical opposing capillaries.

Solutions were prepared using Montreal tap water as used in the hydrodynamic testwork (use of tap water was also because each test consumed about 9 liters (including water for cleaning), a large amount if purified water was to be considered). A total volume of 3 liters was placed in the Acrylic vessel for each test. A halogen lamp provided backlighting after passing through diffuser paper to provide more uniform distribution. A high-speed camera "Fastec Troubleshooter" was used to record the images. The video recordings were processed off-line, and using "Virtual Dub" open source software coalescence time was determined with an accuracy up to 1/2000 s (i.e., using up to 2000 frames per second). Coalescence time is calculated starting from the moment of first contact between the two bubbles (t = 0) and the beginning of coalescence, which is readily determined using frame-by-frame analysis.

Each test was repeated in full (i.e., including freshly prepared solution) at least 3 times and the mean and standard deviation were calculated; error bars on the figures are the 95% CI (confidence interval).

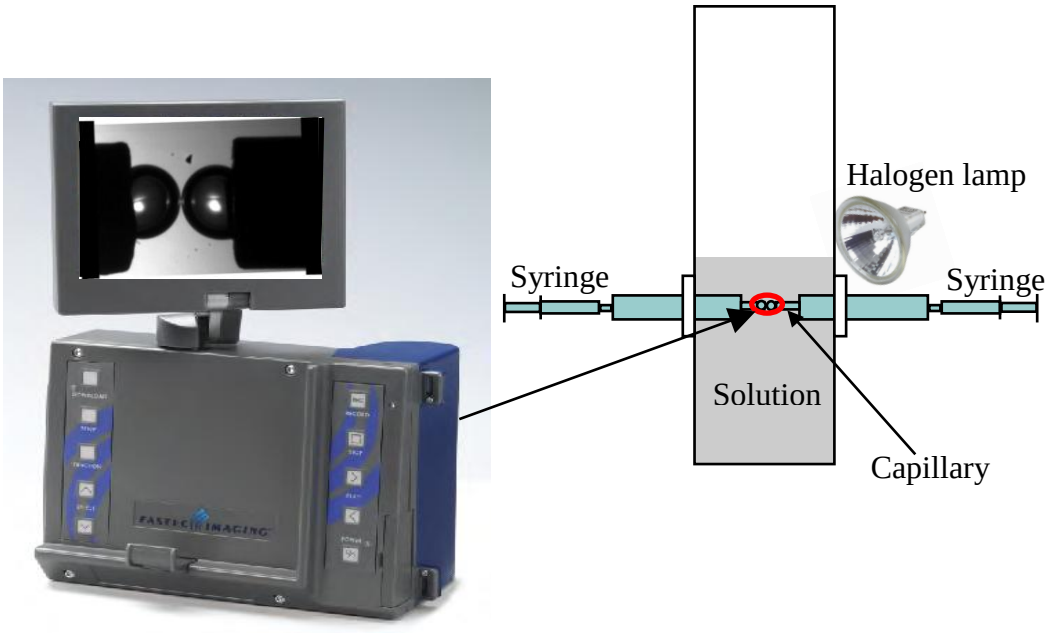

Figure 3.6: Bubble coalescence experimental setup

3.8. Bubble break-up

3.8.1. One-bubble-at-a-time

Figure 3.7 illustrates the experimental setup. A stainless steel capillary, 1.6 mm inner diameter and 3.1 mm outer diameter, was introduced from the side 10 cm above the bottom of a square cross section (15 cm x 15 cm) x 50 cm height Acrylic (transparent) vessel. Air was introduced using a plastic syringe connected to the capillary. Bubbles ca. 3 mm in diameter were generated by applying pressure to the syringe manually. The bubble rises to encounter a three bladed

axial flow impeller (Figure 3.7 right) 4 cm above the capillary tip. The impeller was rotated at 420 rpm for all experiments.

The "Fastec troubleshooter" camera imaged the bubble break-up event at up to 2000 frames per second. The video recording was processed off-line to determine the size of the daughter bubbles.

Solutions again were prepared using Montreal tap water. A total volume of 5 L was used for each test. A halogen lamp was directed to the vessel rear, which was covered by diffuser paper to uniformly distribute the light.

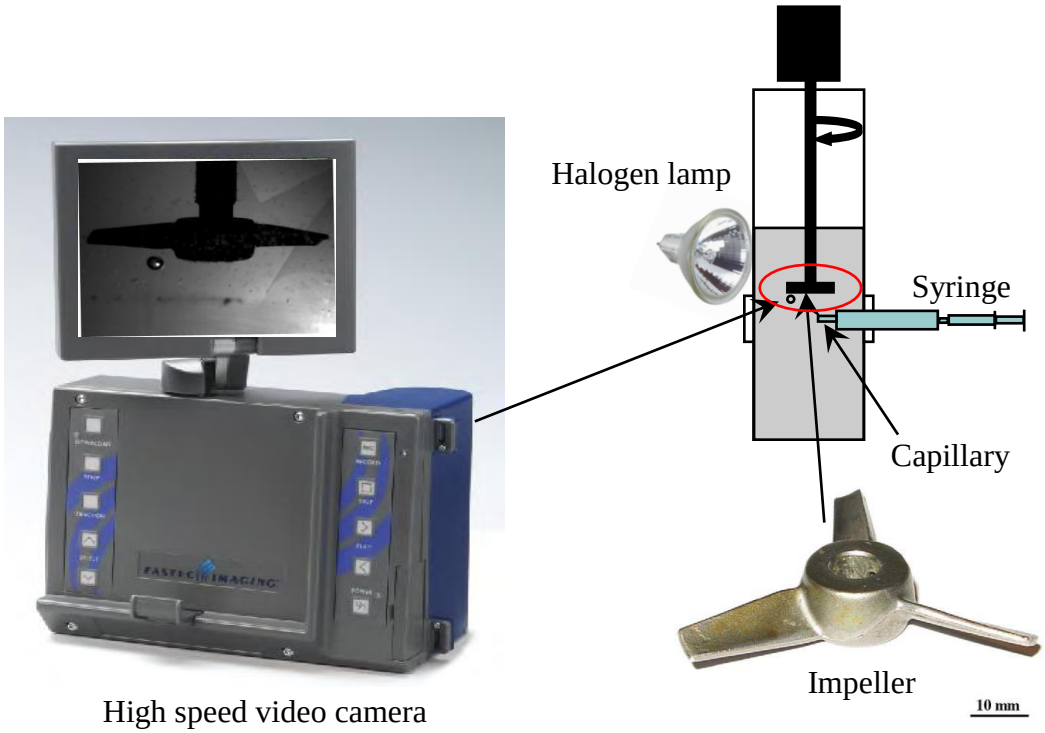

Figure 3.7: Experimental setup for single bubble breakage

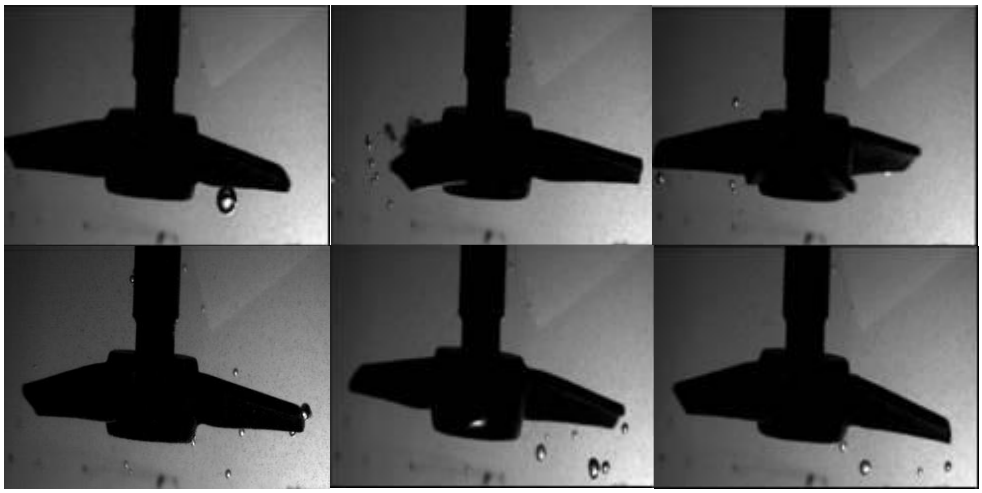

Figure 3.8: Sequence of images recording one-bubble-at-a-time break-up event in the presence of 0.047 mmol/L (20 ppm) F150

Video recordings were transferred to a computer and using "ImageJ" open source software images were processed frame by frame with bubbles selected (and tracked) manually in order to ensure that: bubbles not hit by the impeller were not processed; no bubble was analyzed more than once; and all daughter bubbles were captured for processing. Bubble size distribution was calculated using a macro-code developed by Kracht (2009) within the ImageJ software. Figure 3.8 shows an example of a sequence of images. At least 25 measurements of single bubble break-up events were recorded for each condition.

3.8.2. Break-up (bubble formation) from an air vortex

The same transparent vessel and high-speed camera in the single bubble break-up tests were used (Figure 3.9). Tap water was used to prepare 5 L of

frother solution for each experiment. Bubbles were generated from an air vortex induced by rotation of the impeller (speed 675 rpm) set 3.5 cm below the liquid surface. As the air vortex is drawn downwards, it intercepts the impeller and disperses into bubbles. The aim of this experiment is to image the bubble size immediately after formation which will help capture the role of frother, whether it is just preventing coalescence or is it a combination of break-up and coalescence prevention. This is an attempt at simulating break-up of an air mass (vortex) as in a mechanical machine.

Images were taken at 0.5 s intervals to allow the bubbles to move away from the imaging window just below (ca. 5.6 cm) the impeller (i.e., away from the bubble formation zone) to reduce the probability of imaging a bubble more than once and to try to capture bubbles before coalescence occured. The camera was adjusted to 50 frames per second (the slowest rate). The video was transferred to a computer and the images extracted using "Frame Shots" software with 0.5 s interval. The bubble size distribution was recorded and the Sauter mean bubble size (d_{32}) calculated using Northern Eclipse v6.0 and in-house Empix BSD (bubble size distribution) processor software. Figure 3.10 shows example images with 0.047 mmol/L F150. While the software for the one-bubble-at-a-time and bubble generation from the air vortex was matched to the need each was tested for both experiments and gave the same resulting bubble size.

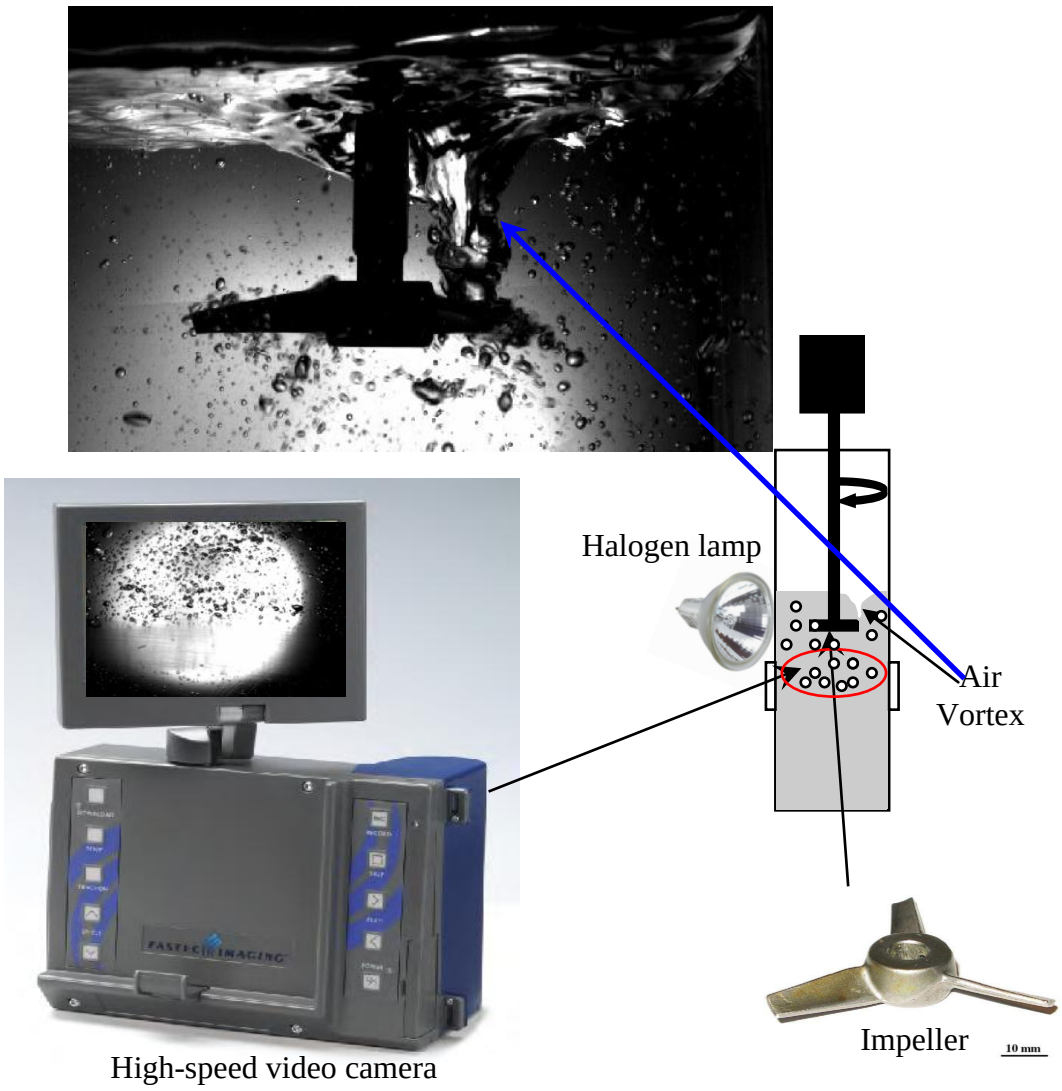

Figure 3.9: Experimental setup for bubble break-up from air vortex

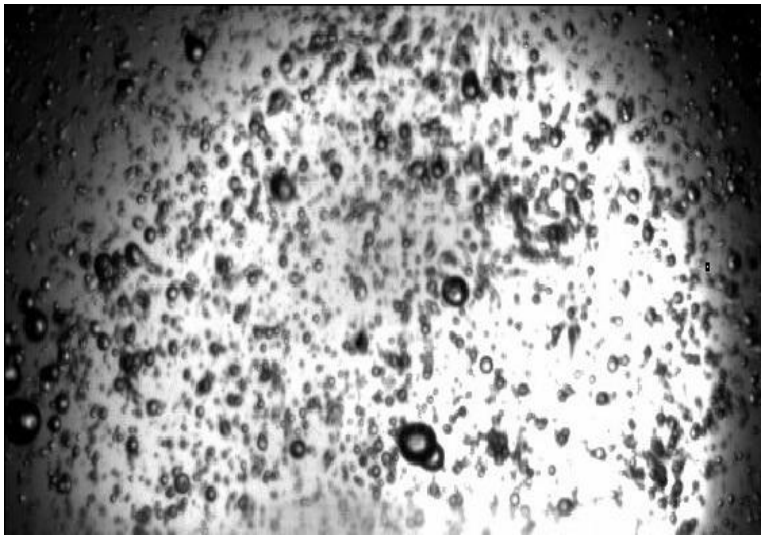

Figure 3.10: Image of bubbles formed from break-up of air vortex in presence of 0.047 mmol/L F150

REFERENCES

Ata, S., 2008, "Coalescence of bubbles covered by particles", Langmuir, Vol. 24, p. 6085-6091.

Duerr-Auster, N., Gunde, R., Mäder, R., and Windhab, E. J., 2009, "Binary coalescence of gas bubbles in the presence of a non-ionic surfactant", Journal of Colloid and Interface Science, Vol. 333, No. 2, p. 579-584.

Fernandez, J.P., "Installation of an Automated Laboratory Flotation Column" M.Eng Thesis, McGill University, 1995.

Gomez, C. O., and Finch, J. A., 2002, "Gas Dispersion Measurements in Flotation Machines", *CIM Bulletin 95,* Vol. 1066, p. 73–38.

Gomez, C. O., and Finch, J. A., 2007, "Gas dispersion measurements in flotation cells", International Journal of Mineral Processing, Vol. 84, p. 51–58.

Hernandez-Aguilar J.R., and Finch J. A., 2005, "An experiment to validate bubble sizing techniques using bi-modal populations of known proportions", In: Graeme J. Jameson (Ed.), Centenary of Flotation Symposium, 6-9 June 2005, Brisbane, Queensland, Australia, p. 465-472.

Hernandez-Aguilar, J.R., Coleman, R.G., Gomez, C.O., and Finch, J.A., 2004, "A comparison between capillary and imaging techniques for sizing bubbles in flotation systems", Minerals Engineering, Vol. 17, No. 1, p. 53-61.

Kracht, W., 2009, "Effect of frother on bubble coalescence, break-up, and initial rise velocity", PhD thesis, McGill University, Quebec, Canada.

Shink, D., Rosenblum, R., Kim, J.Y., and Stowe, K.G., 1992, "Development of Small Scale Flotation Cells and Its Application in Milling Operations", *Proc. 24th Annual Meeting of CMP*, Ottawa, p. 13.

CHAPTER 4 – RESULTS

4.1. Hydrodynamic properties

4.1.1. Reproducibility

At least three repeats were completed for each condition with the 95 % confidence interval (CI) calculated from the pooled estimate of the standard deviation. The reproducibility for froth height (bubble column) was the poorest compared to the other hydrodynamic measurements.

Table 4.1 summrizes the reproducibility for all the techniques (i.e., bubble column, Metso cell, and mini cell) showing absolute (abs) and relative (rel) values of the pooled standard deviation. On the figures, the 95% CI is the "error" bar.

4.2. Bubble column

4.2.1. Gas dispersion properties

Figures 4.1a & b show example bubble size distributions in the presence of single frothers (F150, pentanol, and F150, MIBC) and blends of the alcohols with low concentration of F150. The size distributions in the blends show a higher frequency of large bubbles (> ca. 1.3 mm) compared to the single frothers, as the sample images illustrate (Figure 4.1c).

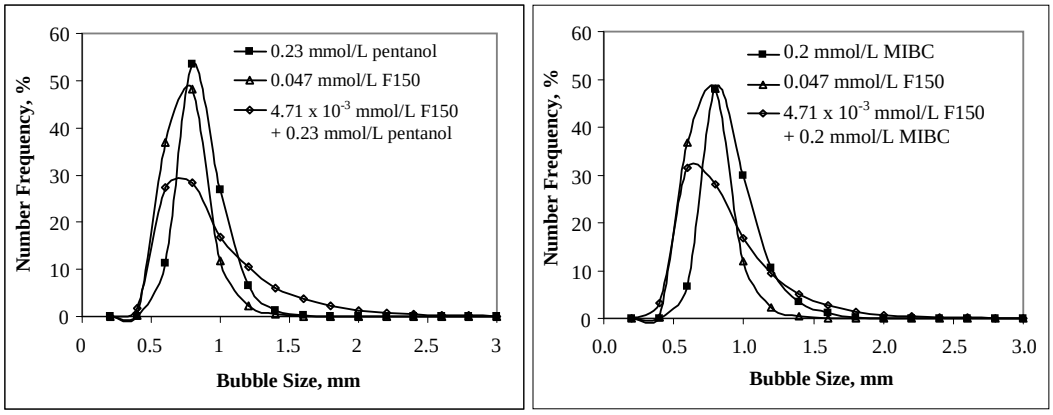

(a) (b)

0.047 mmol/L F150 0.23 mmol/L pentanol 0.2 mmol/L MIBC

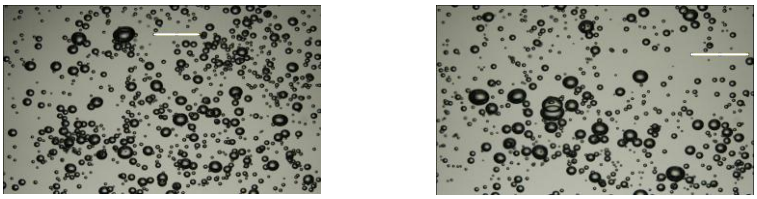

4.71 x 10^{-3} mmol/L F150 + 0.23 mmol/L pentanol

4.71 x 10^{-3} mmol/L F150 + 0.2 mmol/L MIBC

(c)

Figure 4.1: a) Bubble size distribution in the presence of F150-pentanol blend compared to the two frothers alone; b) Bubble size distribution in the presence of F150-MIBC blend compared to frothers alone and c) Corresponding example images. (Note: the white line on each image represents 1 cm)

Table 4.1. Reproduciblity of hydrodynamic properties

Parameter	**Pooled standard deviation**					
	Column		**Metso cell**		**Mini- cell**	
	abs‡	**rel*, %**	**abs**	**rel, %**	**abs**	**rel, %**
Bubble size	0.06 mm	3.7	0.11 mm		-	
Gas holdup	0.3 %	3.2	-		-	
Froth height	3.2 cm	11.2	-		-	
Overflow rate	9.4 g/min	3.6	-		6.4 g/min	2.1

‡ Refers to absolute pooled standard deviation
*Refers to pooled standard deviation divided by the mean value

Figure 4.2 shows the effect of increasing frother concentration on the Sauter mean diameter (d_{32}) for the seven frothers in Table 3.1 individually. For all, the bubble size decreases with increasing frother concentration until a certain concentration is reached (i.e., CCC), in accord with the literature. For each frother the minimum bubble size was ca. 0.8 mm. The results also confirm that F150 and PPG425 yield similar performance.

The trend in bubble size is mirrored by the gas holdup measurements (Figure 4.3). Gas holdup increases with increasing frother concentration, which corresponds to the decrease in bubble size. The relative position of each frother, gas holdup increasing from pentanol to F150/PPG425, is the same as the order of decreasing bubble size, and the same as reported by Azgomi et al. (2007). The notably lower increase in gas holdup with pentanol, e.g. compared to F150, is

because pentanol has markedly less effect on slowing bubble rise compared to F150 for equal sized bubbles (Acuna and Finch, 2008; Rafiei and Finch, 2009).

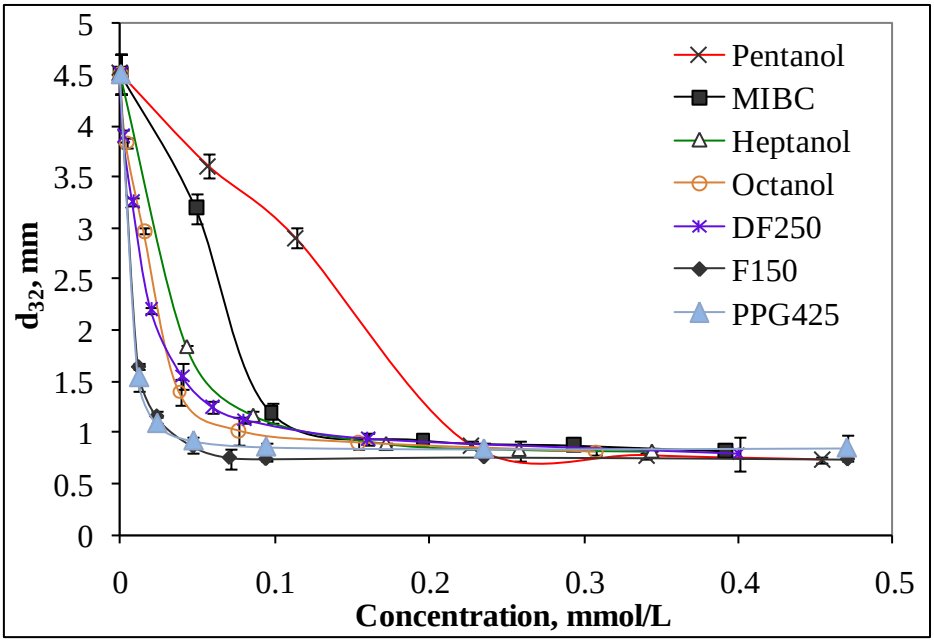

Figure 4.2: Bubble size in presence of the seven frothers individually

For the MIBC – F150 case, the effect on Sauter mean diameter and gas holdup compared to single frothers is shown in Figures 4.4 and 4.5, respectively. The three blends shown represent a fixed amount of F150, namely 1.18 x 10^{-3}, 2.35 x 10^{-3}, and 4.71 x 10^{-3} mmol/L (0.5, 1 and 2 ppm) added to MIBC. In the blends, the bubble size at zero MIBC concentration corresponds to F150 alone.

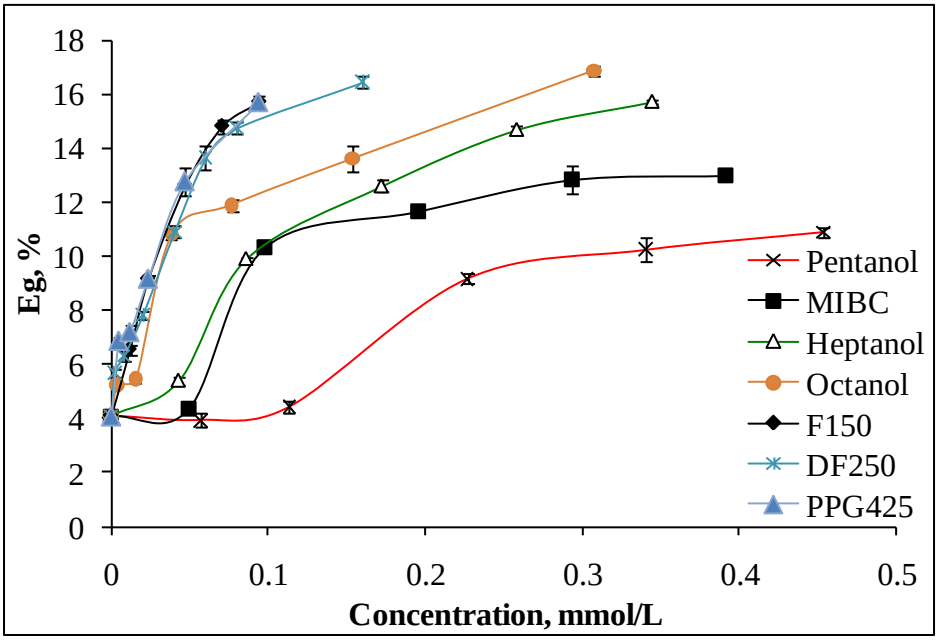

Figure 4.3: Gas holdup as function of concentration for the seven frothers individually

Figure 4.4 suggests the trend for the blends divides into two regions: concentrations below and above the CCC of MIBC. At concentrations lower than the MIBC CCC, the bubble size of the blend is reduced compared to MIBC alone. In contrast, at concentrations above the MIBC CCC the blend gives bubble size significantly larger (ca. 1.3 mm) than in presence of MIBC alone (ca. 0.8 mm). Figure 4.1 b, c also suggested this coarsening effect of the blend. Gas holdup (Figure 4.5) confirms the bubble size results, showing the complementary effects of the blend below the MIBC CCC (gas holdup increases compared to MIBC alone)) and above the MIBC CCC (gas holdup decreases compared to MIBC alone). Below and above the MIBC CCC there is a synergistic but opposite effect on bubble size.

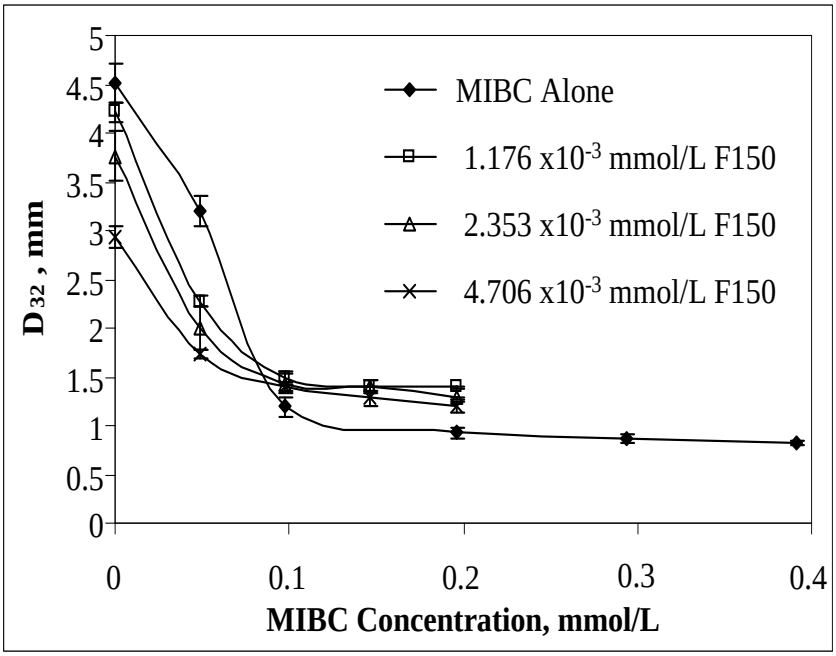

Figure 4.4: Effect of F150 – MIBC blends on bubble size compared to single frothers

The F150 – pentanol case follows the same behavior as for F150 – MIBC: compared to pentanol alone, the bubble size at concentrations lower than pentanol CCC is significantly smaller, and at concentrations greater than pentanol CCC the bubble size is significantly larger than for pentanol alone (the same 1.3 mm vs. 0.73 mm (for pentanol alone), Figure 4.6). The gas holdup for the F150 – pentanol blend supports the bubble size data at concentrations lower than pentanol CCC but above the gas holdup remains larger than for pentanol alone (Figure 4.7). The complication in the case of gas holdup with pentanol systems is because F150 probably has a more marked effect on reducing bubble rise velocity when added to pentanol compared to adding to MIBC (Rafiei and Finch, 2009). This will require more direct testing to confirm the effect of blends on bubble rise velocity which is beyond the scope of this study.

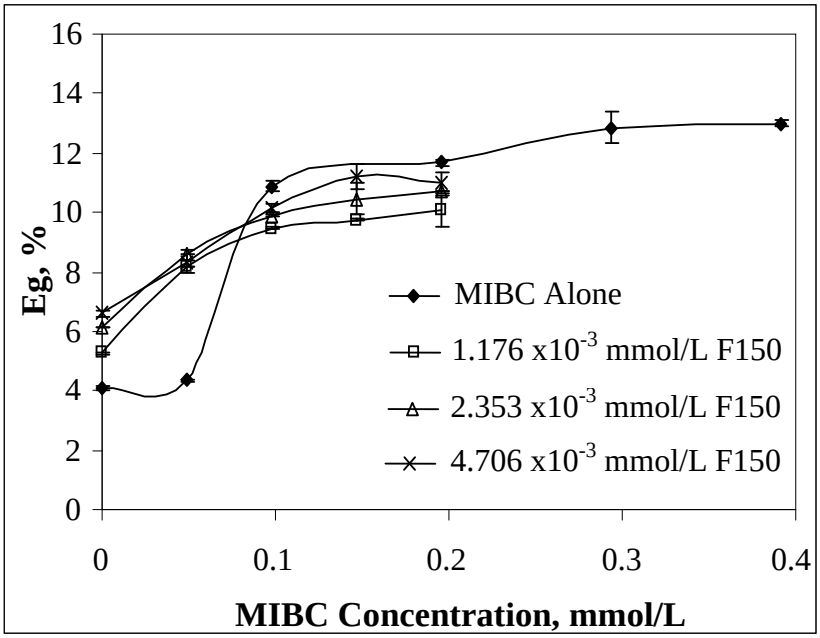

Figure 4.5: Effect of F150 – MIBC blends on gas holdup compared to single frothers

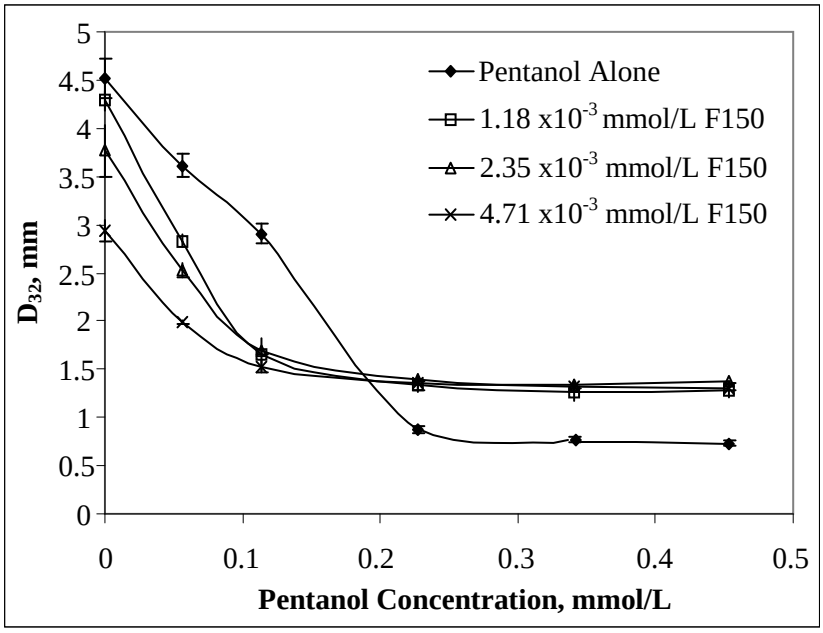

Figure 4.6: Effect of F150 – Pentanol blends on bubble size compared to single frothers

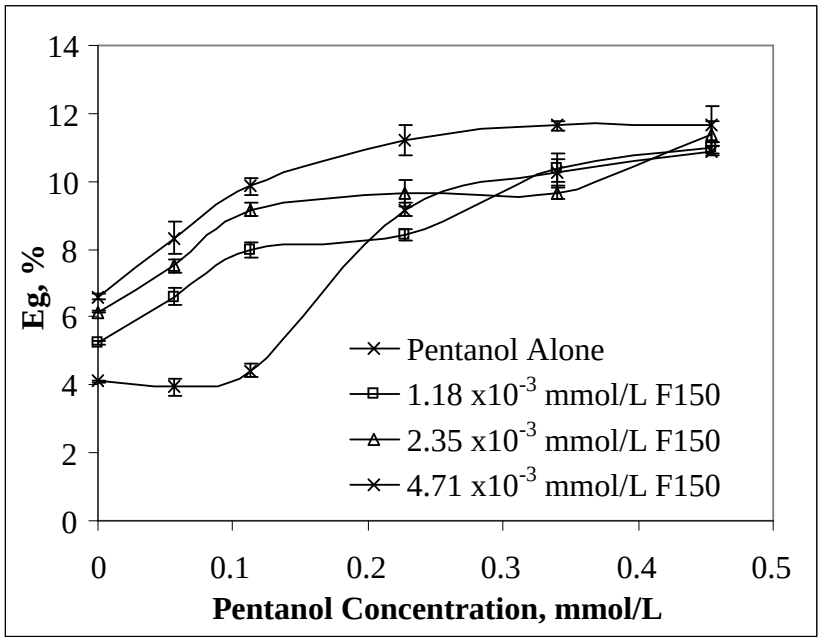

Figure 4.7: Effect of F150 – Pentanol blends on gas holdup compared to single frothers

Figure 4.8 illustrates the effect on bubble size of blending 4.71 x 10^{-3} mmol/L (2 ppm) PPG425 with pentanol compared to pentanol alone. The results are comparable to the F150 – pentanol blend: the minimum bubble size for 4.71 x 10^{-3} mmol/L (2 ppm) PPG425 – pentanol blend (ca. 1.3 mm) is significantly larger than in the presence of pentanol alone (ca. 0.73 mm).

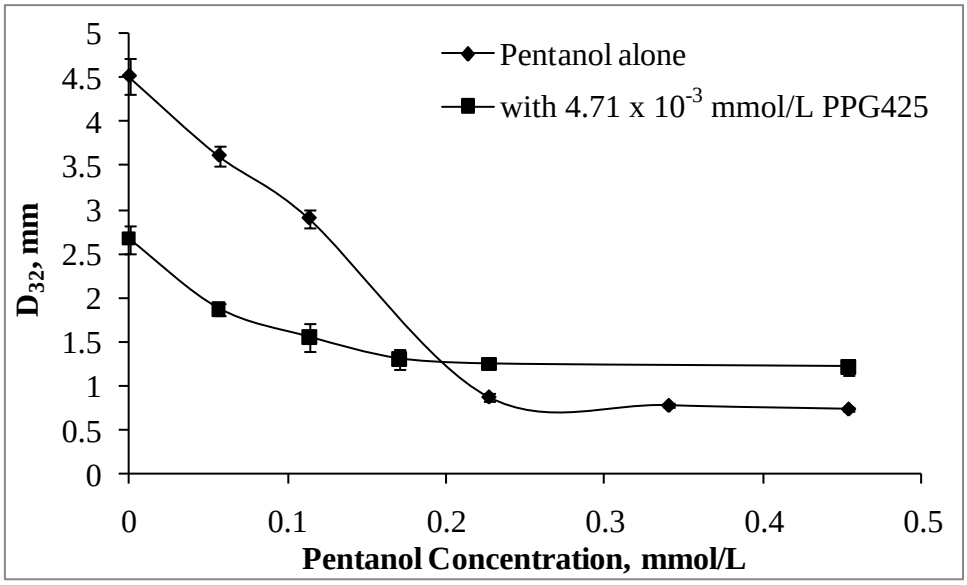

Figure 4.8: Effect of 4.71 x 10^{-3} mmol/L PPG425 – pentanol blend on bubble size compared to pentanol alone

Figures 4.9 – 4.12 show the effect on bubble size and gas holdup of higher concentrations of F150 (up to approximately half the concentration range in Figure 4.3) blends with 0.2 mmol/L (20 ppm) MIBC and 0.23 mmol/L (20 ppm) pentanol compared to the F150 alone. (Note, bubble size and gas holdup in alcohol alone is represented at 0 mmol/L F150.) Figures 4.9 and 4.11 show the bubble size increases upon addition of low F150 concentrations to MIBC and pentanol as reported above. With the further increase in F150 concentration, bubble size in the blend decreases until it returns to the same value as in F150 and MIBC alone. The gas holdup (Figures 4.10 and 4.12) presented a surprise: at the F150 concentrations greater than ca. 0.005 mmol/L (2 ppm) the blend gas holdup is far greater than for F150 alone, rather than approaching the same value in F150 as the Sauter mean diameter data do. Based on prior experience reconciling gas holdup and bubble size data, the reason for the significant increase in gas holdup

implies a significant reduction in the bubble rising velocity (Rafiei and Finch, 2009). This needs to be tested to confirm, but, as noted this is beyond the scope of the thesis.

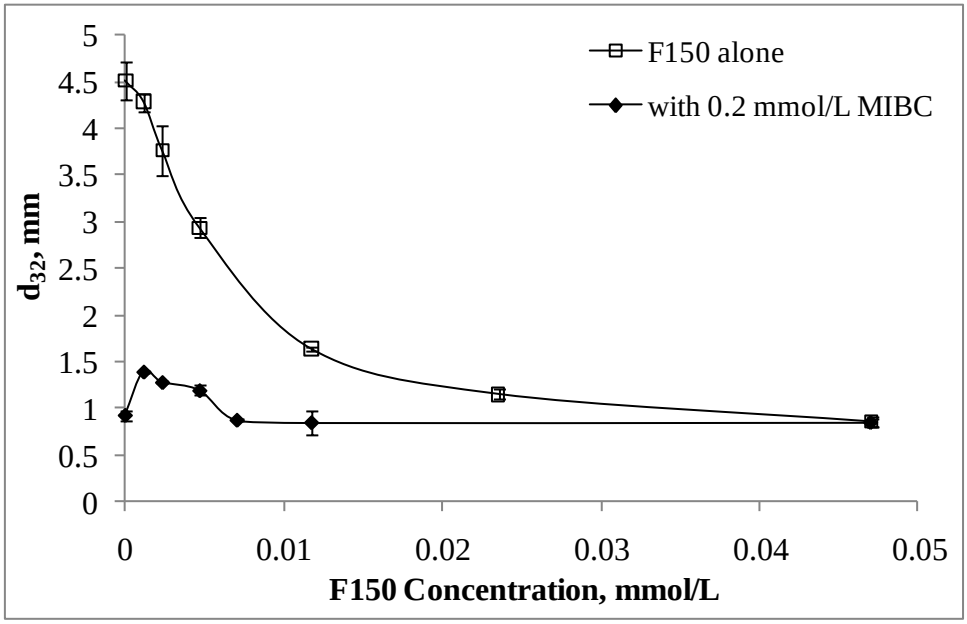

Figure 4.9: Effect of 0.2 mmol/L MIBC blend with F150 on bubble size compared to F150 alone

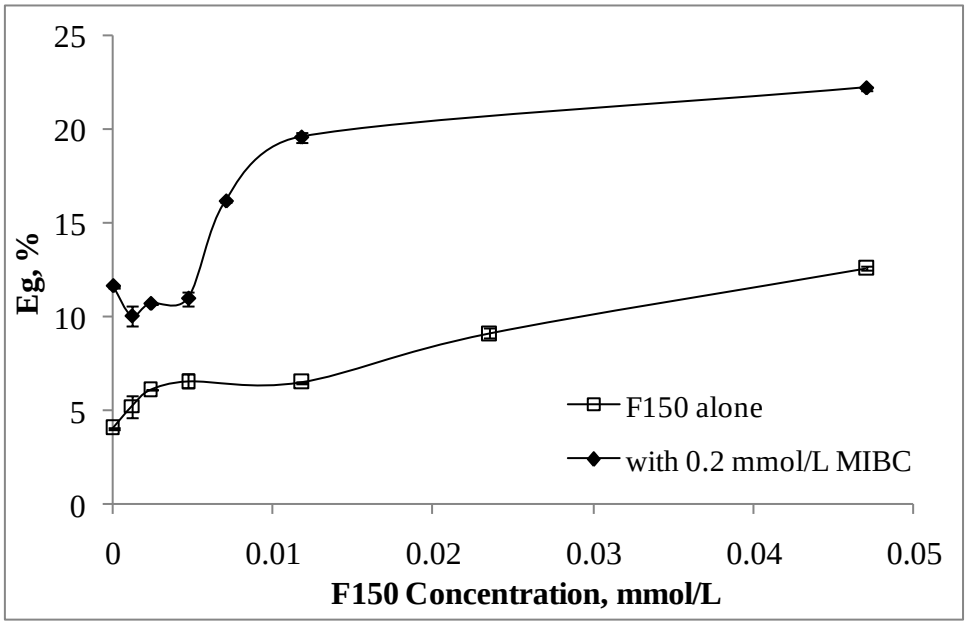

Figure 4.10: Effect of 0.2 mmol/L MIBC blend with F150 on gas holdup compared to F150 alone

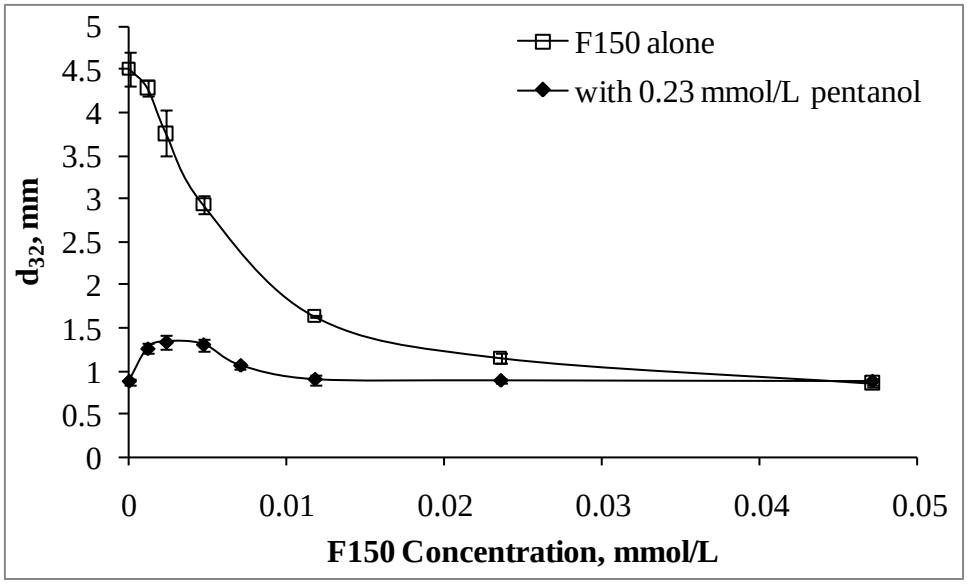

Figure 4.11: Effect of 0.23 mmol/L pentanol blend with F150 on bubble size compared to F150 alone

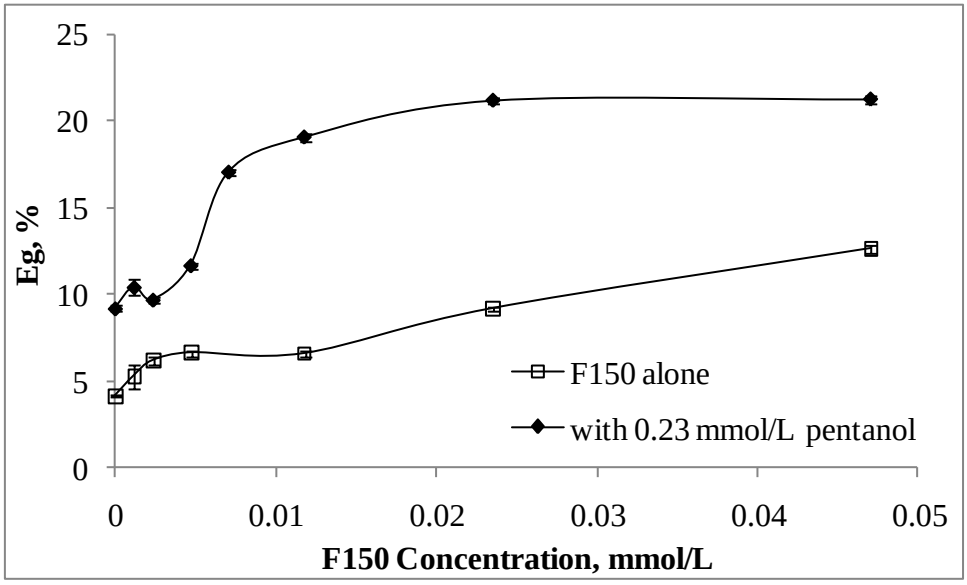

Figure 4.12: Effect of 0.23 mmol/L pentanol blend with F150 on gas holdup compared to F150 alone

Figures 4.13 – 4.16 depict the effect of 2 x 10^{-3} mmol/L (0.5 ppm) DF250 blends with pentanol and MIBC on bubble size and gas holdup. The blends with DF250 follow the same trend as the F150 blends: Figures 4.13 and 4.15 show that blends reduce the bubble size below the alcohol frother CCC compared to alcohol frother alone and increase bubble size above the alcohol frother CCC. The magnitude of the effect above the alcohol CCC is less than in the F150 case: the minimum bubble size in DF250 – pentanol blend is ca. 0.9 mm rather than 1.3 mm for pentanol alone (Figure 4.15) and, in the DF250 – MIBC blend the minimum is ca. 1.1 mm (Figure 4.13). The larger impact of F150 compared to DF250 in the blend is in accord with their relative "strength" (e.g. Moyo et al. (2007); Azgomi et al. (2007)).

Gas holdup measurements for the DF250 – MIBC blend support the bubble size data: below the MIBC CCC gas holdup in the blend is larger than that for MIBC alone and above the MIBC CCC it becomes lower than for MIBC alone. The gas holdup for the DF250 – pentanol blend supports the bubble size data at concentrations lower than pentanol CCC but above the pentanol CCC the gas holdup remains larger than for pentanol alone (Figure 4.16), for reasons discussed earlier in case of F150 blends.

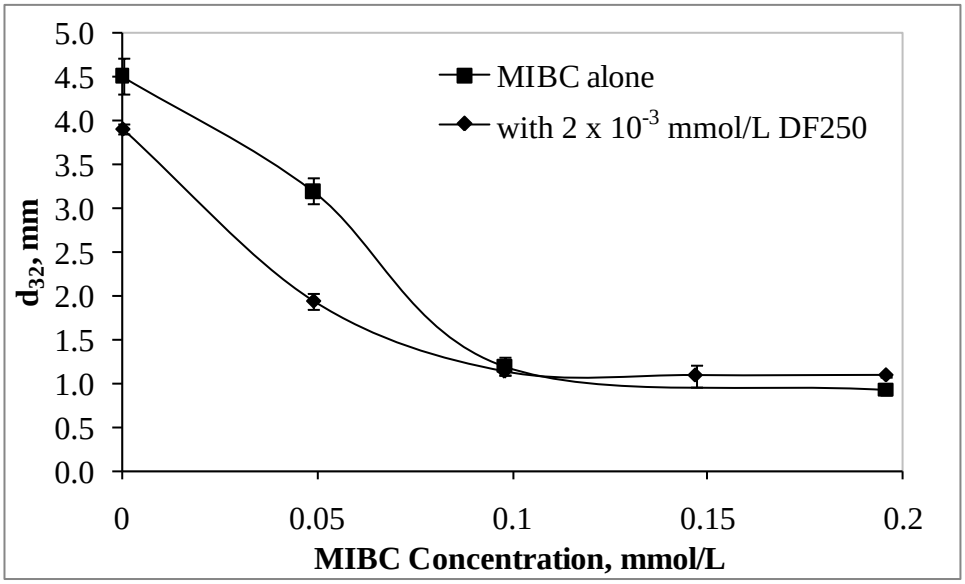

Figure 4.13: Effect of DF250 – MIBC blend on bubble size compared to MIBC alone

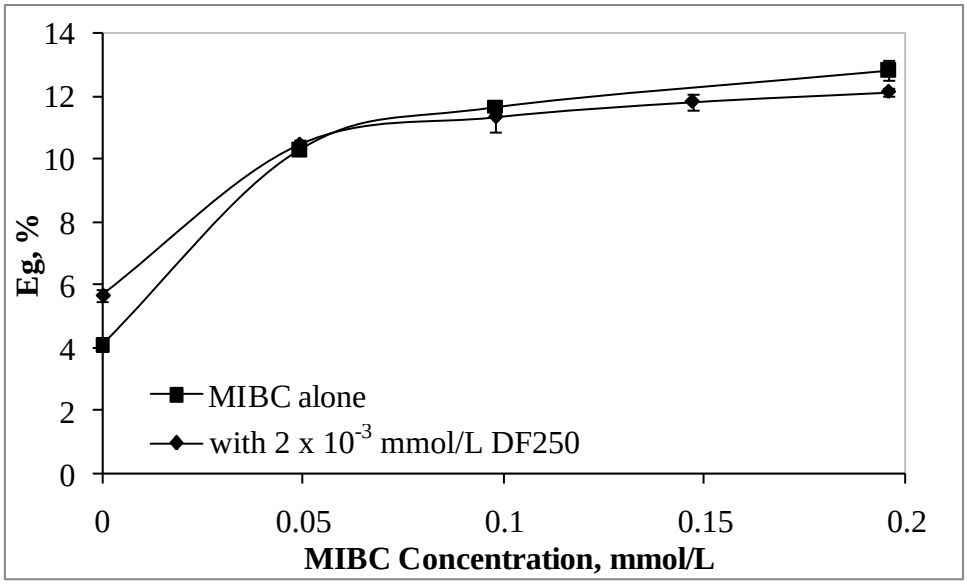

Figure 4.14: Effect of DF250 – MIBC blend on gas holdup compared to MIBC alone

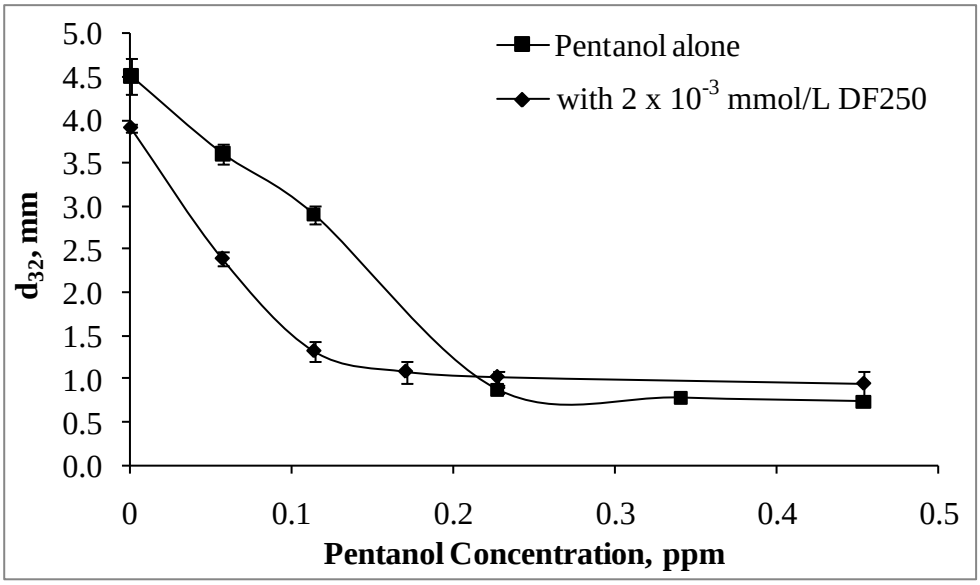

Figure 4.15: Effect of DF250 – pentanol blend on bubble size compared to pentanol alone

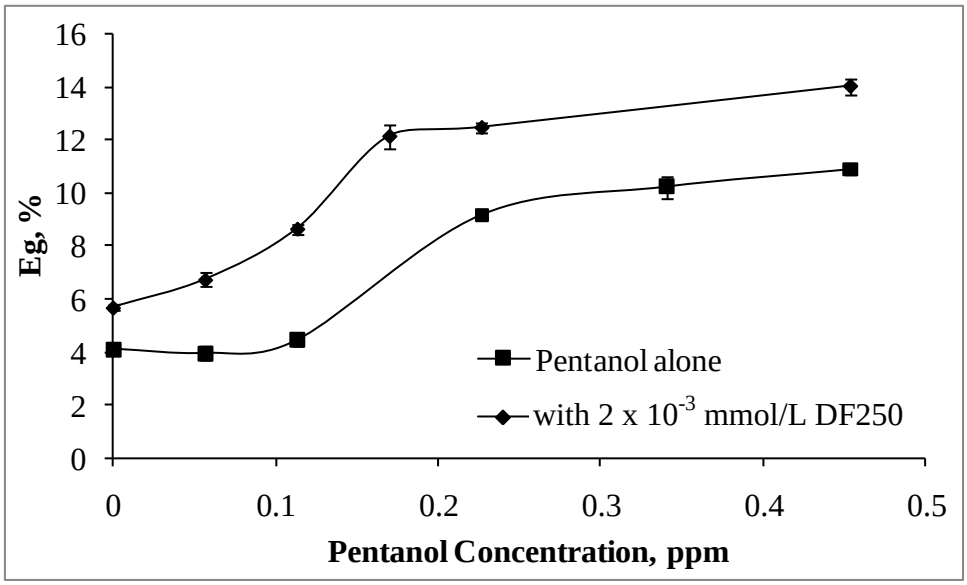

Figure 4.16: Effect of DF250 – pentanol blend on gas holdup compared to pentanol alone

Figures 4.17 – 4.20 show the effect of increasing DF250 concentration in blends with 0.23 mmol/L pentanol (20 ppm) and 0.2 mmol/L MIBC (20 ppm) on bubble size and gas holdup compared to single frothers. As with the F150 blends, Figures 4.18 and 4.19 show that bubble size increases by the addition of low DF250 concentrations compared to the alcohols alone and with continued increase in DF250 concentration bubble size decreases until it returns to the value in the presence of DF250 alone. The effect on gas holdup (Figures 4.18 and 4.20) also mirrors that for the blends with F150: gas holdup increases significantly compared to DF250 alone suggesting a significant impact of alcohol – polyglycol blends in slowing bubble rise.

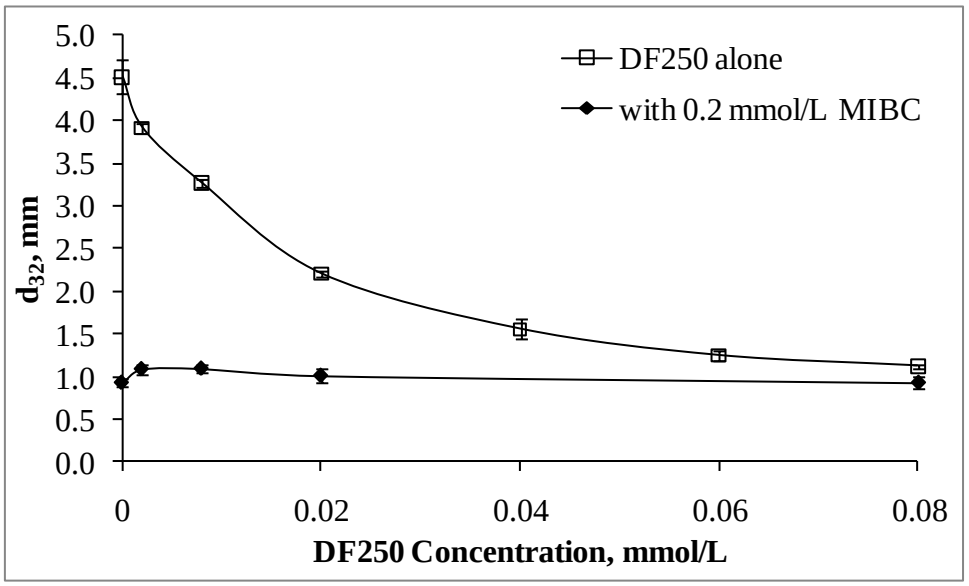

Figure 4.17: Effect of 0.2 mmol/L MIBC blend with DF250 on bubble size compared to DF250 alone

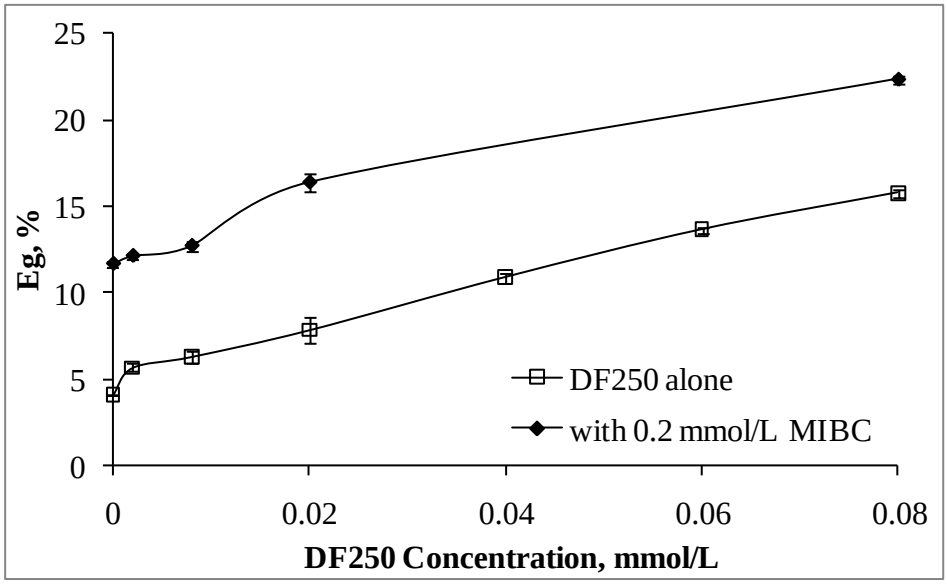

Figure 4.18: Effect of 0.2 mmol/L MIBC blend with DF250 on gas holdup compared to DF250 alone

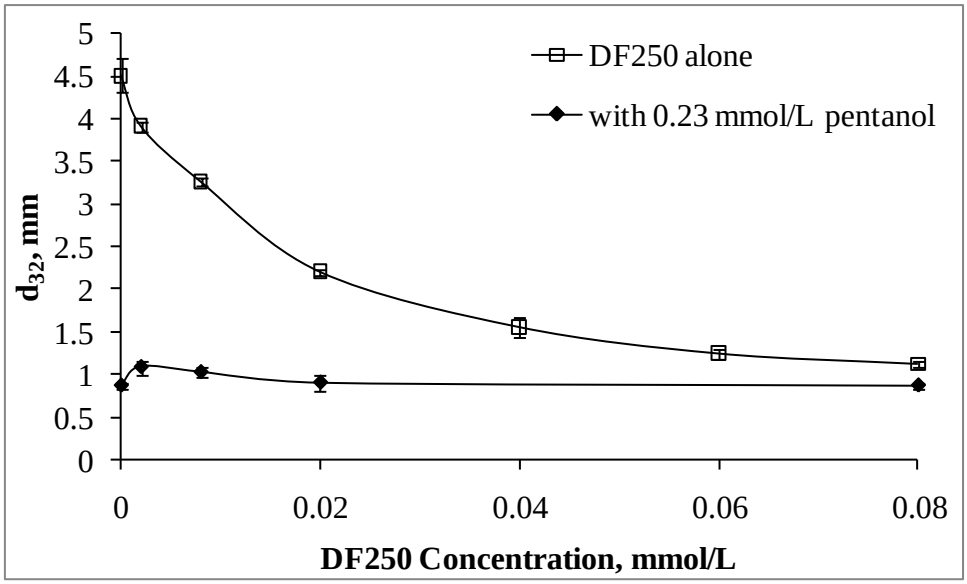

Figure 4.19: Effect of 0.23 mmol/L Pentanol blend with DF250 on bubble size compared to DF250 alone

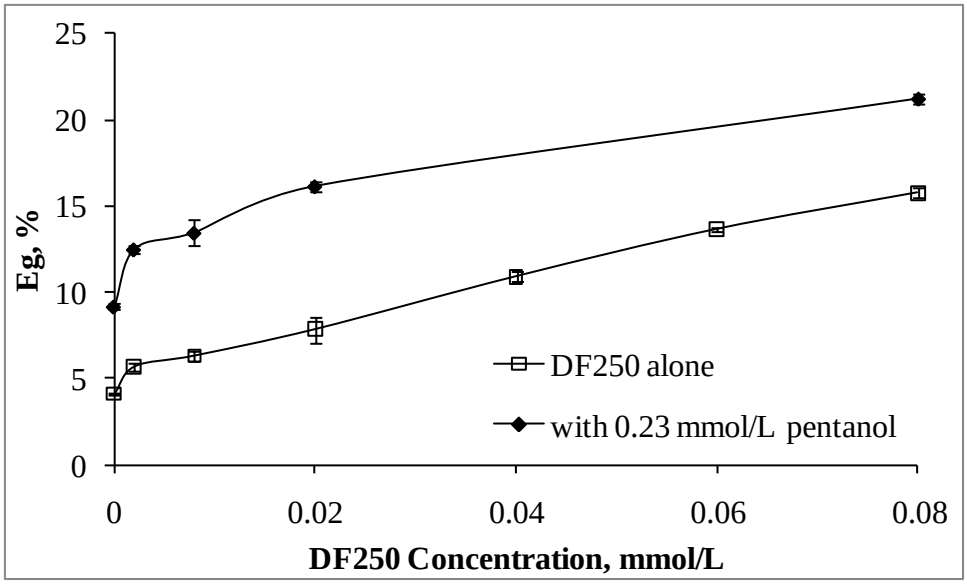

Figure 4.20: Effect of 0.23 mmol/L Pentanol blend with DF250 on gas holdup compared to DF250 alone

To examine if this effect of frother blending on bubble size and gas holdup is limited to frother blends from different families (i.e., alcohol with polyglycol) a "strong" frother from the alcohol family, octanol, was selected based on its effect on bubble size (Figure 4.2) and gas holdup (Figure 4.3). Octanol was blended with 0.23 mml/L (20 ppm) pentanol. As shown in Figure 4.21, the trend in bubble size for the octanol – 0.23 mmol/L pentanol blend follows that for polyglycol – alcohol blends: bubble size in pentanol only (ca. 0.73 mm) initially increasing with increasing octanol concentration in the blend reaching ca. 1.4 mm in the presence of 0.04 mmol/L (5 ppm) octanol (Figure 4.21) but subsequently decreasing to reach the same bubble size as for octanol alone. The difference from the polyglycols is in the gas holdup: in this case gas holdup in the octanol – 0.23 mmol/L pentanol blend is closer to that for octanol alone (Figure 4.22).

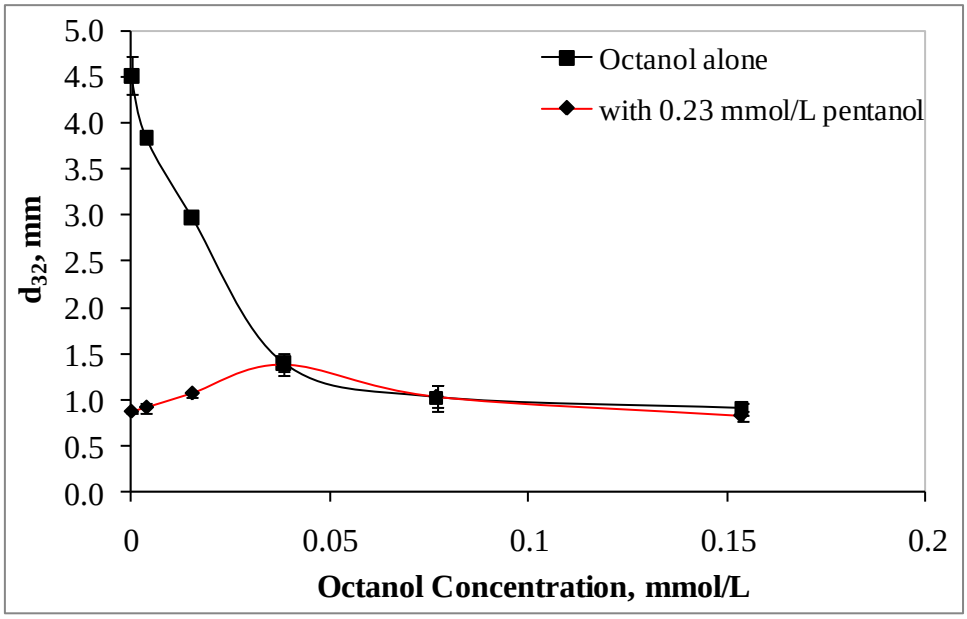

Figure 4.21: Effect of 0.23 mmol/L pentanol blend with octanol on bubble size compared to octanol alone

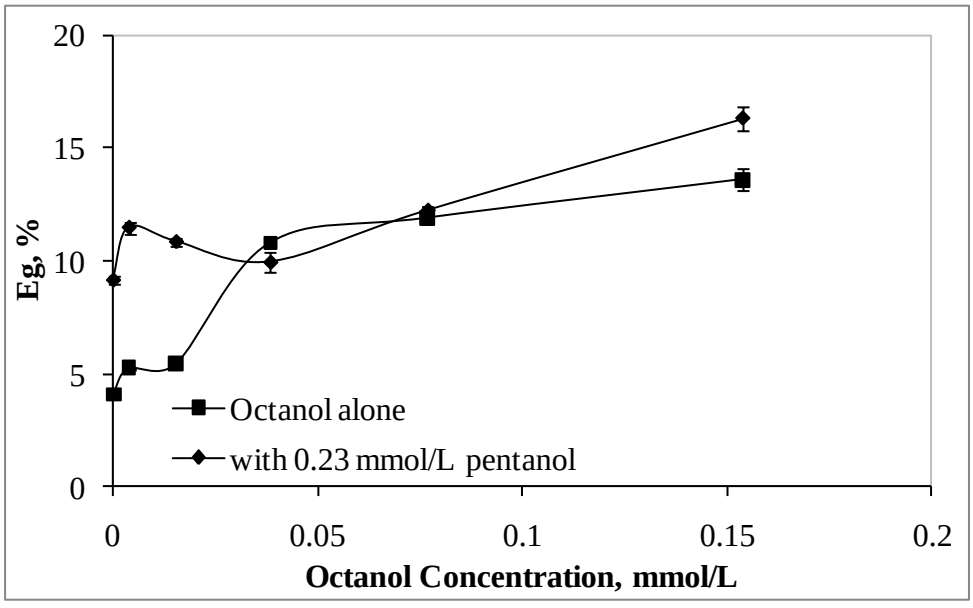

Figure 4.22: Effect of 0.23 mmol/L pentanol blend with octanol on gas holdup compared to octanol alone

4.2.2. Froth properties

For froth properties, the F150 – pentanol blend was explored as the "extreme" case, i.e., "strongest" with "weakest" frother.

4.2.2.1. Froth height

Froth height in presence of single frothers and F150 – pentanol blends is recorded in Figure 4.23. Froth height in the presence of F150 alone increases with increasing concentration reaching a plateau at ca. 33 cm at F150 > ca. 0.05 mmol/L (> 20 ppm). For pentanol, froth height increases to plateau at ca. 3.5 cm. The blends comprise fixed concentration of F150 with increasing pentanol concentration; note that F150 concentrations in the blend are low, within the circle on the figure. The blends significantly increase the froth height compared to that attained by the single frothers. For example at 0.23 mmol/L (20 ppm) pentanol, the presence of only 1.18 x 10^{-3} mmol/L (0.5 ppm) F150 increased froth height from less than 5 cm for either frother alone to more than 15 cm (i.e., significantly more than the sum of their individual heights) and increasing F150 in the blend from 1.18 x 10^{-3} mmol/L to 4.71 x 10^{-3} mmol/L (0.5 ppm to 2 ppm) significantly further increased froth height.

The hypothesis that frother blends can give some independent control over the two frother functions, bubble size reduction and froth building, is explored in Figure 4.24. The Figure shows that increasing F150 concentration from 1.18 x10^{-3}

mmol/L to 4.71×10^{-3} mmol/L (0.5 ppm to 2 ppm) in the presence of 0.17 mmol/L (15 ppm) pentanol the bubble size remained constant whereas the froth height nearly doubled, from 10 to 18 cm. While testing the hypothesis was an objective, the unexpected effect of blends on increasing bubble size above the alcohol CCC is a confounding factor and came to dominate the investigation.

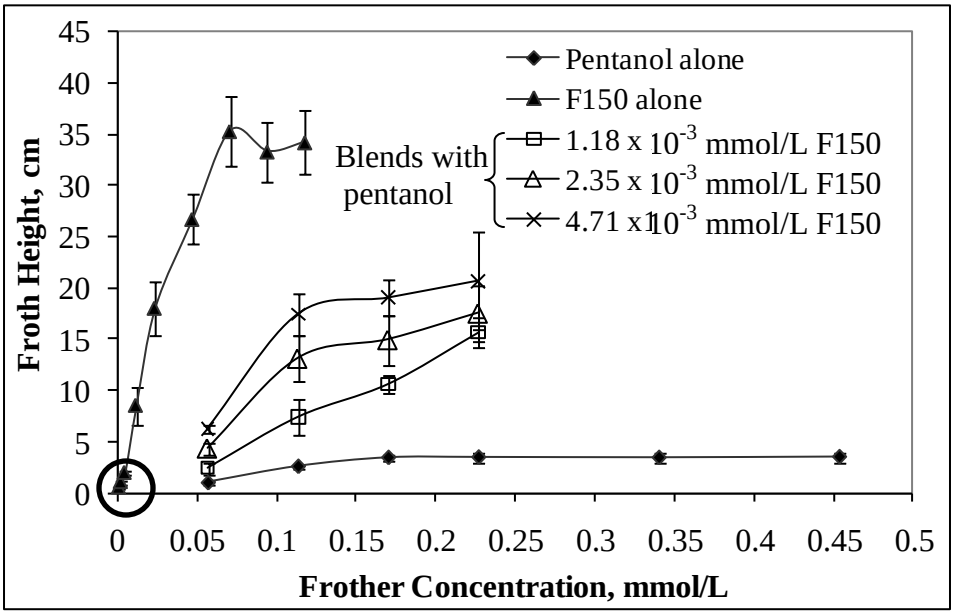

Figure 4.23: Effect of F150 – Pentanol blends on froth height compared to single frothers

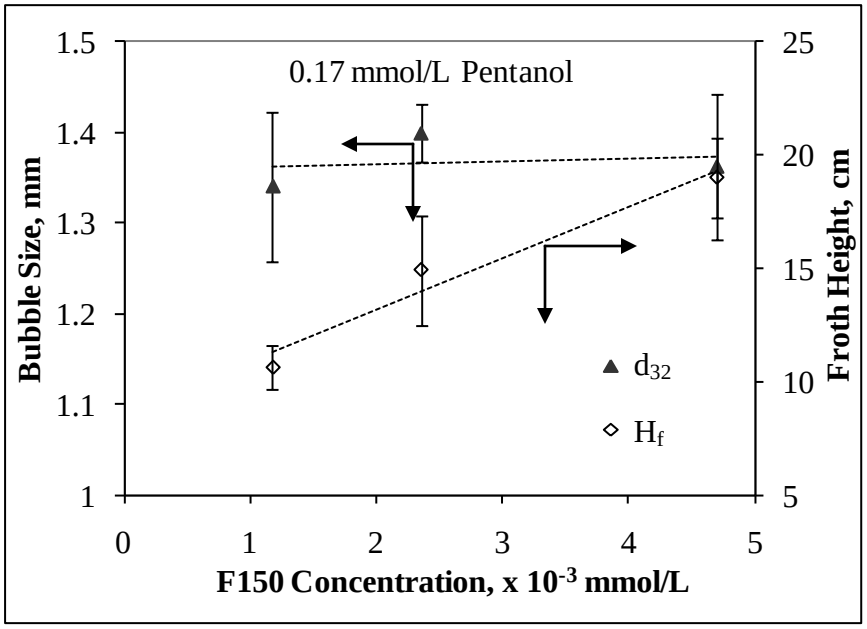

Figure 4.24: Illustration of independent control over the two frother functions: trend in bubble size is independent of F150 concentration but trend in froth height is increasing (dashed line indicates trend only)

4.2.2.2. Water overflow rate

Froth height proved to be the metric with the greatest error (uncertainty). As a measure of froth properties, therefore, water overflow rate was included. Water overflow rate could not be measured reliably for pentanol or F150 alone in the concentration range used for the blends in Figure 4.23 due to the low equilibrium froth height. (Attempts to adjust the froth depth set point below 2 cm to increase water overflow rate caused even more uncontrollably large fluctuation in the rate.) For blends, however, Figure 4.25 shows significant water recovery. The blends consisted of 4.71 x10^{-3} mmol/L (2 ppm) F150 with 0.17 mmol/L and 0.23 mmol/L (15 ppm and 20 ppm) pentanol and overflow was sufficient to track as a function

of froth depth. It is evident that water transport for the blends greatly exceeded that of either frother alone and increased rapidly with decreasing froth depth. The action of the blend in both froth height and overflow rate is reminiscent of the froth stabilizing effect of particles.

Figure 4.26 shows water overflow rate for F150 alone and in a blend with 0.23 mmol/L (20 ppm) pentanol. The blend always exceeded the overflow rate for F150 alone (recall 0.23 mmol/L pentanol gave no overflow at 5 cm froth depth), especially at low F150 dosage: e.g. at 1.18×10^{-3} mmol/L (5ppm) F150 alone overflow rate is ca. 40 g/min, increasing to ca. 200 g/min in the blend. At F150 concentration up to 0.094 mmol/L (40 ppm) in the blend the synergy effect decreases (Figure 4.26): the water overflow rate reached in F150 alone, ca. 410 g/min, is close to that in the blend, ca. 470 g/min. This result implies that blend effect decreases with increasing the concentration of the stronger frother in the blend, as shown in the bubble size data.

Figure 4.27 tests the hypothesis of independent control over the two frother functions, this time using overflow rate. The Figure shows that increasing F150 concentration in the blend from 1.18×10^{-3} mmol/L (0.5 ppm) to 4.71mmol/L (2 ppm) in the presence of 0.17×10^{-3} mmol/L (15 ppm) pentanol did not change the bubble size (ca. 1.3 mm) while water overflow rate nearly doubles, increasing from ca. 13 to 24 g/min.

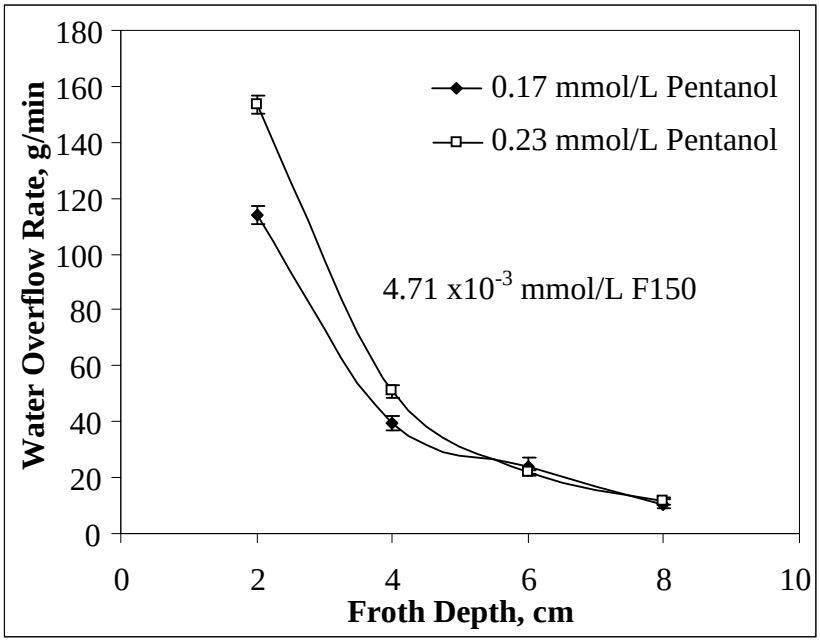

Figure 4.25: Effect of 4.71 x10^{-3} mmol/L (2 ppm) F150 – Pentanol blends on water overflow rate as function of froth depth (Note no water overflow for single frothers at these concentrations)

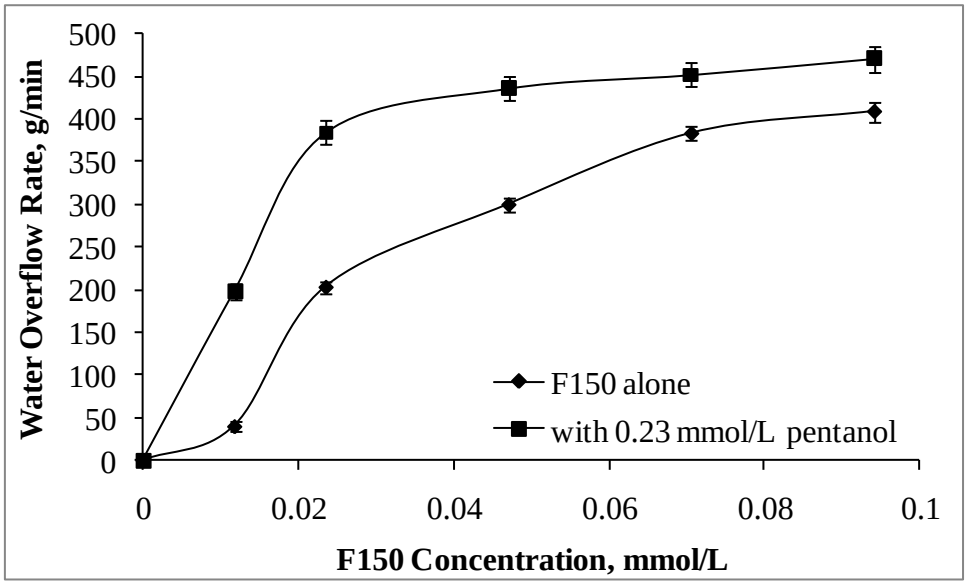

Figure 4.26: Effect of 0.23 mmol/L pentanol blend with F150 on water overflow rate compared to F150 alone at 5 cm froth depth

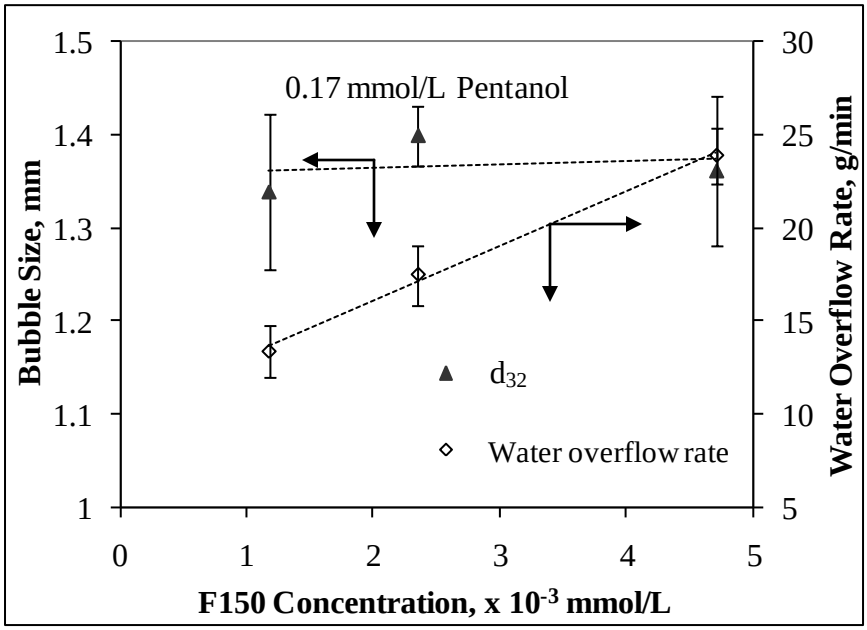

Figure 4.27: Illustration of independent control over bubble size and water overflow rate at froth depth = 5 cm (dashed lines indicate trend only)

4.3. Bubble size in 0.8 m^3 Metso RCS™ mechanical cell

These tests were included to answer whether the blend effect on bubble size evident in the bubble column is replicated in the more realistic (from a flotation perspective) mechanical cell. As in the froth properties case, tests were limited to the F150 – pentanol blend.

Figure 4.28 shows the effect of increasing frother concentration on the bubble size for F150 and pentanol individually: the bubble size decreases with increasing frother concentration until the CCC is reached.

The effect of F150 – pentanol blends on bubble size compared to single frothers is shown in Figure 4.29. The three blends represent a fixed amount of F150, 1.18 x 10^{-3}, 2.35 x 10^{-3}, and 4.71 x 10^{-3} mmol/L (0.5, 1 and 2 ppm), added

to pentanol. In the blends, the bubble size at zero pentanol concentration corresponds to F150 alone.

As seen in Figure 4.29, the trend for the blends follows that in the column (Figure 4.6): at concentrations lower than the pentanol CCC, the bubble size in the blend is reduced compared to pentanol alone, and at concentrations above the pentanol CCC the blend gives a significantly larger bubble size (ca. 1.2 mm - 1.3 mm) than for pentanol alone (ca. 1.0 mm). That is, both below and above the pentanol CCC there is a synergistic but opposite effect on bubble size.

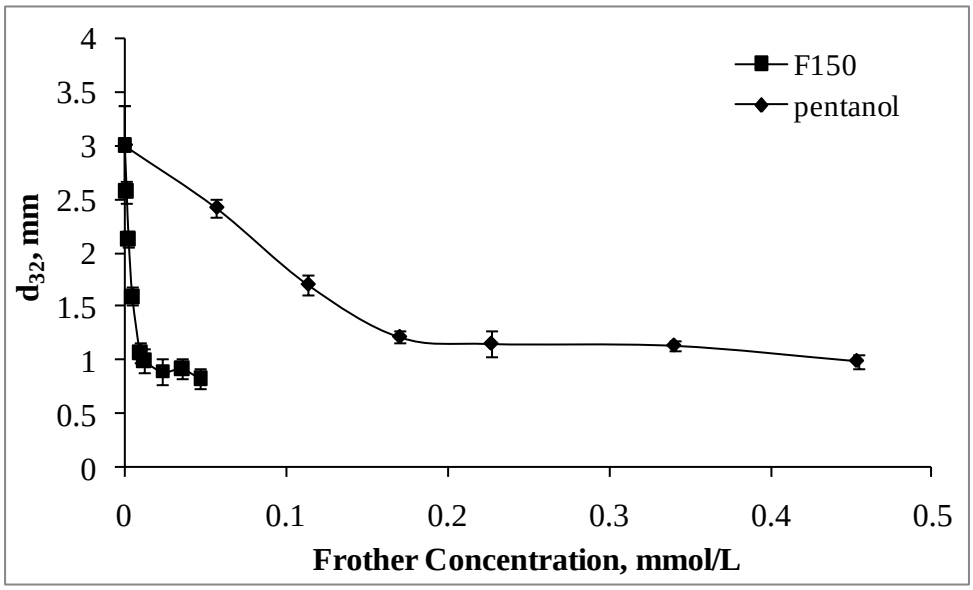

Figure 4.28: Bubble size in presence of the pentanol and F150 individually in the Metso cell (J_g = 0.5 cm/s)

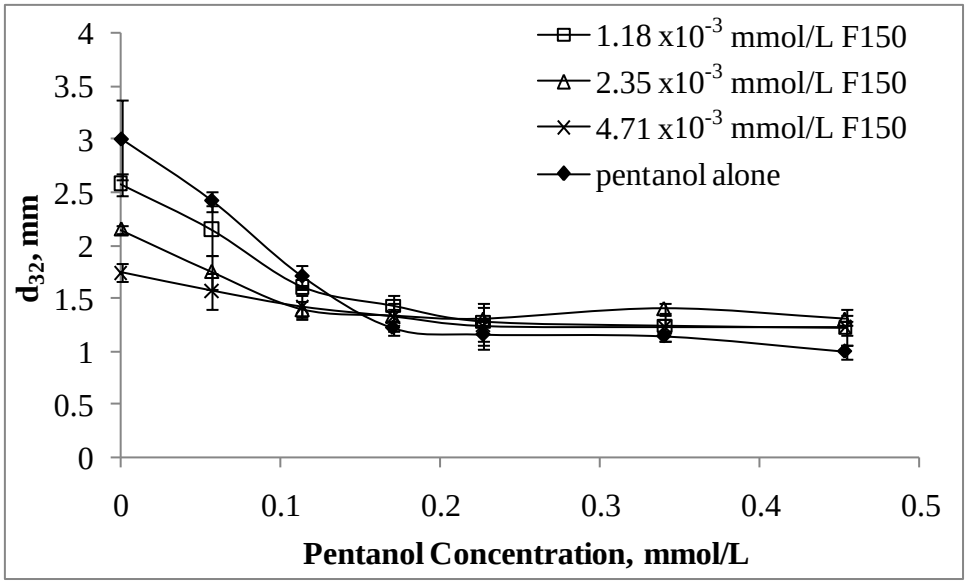

Figure 4.29: Effect of F150 – pentanol blends on bubble size compared to single frothers in the Metso cell (J_g = 0.5 cm/s)

4.4. Water overflow rate in mini-mechanical cell

Overflow rate for F150 and pentanol alone at the concentrations of interest in the blend could not be reliably measured in the bubble column. The mini-cell, however, proved more amenable. Figure 4.30 shows the effect of increasing frother concentration on the water overflow rate for four frothers individually. It is evident that water overflow rate increases with increasing frother concentration until a certain concentration when it plateaus. The order, pentanol to PPG425 (F150) follows that for decreasing bubble size (Figure 4.2) and agrees with Zhang et al. (2009).

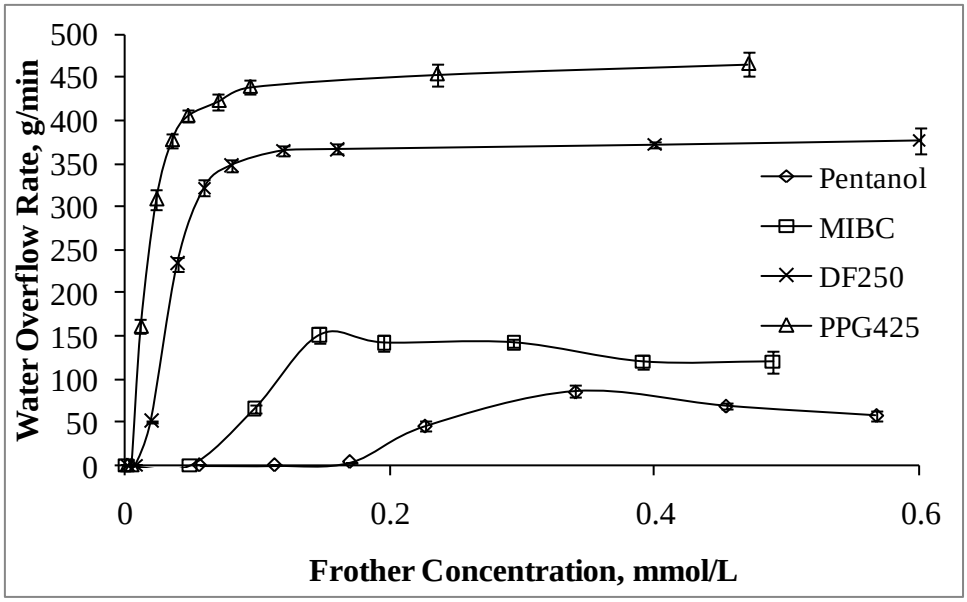

Figure 4.30: Water overflow rate for four frothers alone

The effect of PPG425 – MIBC blends compared to single frothers is shown in Figure 4.31. The three blends represent a fixed amount of PPG425, namely 1.18×10^{-3}, 2.35×10^{-3}, and 4.71×10^{-3} mmol/L (0.5, 1 and 2 ppm), added to MIBC. In the blends, the water overflow rate at zero MIBC concentration corresponds to PPG425 alone. The blends significantly increased the water overflow rate compared to that attained by the single frothers. For example, water overflow rate increased from ca. 150 g/min for MIBC alone to ca. 300 g/min with the addition of 4.71×10^{-3} mmol/L (2 ppm) PPG425, which on its own generated no overflow at this concentration. Increasing PPG425 concentration in the blend increased overflow rate to approach that in 0.1 mmol/L (40 ppm) PPG425 alone (Figure 4.30).

As with MIBC, water overflow rate with PPG425 – pentanol blends increases, from < 100 g/min for pentanol alone it reached 400 g/min in the presence of 4.71 x 10^{-3} mmol/L (2 ppm) PPG425, which alone gave no overflow. Figure 4.32 depicts that at sufficiently high PPG425 concentration in the blend (i.e., 4.71 x 10^{-2} mmol/L (20 ppm)) water overflow rate becomes close to PPG425 alone (about 400 g/min), which suggests that PPG425 dominates at high concentrations.

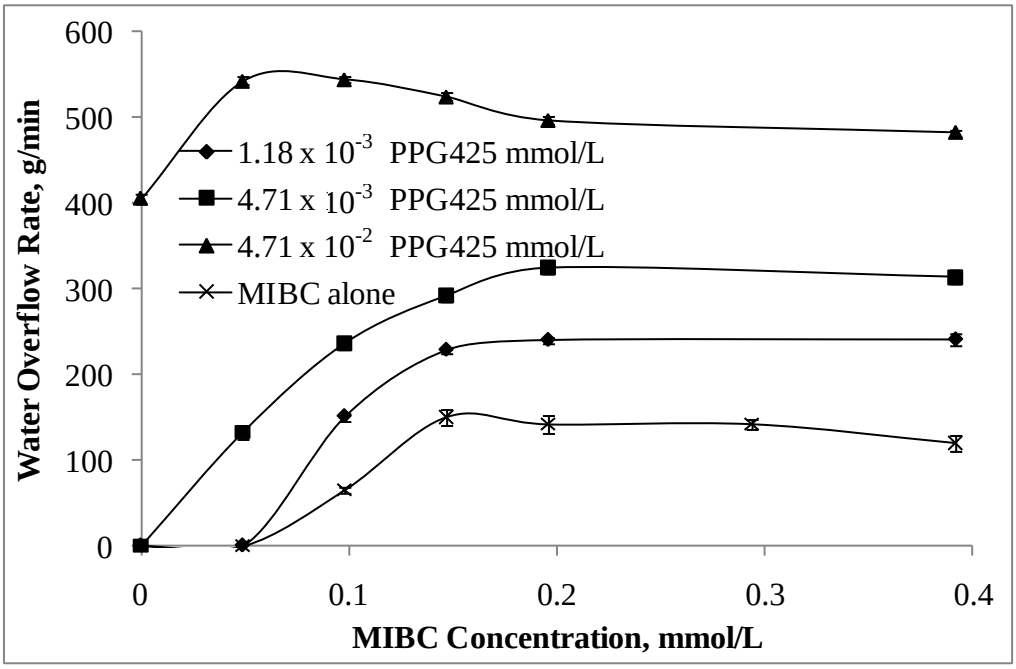

Figure 4.31: Effect of PPG425 – MIBC blends on water overflow rate compared to single frothers

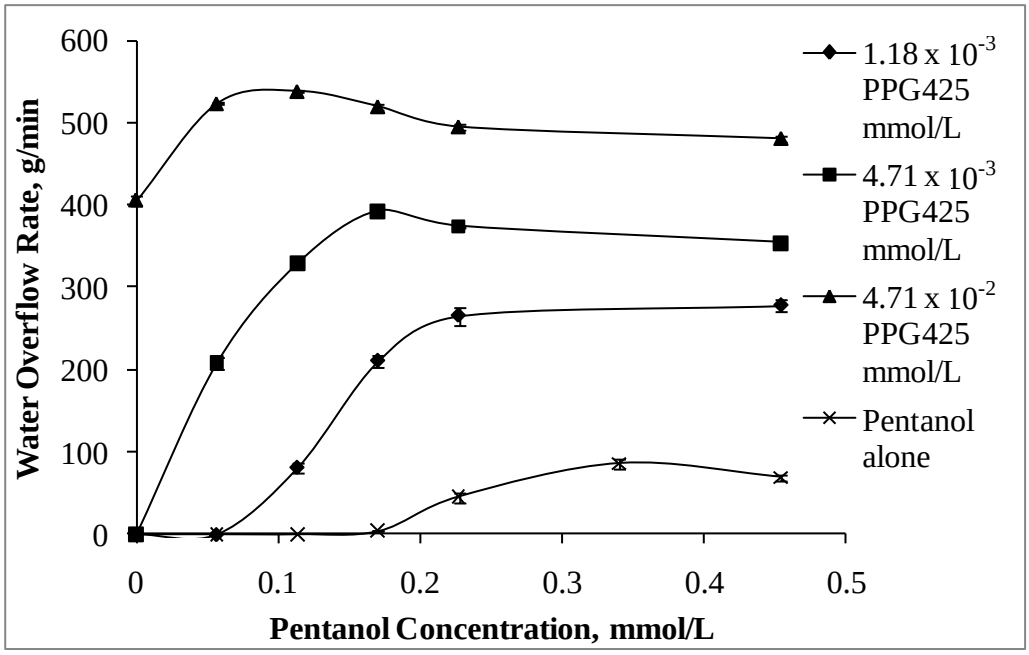

Figure 4.32: Effect of PPG425 – Pentanol blends on water overflow rate compared to single frothers

Figures 4.33 – 4.34 show that DF250 blends with MIBC and with pentanol follow the same trend as their blends with PPG425: water overflow rate increases with addition of the two lowest DF250 concentration which alone produce no overflow, rising to that achieved in high concentration of DF250 alone (> 0.1 mmol/L, Figure 4.30). In general, these overflow results correspond well to the bubble column overflow tests, the mini-cell setup providing more extensive, and reliable, data.

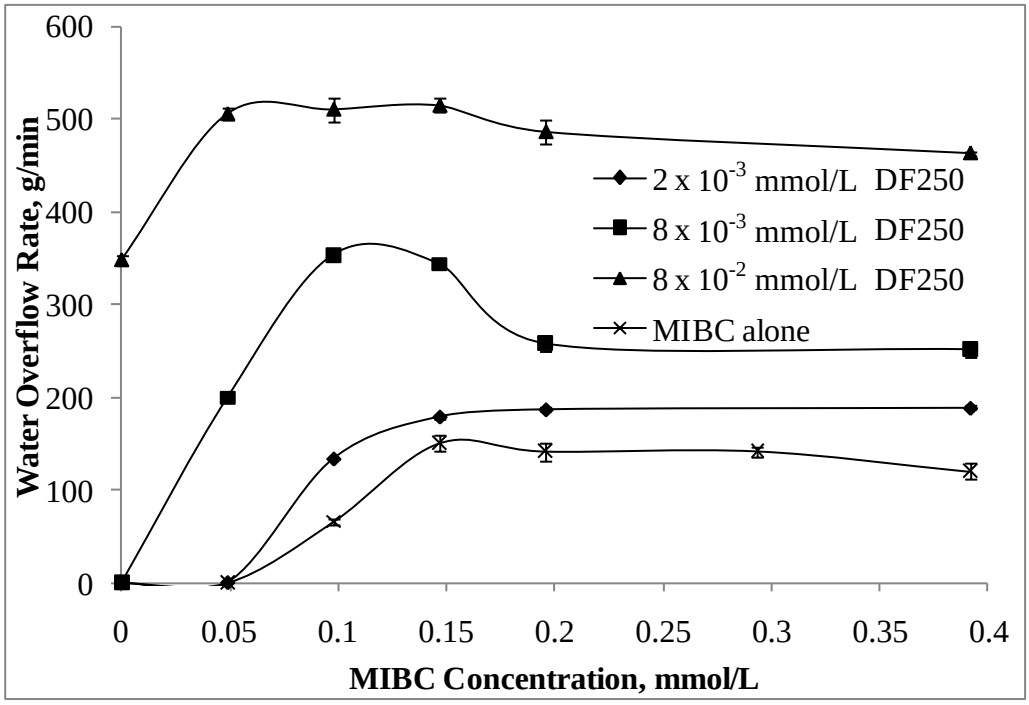

Figure 4.33: Effect of DF250 – MIBC blends on water overflow rate compared to single frothers

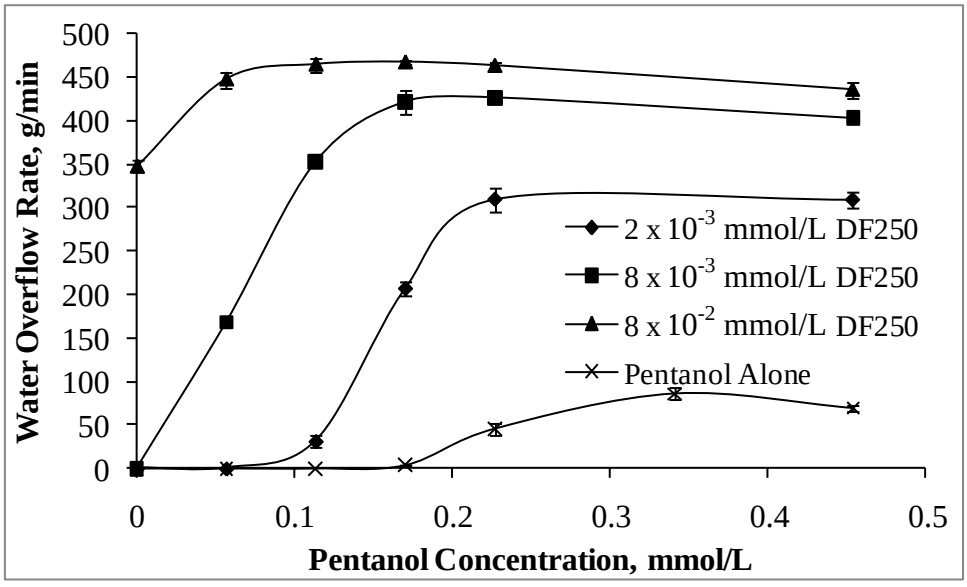

Figure 4.34: Effect of DF250 – pentanol blends on water overflow rate compared to single frothers

4.5. Surface tension

Surface tension measurements for single frothers and F150 – pentanol blends (i.e., strongest – weakest frother blend) are shown in Figures 4.35 and 4.36, respectively. Figure 4.35 shows that pentanol has little effect on decreasing surface tension up to a concentration of 0.454 mmol/L (40 ppm), whereas F150 reduces surface tension by about 10 mN/m at about 0.094 mmol/L (40 ppm).

Figure 4.36 shows that the effect of F150 – pentanol blends on surface tension is comparable to F150 alone at concentrations equal to its fraction in the blend. For example, the blend containing 4.71 x 10^{-3} mmol/L F150 has a surface tension ca. 70.4 mN/m, which is essentially the same (70.6 mN/m) for this concentration of F150 alone.

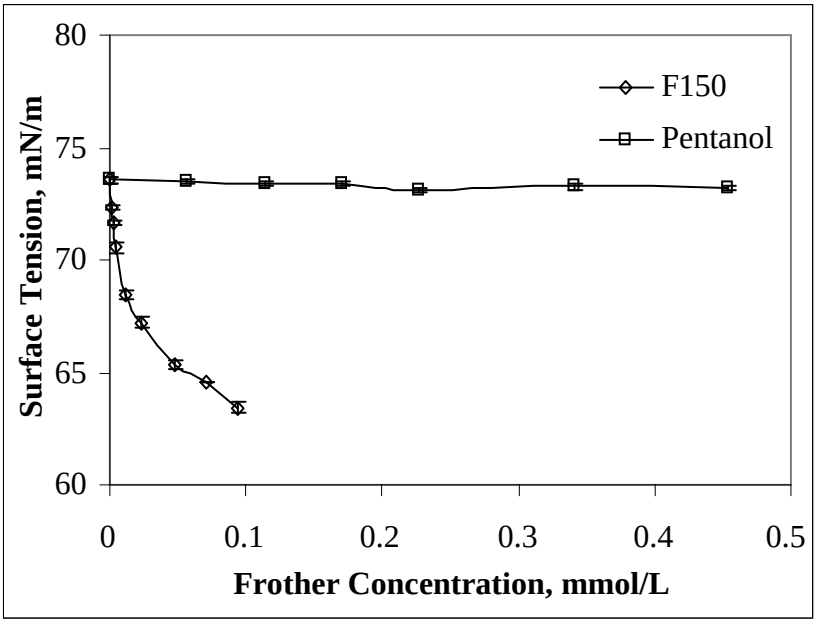

Figure 4.35: Surface tension of deionized water in presence of F150 and pentanol at 22 Cº

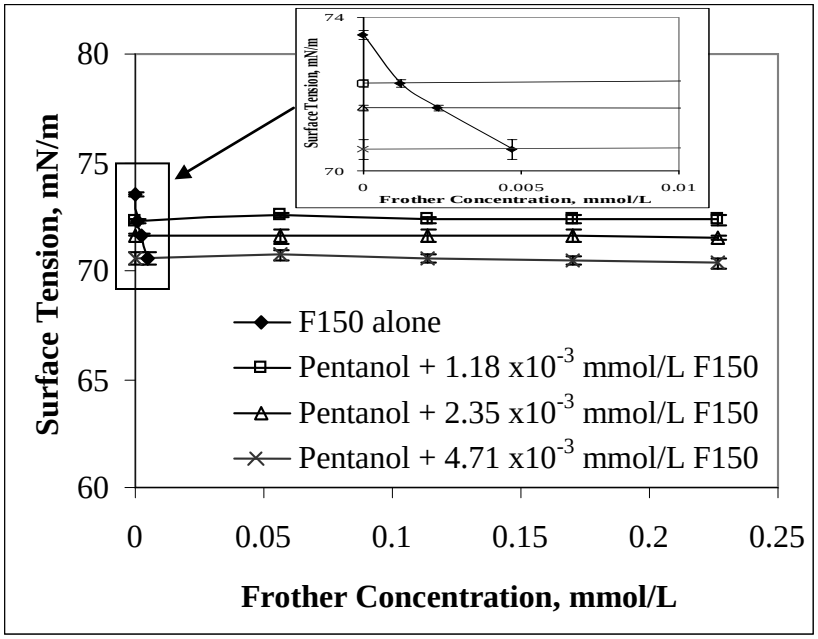

Figure 4.36: Surface tension of F150 – pentanol blends and F150 alone at concentrations equal to its content in the blends at 22 Cº

4.6. Bubble coalescence

4.6.1. Repeatability

The system selected was the F150 – pentanol (strongest – weakest) case. Figure 4.37 shows an example of a sequence of images. The initial contact occurs in the first frame (time t = 0) and coalescence occurs, as indicated in the last frame, with an elapse time (i.e., coalescence time) of 11.9 s. The pooled standard deviation on the coalescence time was 1.03 s for all frothers.

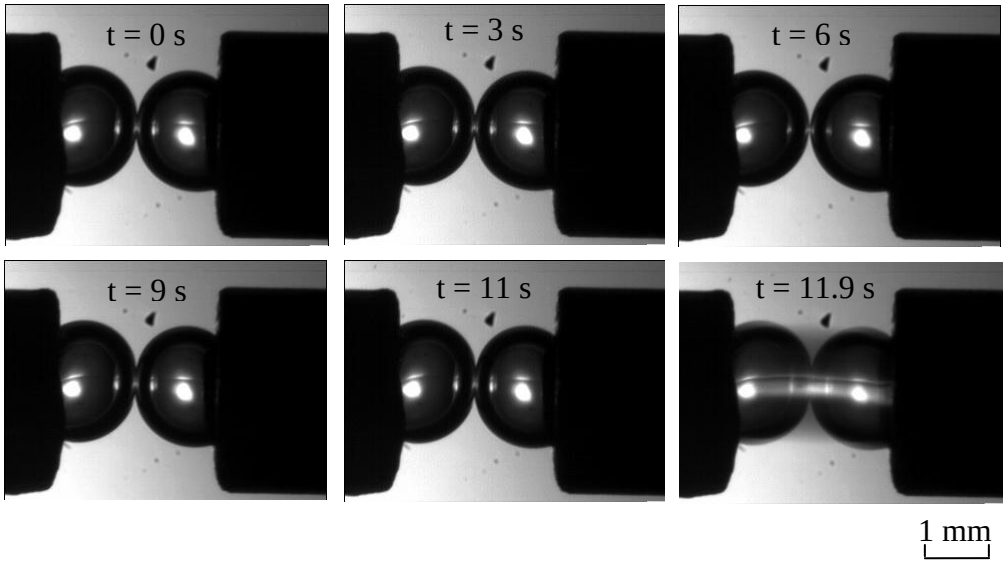

Figure 4.37: Sequence of images using high-speed imaging for bubble coalescence in the presence of 0.024 mmol/L (10 ppm) F150

4.6.2. Single frothers

Figure 4.38 shows coalescence time in the presence of pentanol and MIBC alone as a function of concentration upto 0.28 mmol/L (25 ppm) in case of pentanol and 0.2 mmol/L (20 ppm) for MIBC. Reproducibility decreased markedly for pentanol at concentrations below ca. 0.06 mmol/L, probably due to its high volatility. The coalescence time in both pentanol and MIBC follows the same trend: coalescence time increases with increasing concentration to a maximum of 11.4 s (±1.2 s) at ca. 0.17 mmol/L (15 ppm) for pentanol and 10.4 s (±1.3 s) at ca. 0.05 mmol/L (5 ppm) for MIBC and thereafter decreases to reach an apparently constant value.

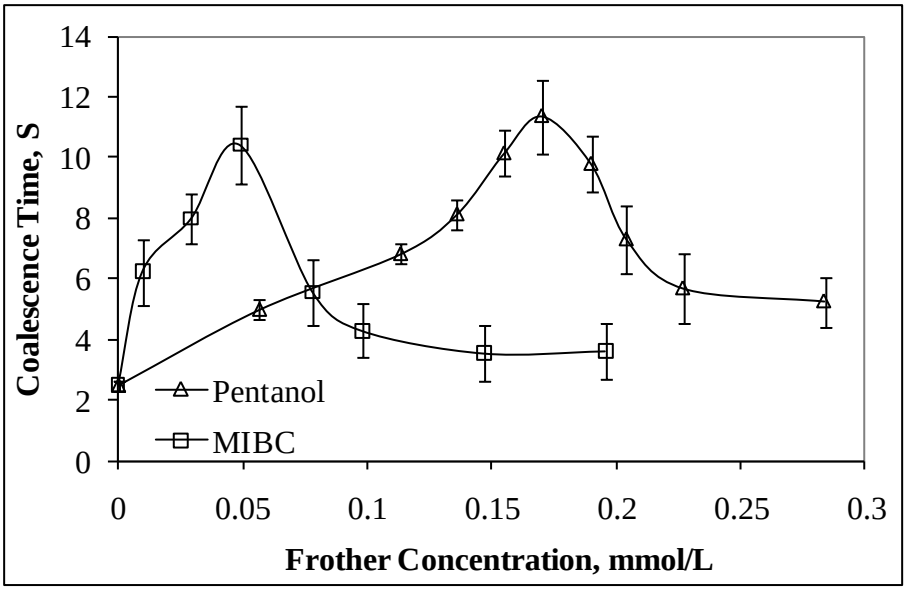

Figure 4.38: Coalescence time as a function of pentanol and MIBC concentration

Coalescence time as a function of F150 concentration upto 0.047 mmol/L (20 ppm) and DF250 upto 0.16 mmol/L (40 ppm) is shown in Figure 4.39 (note, concentration scale is logarithmic). In the F150 case, reproducible coalescence times were measurable to concentrations down to at least 2.35×10^{-5} mmol/L (0.01 ppm) F150. Coalescence time initially increased slowly with increasing F150 concentration, rising more rapidly above ca. 0.001 mmol/L (0.75 ppm) and leveling off to a maximum at around 11.6 s (± 1.1 s) above a concentration of ca. 2.35×10^{-3} mmol/L (1 ppm). For DF250, coalescence time increased rapidly from 4.6 s (± 0.6 s) at 4×10^{-3} mmol/L (1 ppm) to ca. 9.4 s (± 1.4 s) at 0.02 mmol/L (5 ppm) and remained constant upto 0.16 mmol/L (40 ppm).

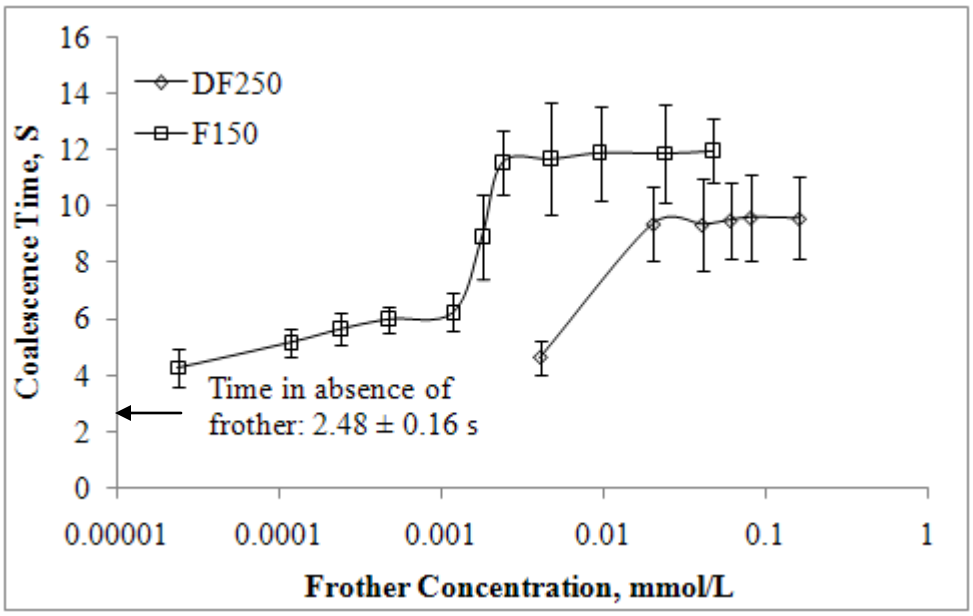

Figure 4.39: Bubble coalescence time as a function of F150 and DF250 concentration

4.6.3. Frother blends

The coalescence time for F150 - pentanol blends is shown in Figure 4.40, given as a function of pentanol concentration for different F150 concentrations. It is observed that the coalescence time at a given F150 concentration is almost constant independent of pentanol concentration (considering the 95% CI). For the two lowest F150 concentrations, 1.18 and 2.35 x 10^{-3} mmol/L (0.5 and 1 ppm), coalescence time is about 8 s rising to ca. 10 s when F150 concentration is raised to 4.71 x 10^{-3} mmol/L (2 ppm).

The comparison between coalescence time for single frothers and F150 – pentanol blends is shown in Figure 4.41. It can be concluded that blends gave generally higher coalescence times than pentanol alone but lower than for F150 alone. The maximum in coalescence time found for pentanol alone at ca. 0.17 mmol/L is eliminated in the blends.

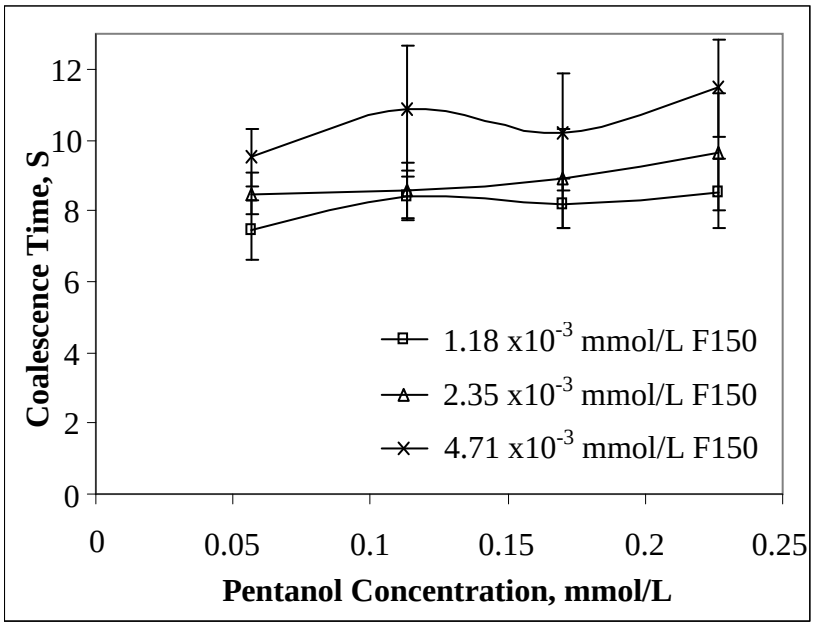

Figure 4.40: Bubble coalescence time in the presence of F150 – pentanol blends

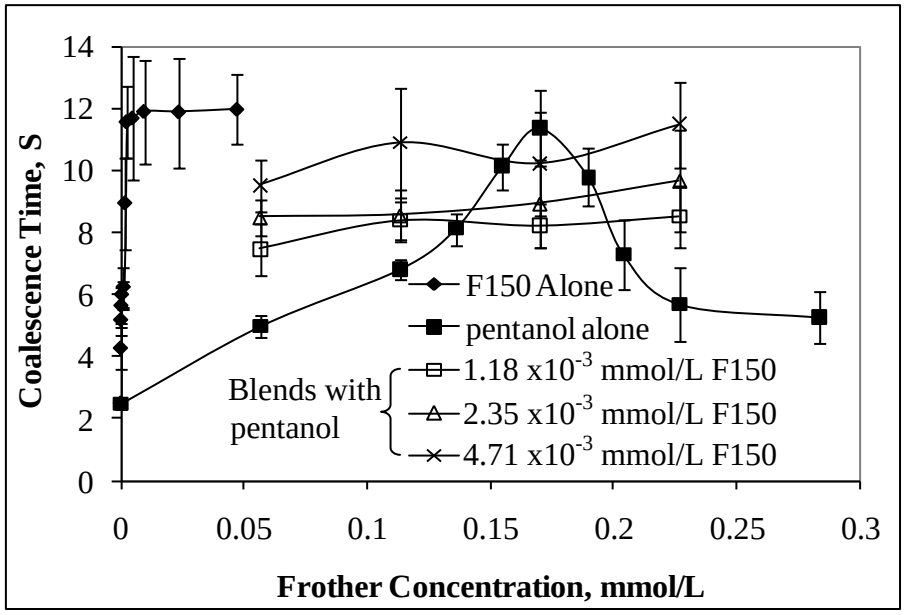

Figure 4.41: Comparison of bubble coalescence time in the presence of single frothers and F150 – pentanol blends

4.7. Bubble break-up

4.7.1. One-bubble-at-a-time

Results are reported as number frequency of daughter bubbles versus the ratio of daughter bubble size to the mother bubble size, d/d_0 (Figure 4.42). Using d/d_0 normalizes for the slight variation in original bubble size between tests (3.04 mm ± 0.3 (95% CI)). The number frequency represents a 10% range in d/d_0 (e.g., d/d_0 = 45% represents all bubbles within the range 40-50% d/d_0). Each frequency represents the sum of all 25 break-up experiments and not an average. This strategy was adopted because the extent of the break-up depends on where the mother bubble encounters the impeller (or eddy) (close to or far from bubble

centre, for instance). One consequence is lack of confidence interval (error bar) on the data.

Figure 4.42 shows the results for single and blended frothers. The daughter bubble size distributions are near normal (Gaussian). For F150 and pentanol alone the size distributions are similar (i.e., bubble break-up is similar) with mean d/d_0 ca. 35%. The distribution for the frother blend, on the other hand, shows a shift to larger sizes with a mean ca. 45% of the original size. This shift means a decrease in population of small bubbles and a corresponding increase in the population of larger bubbles compared to the two frothers on their own. In other words, this result indicates that frother blends reduce bubble break-up and cause the resulting daughter bubble size to increase.

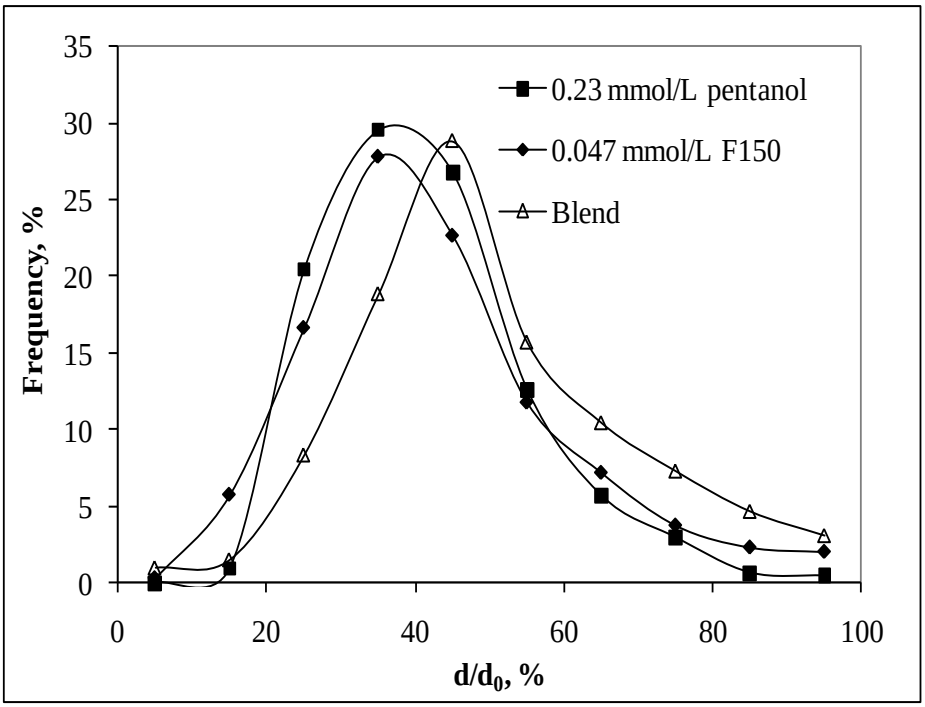

Figure 4.42: One-bubble-at-a-time break-up in the presence of single frothers and F150 – Pentanol blend (4.71×10^{-3} mmol/L F150 + 0.23 mmol/L pentanol) using 420 rpm impeller rotation speed

4.7.2. From an air vortex

Figure 4.43 summarizes the Sauter mean for bubbles produced by shear of the air vortex. The figure shows that bubbles formed in F150 – pentanol blends are larger than the bubbles generated in the presence of single frothers. Figure 4.44 shows that the size distribution shifts to larger size for the blend and Figure 4.45 shows the blend size distribution approaches that in the tap water.

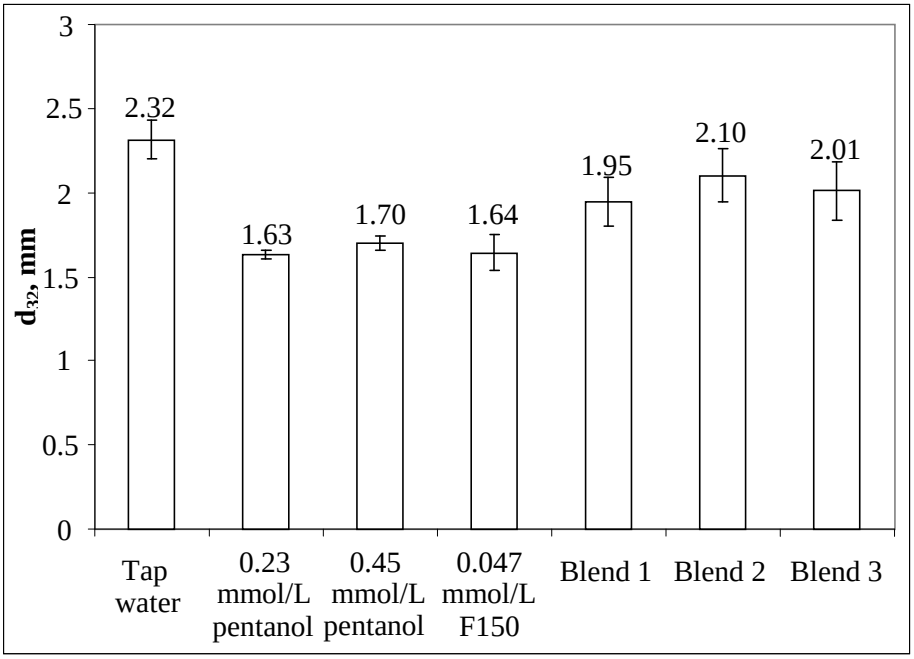

Figure 4.43: Bubble break-up from air vortex in the presence of single and blended frothers (blend 1 is 4.71 x 10^{-3} mmol/L F150 + 0.23 ml/L pentanol; blend 2 is 2.35 x 10^{-3} mmol/L F150 + 0.23 mmol/L pentanol; and blend 3 is 1.18 x 10^{-3} mmol/L F150 + 0.23 mmo/L pentanol)

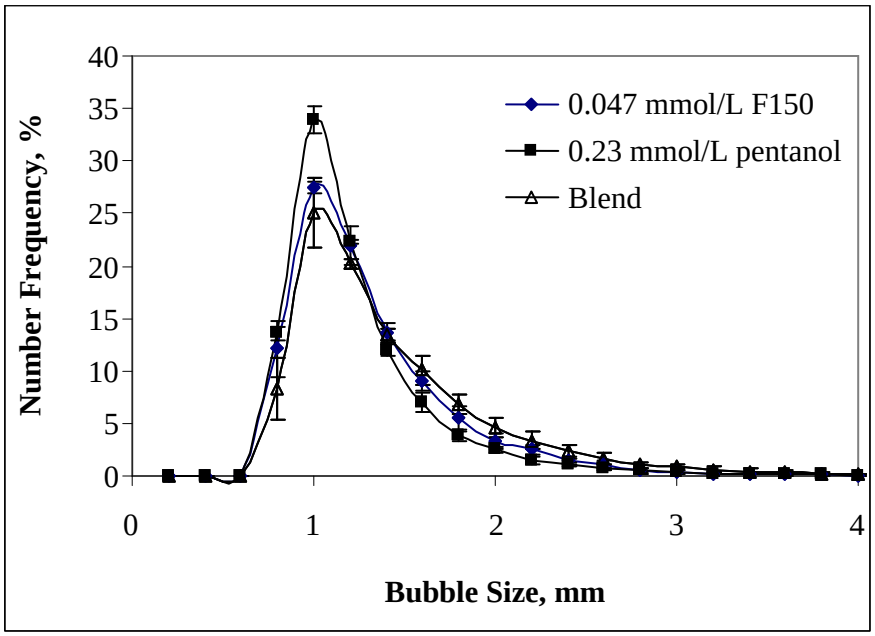

Figure 4.44: Bubble size distribution in the presence of single and blended frothers. Blend is 4.71 x 10^{-3} mmol/L F150 + 0.23 mmol/L pentanol

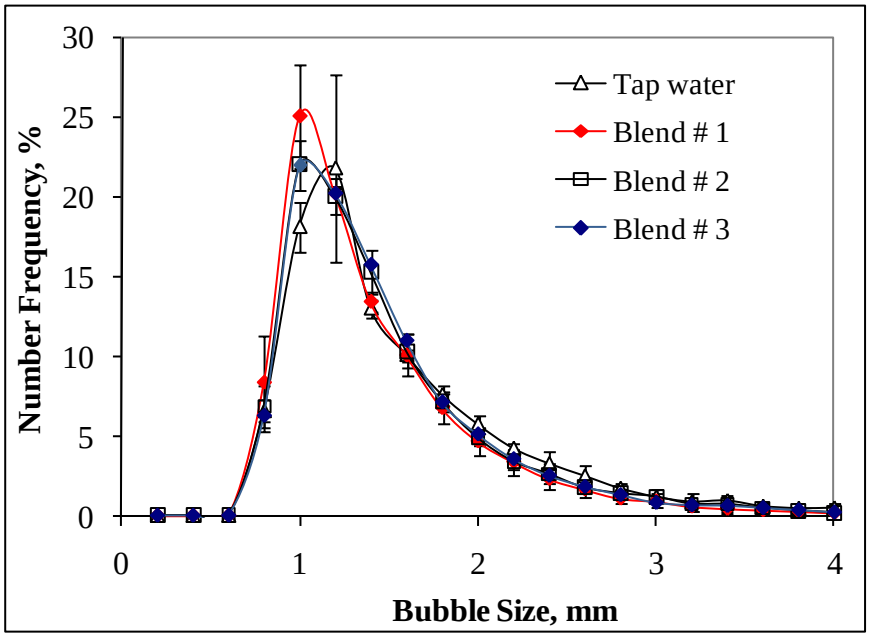

Figure 4.45: Bubble size distribution in tap water and in the presence of frother blends containing 0.23 mmol/L pentanol and 4.71 x 10^{-3} mmol/L F150 (Blend # 1), 2.35 x 10^{-3} mmol/L F150 (Blend # 2), and 1.18 x 10^{-3} mmol/L F150 (Blend # 3)

REFERENCES

Acuna, C. and Finch, J. A., 2008, " Motion of Individual Bubbles Rising in a Swarm", International Mineral Processing Congress, D. Wang et al., Eds., Vol. 1, Beijing, China, p. 891-901.

Rafeie, A. A., and Finch, J. A., 2009, "A comparison of bubble rise velocity profile of two surfactants to explain gas holdup data", In: Proceedings of the 7th UBC-McGill-UA International Symposium on Fundamentals of Mineral processing, Editors: Gomez, C. O., Nesset, J. E., and Rao, S. R., Sudbury, Ontario, p. 183-192.

Schwarz, S., and Grano, S., 2005, "Effect of particle hydrophobicity on particle and water transport across a flotation froth", Colloids and Surfaces A: Physicochemical and Engineering Aspects, Vol. 256, No. 2-3, p. 157-164.

Zhang, W., Nesset, J. E., and Finch, J. A., 2009, "Water recovery and bubble surface area flux", In: Proceedings of the 7th UBC-McGill-UA International Symposium on Fundamentals of Mineral processing, Editors: Gomez, C. O., Nesset, J. E., and Rao, S. R., Sudbury, Ontario, p. 155-168.

CHAPTER 5 - DISCUSSION

5.1. Hydrodynamic properties

5.1.1. Gas dispersion properties

Although frothers have been used in flotation for over a century, the mechanism behind their role is still a subject of enquiry. In control of bubble size Gomez et al. (2000) testing porous spargers in a bubble column suggested that at sufficient concentration frothers preserve the original bubble size produced by the bubble generator, i.e., gave the minimum bubble size. This 'sufficient concentration' can be linked to the CCC concept of Cho and Laskowski (2002a). Grau and Laskowski (2006) made a similar observation to Gomez et al. suggesting that the bubble size at concentrations above the CCC is the size generated by the rotor-stator mechanism in a mechanical cell at the hydrodynamic conditions prevailing in the cell. This implies that this minimum bubble size should be the same for any frother and presumably, therefore, any frother blend under the same hydrodynamic conditions.

This proved not to be the case. Figures 4.4, 4.6, 4.13, 4.15, 4.21, and 4.29 show that the blends of F150, DF250, and octanol with pentanol and MIBC significantly increased bubble size above the “weak” alcohol frother CCC compared to either frother alone regardless of the bubble generation mechanism (i.e., in the column and mechanical cell).

This unexpected finding, that the minimum bubble size in the case of blends is larger compared to single frothers, was supported by the corresponding gas

holdup data, particularly in the blends with MIBC where gas holdup decreased above the MIBC CCC in accord with the bubble size data (Figures 4.5 and 4.14). The combination of bubble size and gas holdup measurements provides evidence that either bubble size or gas holdup alone might leave open for debate. It does imply that the frother appears to play a direct role in the bubble formation process and the simple 'machine produces frother preserves' concept of small bubble production is not quite correct. A direct role of frother in formation has been speculated (Nesset et al., 2007) and the data here adds to that suspicion. Other than entertaining that blends somehow cause loss of frother from the system, the finding implies that blends either exhibit reduced coalescence inhibition or reduced break-up of the air mass which was the motivation behind the bubble coalescence and break-up experiments which are discussed later in this chapter.

That blends produce a larger bubble size above the "weak" frother CCC has not been reported previously and can be considered a negative effect. In practice, however, the "weak" frother (e.g. MIBC) concentration is often below its CCC (Gelinas and Finch, 2007) in which case the addition of F150 or DF250 (and likely other polyglycols) will see a reduction in bubble size (Figures 4.4, 4.6, 4.13, 4.15, and 4.29). In other words, the blend may be found to have a beneficial impact on reducing bubble size in practice.

Apparently, coalescence prevention is not sufficient to explain the bubble size data. Grau and Laskowski (2006) and Gupta et al. (2007) have speculated that frothers affect bubble break-up under turbulent conditions but do not offer any mechanism. Finch et al. (2008) also suggested that coalescence prevention is not

the only mechanism involved in reducing bubble size. One of their arguments was numerical: noting that bubble size (d_{32}) at frother concentrations above CCC is typically 1 mm, i.e., this is the size produced by the machine on the 'frother preserves' concept, and bubbles in the absence of frother are typically 4 mm, i.e., as a result of uncontrolled coalescence, means that 64 coalescence events must occur to grow the 1 mm to the 4 mm bubble size. They thought this number of apparently simultaneous coalescence events unrealistic and that a component of frother impact on bubble break-up appeared to be needed. Finch et al. (2008) went on to suggest a mechanism based on the force associated with surface tension gradients produced by variations in surface concentration (adsorption density) of frother caused by transient deformation of the air-water interface. The model is described in some detail later in this chapter, when we return to the question of the increased minimum bubble size in the blends.

5.1.2. Froth properties

The bubble size data do show a synergistic effect even if above the "weak" frother CCC it is negative. The froth properties, froth height and water overflow rate, in contrast show positive synergy: both paramerters increase in the blend by more than the sum of the individual frother results. This synergistic action agrees with the observations of Tan et al. (2005). Their results showed synergy in blends containing small proportions of polyglycol frothers, less than ca. 10 % by mass of the blend, with MIBC. On increasing the proportion of polygylcol in the blend the

froth became dominated by the polyglcols. This latter observation is probably the reason why Laskowski et al. (2003) did not report synergies, the polyglycol was dominating as they used a large proportion of polyglycol, representing 35% of the mass of the blend with MIBC.

The froth properties work in the bubble column focused on pentanol and F150, the 'weakest' and 'strongest' frothers tested. The mini-mechanical cell setup allowed better control of froth depth resulting in more consistent water overflow rate data which encouraged testing more frothers, and blends. Pentanol alone showed poor frothing properties, in the work here the maximum froth height reached (in the bubble column) was ca. 3.5 cm at concentration of 0.17 mmol/L (15 ppm). F150 gave more froth height increasing to reach a maximum of ca. 35 cm at a concentration of 0.071 mmol/L (30 ppm) where it plateaued (Figure 4.23). Tan et al. (2005) also found that froth height reached a plateau with increasing concentration (and going to even higher concentrations, much larger than encountered in practice, froth height would start to decrease).

The enhanced froth stability with the F150 – pentanol blends indicated by the increase in froth height in the column (Figure 4.23) and water overflow rate in the column (Figures 4.25 – 4.26) and in the mini-mechanical cell (Figures 4.31 – 4.34), is significant. The mechanism might be associated with increased water transport into the froth; i.e., the blend increases δ in the Herbst/Bascur model (equation 2.5). This is difficult to establish as most water overflow experiments include froth, i.e., it is difficult to isolate the transport through the froth from that

into the froth. This was the difficulty calculating δ in the work of Zhang et al. (2010).

The alternative is that the blends increase water retention and flow through the froth. Water is retained if bubbles are stable in the froth, i.e., do not coalesce rapidly. Surface elasticity generated by surface tension gradients contributes to this stability (equations 2.15 – 2.16). An associated mechanism, the Marangoni effect, could increase water flow into and through the froth (Tan et al., 2004; 2005; Goosh, 2009). Figure 5.1 illustrates the origin of this flow, the surface tension gradient inducing flow in the adjacent water layer. These surface tension gradient – driven flows can be visualized (e.g. Acuna et al., 2008). The argument, then, is that the blends increased surface tension gradients. The surface tension data did not suggest any synergy in the blends which behaved as F150 alone, but dynamic surface tension data might be more revealing. Later, in discussing bubble size effects, we entertain that blends reduce surface tension gradients.

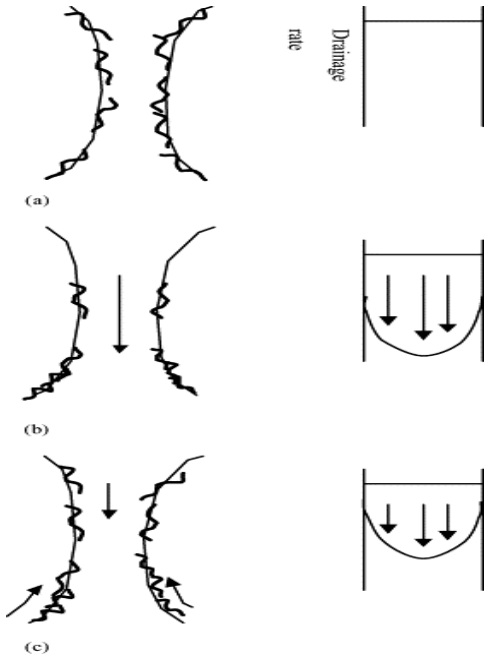

Figure. 5.1: (a) Surfactants at the air–liquid interface in the absence of thin film drainage. (b) Surface tension gradient on the surface is created as the surfactants are displaced due to the bulk viscous drag force in the presence of drainage. (c) The Marangoni effect results in a decrease in the net drainage rate. (Tan et al., 2004. Reprinted with permission from Elsevier)

Another water transport mechanism in the froth might be through blends causing an increase in surface viscosity. Non-ionic surfactants (e.g., frothers) added to ionic surfactants have been found to increase foam stability, which was attributed to formation of more highly condensed films (Pugh, 1996). The same mechanism might be applicable for blends of two non-ionic surfactants given that one, F150, has strong frothing properties, closer to ionic surfactants, and the other, pentanol, has low frothability.

5.2. Bubble coalescence

5.2.1. Single frothers

In the absence of frother (i.e., tap water only) coalescence time was ca. 2.5 ± 0.16 s (95% CI), which, when compared to the increase that occurs upon adding even small amounts of frother (e.g. < 0.0001 mmol/L F150), indicates that water quality has a minor ('background noise') effect on coalescence time. In this regard the measurements show that frothers acted as expected, i.e., they inhibited coalescence.

It has been suggested that coalescence inhibition plays the key role in forming small bubbles (Harris, 1976). Therefore, it was anticipated that coalescence time would increase with increasing frother concentration. In the presence of polyglycol frothers alone (Figure 4.39) coalescence time did follow the anticipated response, increasing with increasing concentration to reach a plateau. However, pentanol and MIBC alone did not show this behaviour. With increasing concentration coalescence time did initially increase but displayed a maximum (ca. 10 - 11s) at ca. 0.17 mmol/L for pentanol and at ca. 0.05 mmol/L (5 ppm) for MIBC. By further increasing frother concentration, coalescence time decreased significantly, to ca. 6 s at ca. 0.23 mmol/L pentanol and 0.08 mmol/L MIBC.

The maximum in coalescence time was not expected. However, Wang and Yoon (2008) may have made a potentially relevant observation in the case of MIBC. Examining foam stability they calculated that the critical film rupture

pressure between bubbles reaches a maximum at ca. 0.01 mmol/L MIBC then decreased by further increasing MIBC concentration. While the maximum here occurs at 0.08 mmol/L, and there are insufficient data to perform similar calculations to Wang and Yoon, the notion that film rupture pressure first increases then decreases with concentration offers some support to the present findings. Foam stability tests typically show a maximum at a given range of concentration (Tan et al., 2005; Wang and Yoon, 2008). These concentrations, however are significantly greater than those corresponding to the maximum in coalescence times seen here. The argument advanced by Tan et al. (2005) that solubility is exceeded and hydrophobic droplets de-stabilize the inter-bubble films does not offer a plausible explanation here. An alternative explanation for a maximum in foam stability is that high concentration means too rapid 'repair' of surface tension gradients, loosening their ability to preserve stability (Harris, 1982).

The concentration at the maximum in coalescence time in case of alcohols and the plateau in the case of the polyglycols is well below the corresponding CCC (Figure 4.2) indicating that the coalescence data do not correspond easily to the CCC.

One difference between formation of small bubbles and most coalescence test work (as here) is one of bubble age: in most coalescence tests the bubble is arguably older than in the corresponding bubble production situation and therefore has more adsorbed frother. In the case of bubble production, bubble age approaches zero and the surface concentration approaches the bulk concentration

(i.e., there is no ‘excess’, e.g. as given by Gibbs adsorption equation). Generally, the minimum in bubble coalescence (i.e., inferred from maximum in coalescence time) occurs at bulk concentrations below the CCC which could be the result of the “extra” adsorption in the coalescence test.

The experimental approach of Kracht and Finch (2009b) aimed to measure coalescence events at essentially time zero. They found that bulk concentrations in that case exceeded the CCC to retard coalescence. This can be taken to mean that in the actual bubble formation process bubble surfaces are somewhat older than true zero. Regardless, the argument is that surface concentrations need to be considered when using a coalescence test system aimed at probing the bubble production process (as opposed to foam formation) in the presence of surfactants.

5.2.2. Frother blends

The coalescence time – concentration trend in the presence of F150 – pentanol blends can be divided into three regions when compared to pentanol alone (Figure 4.41). At concentrations < 0.17 mmol/L (15 ppm) pentanol, all blends show greater coalescence time than for pentanol alone. At 0.17 mmol/L pentanol, where a maximum in coalescence time with pentanol alone is reached, all blends show coalescence times lower than that of pentanol alone. In the third region, above 0.17 mmol/L pentanol, although coalescence time decreases rapidly for pentanol alone the blend coalescence time remains constant approaching

similar coalescence times to F150 alone. The blends do not show any synergy reflective of that shown in the gas dispersion or froth stability properties.

Bikerman (1973) noted enhanced foamability of some surfactant blends and suggested that this might result from enhanced solubility of one surfactant due to the presence of the other. Based on Bikerman's reasoning the blend behavior might be that the presence of F150 enhances the solubility of pentanol, so phase transition will occur at higher pentanol concentrations in the blends compared to pentanol alone. However, this seems unlikely. Another possibility is simply that F150 properties dominate and the blends then show coalescence times close to that of F150 alone, as observed. Laskowski et al. (2003), for example made this claim for polyglycol-alcohol blends.

Figure 5.2 compares the bubble size and coalescence time obtained in the presence of 0.23 mmol/L (20 ppm) pentanol blended with 1.18×10^{-3} mmol/L F150, 2.35×10^{-3} mmol/L F150, and 4.71×10^{-3} mmol/L F150, conditions which represent the minimum bubble size obtained using the blends (which is ca. 0.5 mm larger than for single frothers). It is evident that while bubble size is almost the same for the three blends the coalescence time increases with increasing F150 concentration (from 1.18×10^{-3} mmol/L to 4.71×10^{-3} mmol/L). In other words, the lack of change in bubble size does not reflect the decrease in probability of coalescence (as indicated by increase in coalescence time) which in turn might be taken to imply that coalescence prevention alone is not responsible for bubble size reduction. By extension, reduced coalescence prevention does not offer an

explanation for the coarser bubble size in polyglycol blends above the alcohol CCC.

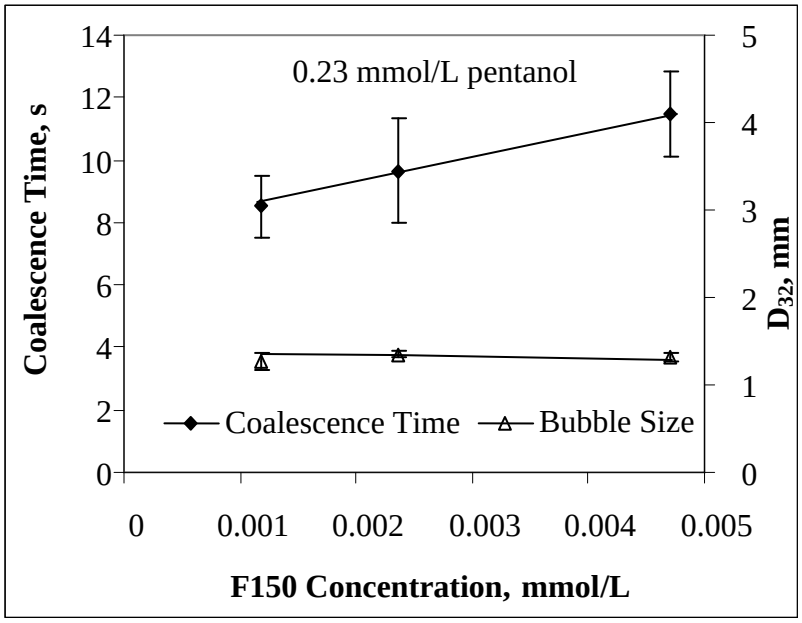

Figure 5.2: Bubble size and coalescence time in the presence of 0.28 mmol/L pentanol blended with (1.18, 2.35, and 4.71) x 10^{-3} mmol/L F150

The evidence that reduced coalescence prevention is not the source of the larger minimum bubble size in the blend above the alcohol frother CCC opened other possibilities. The surface tension data do not support that F150 and pentanol interact to enhance surface activity. There may be differences in the distribution (partitioning) of frother between solution and froth that occurs on blending but the decrease in bubble size for blends compared to single frothers before the CCC of the 'weak' frother. i.e., the expected effect, tends to rule that out. The considered possibility is a reduction in break-up of the air mass, which will be discussed later in this chapter.

5.3. Bubble break-up

5.3.1. Method of generation and nature of the distributions

The refinement of the setup of Kracht and Finch (2009a) aimed to remove the opportunity for coalescence events in order to de-couple from break-up events. The one-bubble-at-a-time setup approached providing that feature. Another refinement was to ensure that each bubble is imaged only once. The current setup also ensured that all bubbles encountered the impeller: after a break-up event the daughter bubbles were allowed to disperse before the next single bubble was introduced enabling unambiguous evidence of the encounter with the impeller. The main disadvantage of the method is the small number of bubbles analyzed. To collect and analyze data on the 25 individual bubbles required several weeks.

In bubble break-up from the air vortex, bubbles were imaged immediately below the rotating impeller, again aiming to minimize coalescence events that might occur as the bubbles later rise. The imaging rate was adjusted to ensure that each bubble was imaged only once.

The shift to a larger daughter bubble size between single and blended frothers at concentrations greater than the alcohol CCC found in the bubble column, mechanical cell, and vortex shear tests indicates the phenomenon is general.

The daughter bubble frequency curves obtained in the one-bubble-at-a-time study showed near-normal distributions (Figure 4.42) centered not far from d/d_0 =

50%. Some researchers (Nambiar et al. 1992; Wang et al, 2003) have argued that the daughter bubble distribution from break-up should show a minimum in frequency at d/d_0 = 50% being the least probable as it represents the maximum increase in surface area and thus maximum increase in associated surface energy relative to the mother bubble. In other words, bubble break-up should be strongly asymmetric. Other researchers have suggested that the probability of d/d_0 = 50% is the maximum (Lee et al., 1987; Martinez-Bazan et al., 1999). The results of Kracht and Finch (2009a) tended to support the first argument (i.e., low probability of d/d_0 = 50%) but as noted there is some difficulty in distinguishing break-up from coalescence in their approach. The present results, where break-up predominates, do not support the first argument. While the number of mother bubbles is limited the resulting distributions always approximated normal distributions with no suggestion that strongly asymmetric break-up was occurring.

5.3.2. Blended vs. single frothers

The role of frother in bubble size reduction is commonly attributed to coalescence prevention (Harris, 1976). This is illustrated by the name critical coalescence concentration, CCC, given to the frother concentration at which bubble size (d_{32}) reduction stops and reaches a minimum. Some researchers (Gomez et al., 2000; Grau and Laskowski, 2006) have extended this notion to suggest that this minimum bubble size is the size generated by the machine with frother acting to preserve this size. That implies the minimum bubble size

generated in a certain machine operated in a certain manner should remain the same regardless of the kind of frother, or by extension, frother blend being used. The bubble size measurements showed that this is not the case, with the alcohol – polyglycol frother blends giving a significantly larger minimum bubble size than the single frothers. Various authors (Grau and Laskowski, 2006; Gupta et al., 2007; Nesset et al., 2007; Finch et al., 2008) have speculated that frother also affects bubble break-up. The work reported here using the one-bubble-at-a-time approach is the first to examine break-up independent of coalescence.

As demonstrated in Figure 4.42 it is evident that the F150 – pentanol blend produced fewer small daughter bubbles and more large daughter bubbles compared to the two frothers on their own, i.e., the bubble size is increased in the blend. Figure 4.43 reports a similar finding from the break- up of the air mass (Figure 4.44 and 4.45). These findings support the column/mechanical cell results that indicated the minimum bubble size in the presence of frother blends was larger compared to that with single frothers. The evidence in this chapter identifies this blend effect with reduced bubble break-up. To the author's knowledge, this is the first unambiguous evidence that frother plays a role in break-up of the air mass.

5.3.3. Proposed mechanism of increased minimum bubble size in blends

The results have shown that below the "weak" frother CCC the bubble size decreased in the blend compared to single frothers. This was the expected

outcome. The unexpected result was that a small addition of "strong" frother (F150, DF250, and octanol) to "weak" frother (pentanol or MIBC) caused the bubble size to increase significantly above the “weak” frother CCC; and that with further increasing “strong” frother concentration the bubble size decreased to the original, pre-blend, value. Therefore, this section focuses on the mechanism of the increase in the minimum bubble size.

The approach to the mechanism starts by considering the arrangement of frother molecules at the air/water interface (bubble surface) (Figure 5.3). A bubble surface in presence of single frother (e.g. pentanol) under equilibrium conditions with no forces acting will tend to a uniform surface distribution of frother molecules, as in Figure 5.3a. There will be an associated surface tension corresponding to this surface concentration (adsorption density). Any disturbance to this arrangement will produce a surface tension gradient and thus associated Gibbs-Marangoni effects. A form of disturbance is to introduce a second "strong" frother molecule, e.g. F150. The arrangement may then look something like in Figure 5.3b (where "strong" frother is represented by the open circle and longer ‘chain’ to distinguish from the "weak" frother symbol). A surface tension gradient will be generated due to the larger local surface tension depression associated with "strong" frother compared to "weak" frother. The "weak" frother molecules will be pushed away from the "strong" frother molecule by this surface tension gradient, which, for discussion purposes, will be referred to as the ‘blend – Marangoni’ effect.

Finch et al. (2008), based on Miller and Neogi (1985), suggested that local stresses generated due to opposing surface tension gradient forces originating around frother molecules might be a possible mechanism contributing to bubble break-up (Figure 5.4). This is one of the Gibbs- Marangoni effects.

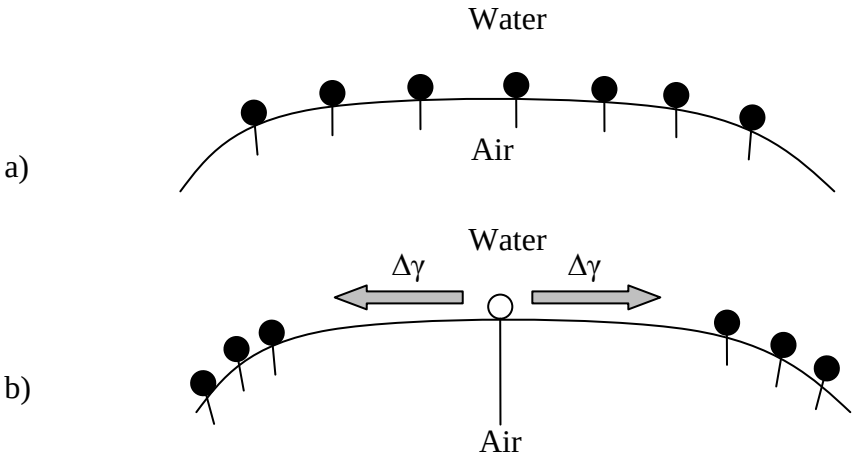

Figure 5.3: Schematic for bubble surface under equilibrium conditions in the case of a) single frother (pentanol), and b) addition of F150 (to form a blend with low ratio of F150 : pentanol)

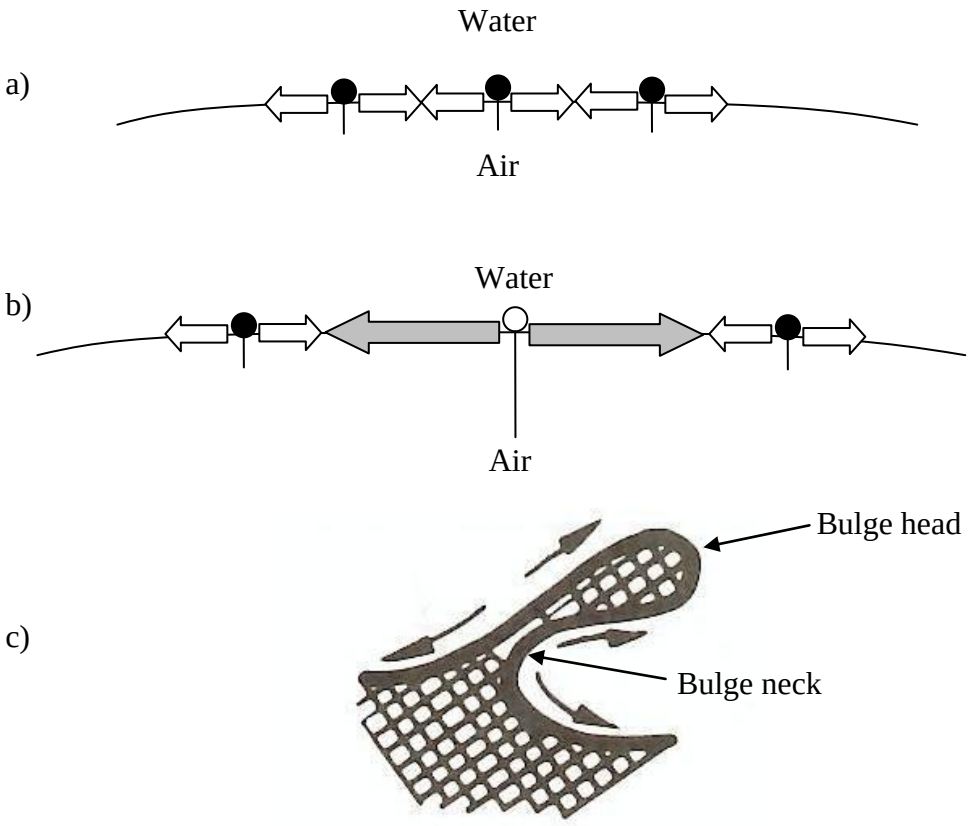

Figure 5.4: Schematic showing opposing forces from frother molecules in case of a) single frother (adapted from Finch et al., 2008), b) frother blend, and c) schematic showing break-up due to opposing surface tension gradients (adapted from Miller and Neogi, 1985)

In the Finch et al. model, random fluctuation in the air/water interface due to turbulence in the vicinity of the bubble generating device results in bulges and if frother (surfactant) concentration at the neck is higher than at the head this adds a force promoting breakaway of the head (i.e., bubble break-up) (Figure 5.4c). Of course frother concentration may be higher at the head (the process is random) and this would oppose break-up (Miller and Neogi, 1985). However, the net effect is to favour break-up as opposing is not the same as reversing break-up: assuming

excess accumulation at both neck and head is equally likely then break-up will occur half as frequently but break-up will still occur and effectively be promoted by frother. The arguments can be extended to explain the effect of frother concentration: when concentration is increased, the corresponding higher adsorption density will result in more low surface tension regions giving rise to more break-up events and hence leading to formation of smaller bubbles.

To apply the hypothesis to frother blends, two types of surface tension gradient, namely, the Marangoni effect (associated with a single frother) and the blend – Marangoni effect, are proposed. When the surface is deformed, the two types of frother molecules will accumulate differently creating the two types of surface tension gradient. As depicted in Figure 5.5, the blend – Marangoni effect tends to oppose the Marangoni effect associated with one frother. As a result, the magnitude of the resultant (net) surface tension gradient is reduced leading to larger bubbles being formed. Note the depiction suggests that the mechanism is associated with low concentration of the strong frother compared to the weaker one. Based on this hypothesis frother blends with a small component of strong frother inhibit bubble break-up by reducing the surface tension gradients produced, i.e., reducing the effective concentration of single frother.

Following the argument, increasing the ratio of strong frother to weak frother (pentanol or MIBC) above a critical limit will lead to reduction (even elimination) of the blend – Marangoni effect (Figure 5.6). The reduction in the blend-Marangoni effect will increase the resultant surface tension gradient force returning it to the single frother case. This is the evidence here: as concentration

of “strong” frother increases bubble size returns to the single frother case. For blends to show the effect of increasing minimum bubble size (i.e., increasing blend – Marangoni effect) it is suggested that a weak frother concentration above its CCC has to be used with a small addition of strong frother that is well below its CCC.

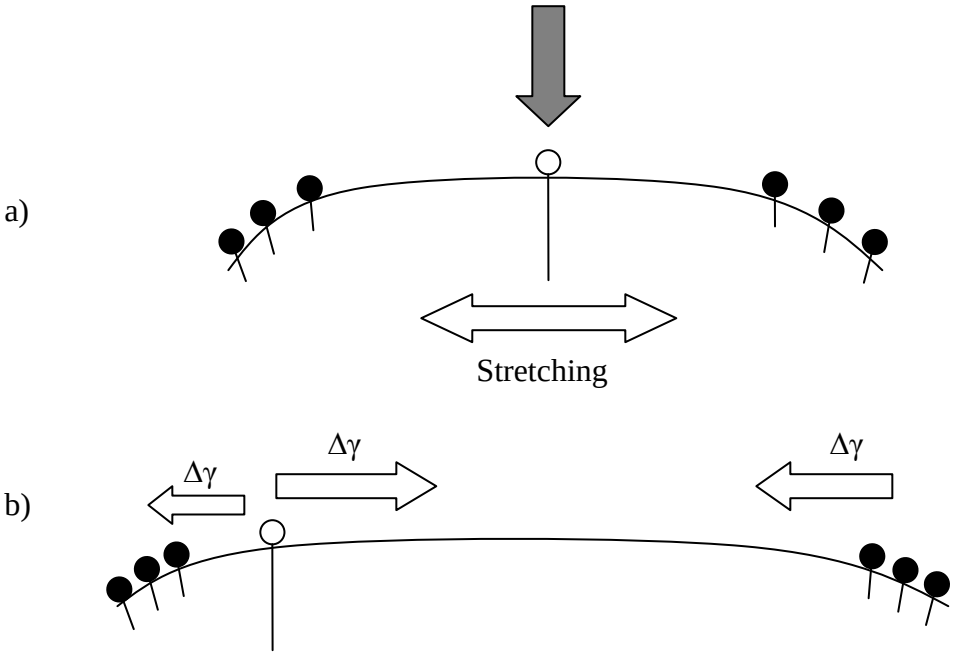

Figure 5.5: Schematic drawing showing air/water interface in the presence of frother blend: a) before deformation, and b) after deformation and the formation of two opposing surface tension gradient forces.

There is little bubble size distribution data for blends in the literature. Laskowski et al. (2003) measured bubble size for blends consisting of MIBC (alcohol) with each of three Dowfrothers (polyglycol frothers) DF-200, DF-250, and DF-1012 (which has molecular weight (ca. 400 g/mol) very close to that of

F150). They did not find any significant change in the minimum bubble size with blends compared to the individual frothers. To compare with the present work DF-1012 is chosen as it is similar to F150 (i.e. both are polypropylene glycol, molecular weight 400 – 425 g/mol). The reason they did not see an effect on the minimum bubble size might be their use of a constant molar ratio for all blend concentrations of 1 DF-1012 to 9 MIBC giving 1:2 by weight. This ratio is much higher than in the current study (1:48 to 1:193 F150 to pentanol by molecular weight giving 1:10 to 1:80 by weight) and thus, it can be argued, there is too much strong frother in the Laskowski et al. work to generate the blend – Marangoni effect and the blend will be giving bubble size reduction similar to the strong frother alone, as the Laskowski et al. and the present work found.

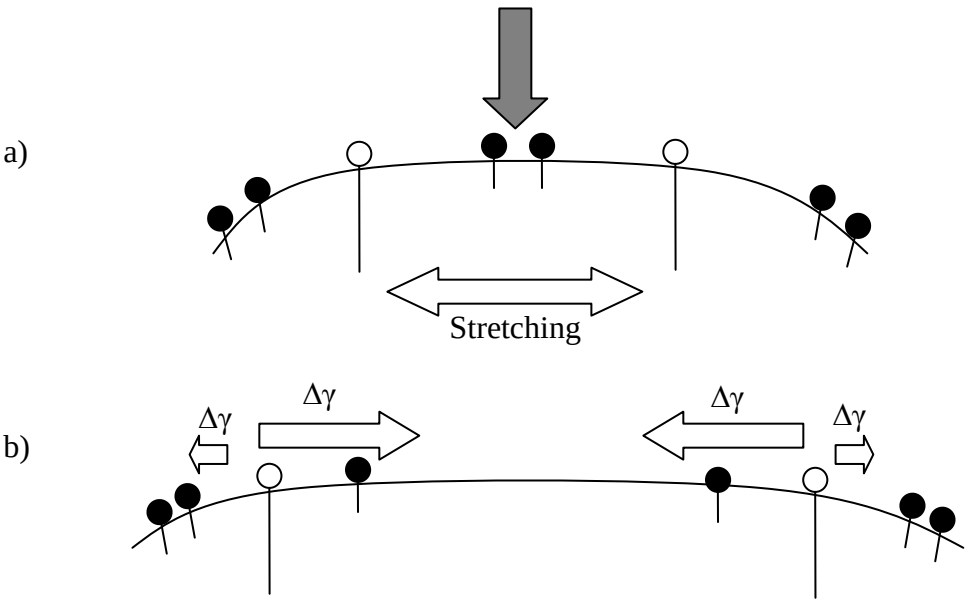

Figure 5.6: The effect of increasing "strong" frother molecular ratio in blends with "weak" frothers on surface tension gradient: a) before deformation, and b) after deformation

This discussion has focused on break-up. A case could be made that minimum bubble size observed when frother concentration is taken beyond some limit is associated with there being no further enhancement of break-up. In other words the CCC might be equally well named the Critical Breakage Concentration (CBC).

REFERENCES

Acuna, C. and Finch, J. A., 2008, " Motion of Individual Bubbles Rising in a Swarm", International Mineral Processing Congress, D. Wang et al., Eds., Vol. 1, Beijing, China, p. 891-901.

Acuña, C. A., Radman, J., and Finch, J. A., 2008, "Measurement of flow visualized on surface of bubble blown in air", Colloids and Surfaces A: Physicochemical and Engineering Aspects, Vol. 330, No. 2-3, p. 112-115.

Arzhavitina, A., and Steckel, H., 2010, " Foams for pharmaceutical and cosmetic application", International Journal of Pharmaceutics, Vol. 394, No. 1-2, pp. 1-17.

Bikerman, J. J., 1973, “Foams”, Springer Verlag, New York.

Cho, Y. S, and Laskowski, J. S., 2002 a, “Effect of flotation frothers on bubble size and foam stability”, International Journal of Mineral Processing, Vol. 64, p. 69-80.

Finch, J. A., Nesset, J. E., and Acuna, C., 2008, "Role of frother on bubble production and behavior in flotation", Minerals Engineering, Vol. 21, p. 949-957.

Gelinas, S., and Finch, J.A., 2007, "Frother analysis: procedure and plant experiences", Proceedings 39th Annual Meeting of the Canadian Mineral Processors of CIM, Jan. 23–25, 387–398.

Ghosh, P., 2009, "Coalescence of bubbles in liquid", Bubble Science, Engineering and Technology, Vol. 1, No. 1-2, p. 75-87.

Gomez, C. O., Escudero, R., and Finch, J. A., 2000, "Determining equivalent pore diameter for rigid porous spargers", The Canadian Journal of Chemical Engineering, Vol. 78, 785-792.

Grau, R. A., and Laskowski, J. S., 2006, “Role of frothers in bubble generation and coalescence in a mechanical flotation cell”, The Canadian Journal of Chemical Engineering, Vol. 84, p. 170-182.

Gupta, A. K., Banerjee, P. K., Mishra, A., Satish, P., and Pradip, 2007, " Effect of alcohol and polyglycol ether frothers on foam stability, bubble size and coal flotation", nternational Journal of Mineral Processing, Vol. 82, p. 126-137.

Harris, C.C., 1976, "Flotation machines", In: M.C. Fuerstenau, Editor, A.M. Gaudin Memorial Volume, Vol. 2, SME, pp. 753–815.

Kracht, W. and J. A. Finch, 2009a, "Bubble break-up and the role of frother and salt", International Journal of Mineral Processing**,** Vol. 92, No. 3-4, p. 153-161.

Kracht, W., Finch, J. A., 2009b, "Using sound to study bubble coalescence", Journal of Colloid and Interface Science, Vol. 332, No. 1, p. 237-245.

Laskowski, J. S, Tlhone, T., Williams, P., and Ding, K., 2003, "Fundamental properties of polyoxypropylene Alkyl ether flotation frothers", International Journal of Mineral Processing, Vol. 72, p. 289-299.

Lee, C.H., Erickson, L.E., and Glasgow, L.A., 1987, "Dynamics of bubble size distribution in turbulent gas–liquid dispersions", Chemical Engineering Communications, Vol. 61, p. 181–195.

Martínez-Bazán, C., Montañés, J.L., and Lasheras, J.C.,1999, "On the breakup of an air bubble injected into a fully developed turbulent flow. Part 2. Size PDF of the resulting daughter bubbles", Journal of Fluid Mechanics, Vol. 401, p. 183–207.

Miller C. A., and Neogi, P., 1985, "Interfacial phenomena: equilibrium and dynamic effects", In: Surfact science series, Vol. 17, Chapter VI: Transport effects on interfacial phenomena, p. 240-298.

Nambiar, D. K. R., Kumar, R., Das, T. R., and Gandhi, K. S., 1992, "A new model for breakup frequency of drops in turbulent stirred dispersions", Chemical Engineering Science, Vol. 47, No. 12, p. 2989-3002.

Neethling, S.J., and Cilliers, J.J., 2002, “The entrainment of gangue into a flotation froth”, International Journal Mineral Processing, Vol. 64, p.123-134.

Nesset, J.E., Finch, J.A., Gomez, C.O., 2007, "Operating variables affecting the bubble size in forced-air mechanical flotation machines", In: Proceedings AusIMM 9th Mill Operators Conference, Fremantle, Australia, p. 66–75.

Pugh, R. J., 1996, “Foaming foam films, antifoaming and defoaming”, Advances in Colloid and Interface Science, Vol. 64, p. 67-142.

Rafeie, A. A., and Finch, J. A., 2009, "A comparison of bubble rise velocity profile of two surfactants to explain gas holdup data", In: Proceedings of the 7th UBC-McGill-UA International Symposium on Fundamentals of Mineral processing, Editors: Gomez, C. O., Nesset, J. E., and Rao, S. R., Sudbury, Ontario, p. 183-192.

Schwarz, S., and Grano, S., 2005, "Effect of particle hydrophobicity on particle and water transport across a flotation froth", Colloids and Surfaces A: Physicochemical and Engineering Aspects, Vol. 256, No. 2-3, p. 157-164.

Tan, S. N., Fornasiero, D., Sedev, R., and Ralston, J., 2004, "The interfacial conformation of polypropylene glycols and foam behaviour", Colloids and Surfaces A: Physicochemical and Engineering Aspects, Vol. 250, No. 1-3, p. 307-315.

Tan, S. N., Pugh, R.J., Fornasiero, D., Sedev, R., and Ralston, J., 2005, “Foaming of polypropylene glycols and glycol/MIBC mixtures”, Minerals Engineering, Vol. 18, p. 179–188.

Wang, T., Wang, J., and Jin, Y., 2003, "A novel theoretical breakup kernel function for bubbles/droplets in a turbulent flow", Chemical Engineering Science, Vol. 58, No. 20, p. 4629-4637.

Wang, L., and Yoon, R. H., 2008, “Effect of surface forces and film elasticity on foam stability”, International Journal of Mineral Processing, Vol. 85, p. 101

Zhang, W., Nesset, J. E., and Finch, J. A., 2009, "Water recovery and bubble surface area flux", In: Proceedings of the 7th UBC-McGill-UA International Symposium on Fundamentals of Mineral processing, Editors: Gomez, C. O., Nesset, J. E., and Rao, S. R., Sudbury, Ontario, p. 155-168.

CHAPTER 6 – CONCLUSIONS, CONTRIBUTIONS, AND FUTURE WORK

6.1. Conclusions

This thesis addressed the effect on gas dispersion and froth properties of blending strong frothers, polyglycols (F150 and DF250) and octanol, with two weak alcohol frothers pentanol and MIBC, with supporting basic bubble coalescence and break-up studies and formulation of mechanisms. The following conclusions can be drawn:

Gas dispersion and froth properties:

1. Bubble column and pilot mechanical cell tests showed that compared to single frothers a small amount of strong frother (below CCC) reduced the blend Sauter mean bubble size at concentrations below the (critical coalescence concentration (CCC) of the alcohol frother and increased it (from ca. 0.8 mm upto 1.3 mm) at concentrations above the alcohol CCC. This response was also indicated by the gas holdup measurements in the bubble column. When increasing strong frother concentration in the blend, the bubble size returned back to its value in the presence of single frothers

2. The larger bubble size above the alcohol frother CCC suggests that frother affects the bubble size at production which in turn means the common explanation that the machine produces the bubble size which frother preserves by preventing coalesence is not supported.

3. For the same small polyglycol addition to alcohol blend froth height and water overflow rate significantly increased compared to the frothers alone in both column and mini-mechanical cell tests.

4. The possibility of independent control of the frother functions (bubble size and froth properties) in the case of the F150 – pentanol blend was demonstrated.

Coalescence and break-up:

5. For single alcohols, coalescence time increased with increasing concentration reaching ca. 0.17 mmol/L pentanol and ca. 0.05 mmol/L MIBC. The possibility of the maximum corresponding to a maximum in disjoining pressure based on based on Wang and Yoon was entertained.

6. With polyglycol alone coalescence time increased to plateau at about 12 s at concentration greater than ca. 2.35×10^{-3} mmol/L F150 and 0.02 mmol/L DF250 .

7. The F150 – pentanol blends showed a constant coalescence time which was less than that for F150 alone and generally greater than that for pentanol alone with no maximum.

8. The trend in coalescence time results for the blends do not follow those for the bubble size results suggesting the increase in minimum bubble size found with the blends above the alcohol frother CCC is not related to increased probability of coalescence.

9. Frother blends showed a significant increase in bubble size in both the one-bubble-at-a-time break-up and break-up from an air vortex test procedures compared to single frothers.

10. The results of the break-up tests provide evidence for a role of frother in break-up at bubble formation.

11. Based on a surface tension gradient (Marangoni effect) hypothesis of break-up, a blend – Marangoni effect was introduced to explain the reduced effect of frother blends on break-up.

6.2 Contributions to original knowledge

1. It is the first study on frother blends considering both bubble size reduction and froth stability with mechanisms being proposed and tested.

2. The first study to show that the minimum bubble size can increase in a blend.

3. The first experimental evidence showing that the hypothesis of "machine produces and frother preserves" is not entirely supported.

4. The first practical demonstration of the blend ability to control the two frother functions independently.

5. Development of a technique (one-bubble-at-a-time break-up), based on image analysis, able to discriminate between bubble coalescence and break-up for a single bubble.

6. Development of a technique (break-up from an air vortex), based on image analysis, able to discriminate between bubble coalescence and break-up in a turbulent field.

7. Provided experimental evidence that frothers are involved in break-up at bubble formation.

8. A novel mechanism, the blend – Marangoni effect, was introduced to explain the frother blend behaviour in producing larger minimum bubble size at concentrations above the weak alcohol CCC.

6.3. Recommendations for future work

The test of whether frother blends could control the two frother functions independently was compromised by the unexpected effect on bubble size. A blend free of this effect is required to properly test the hypothesis. Extension to actual flotation (i.e., three-phase) is then required, including allowance for frother-particle interaction and frother-collector interaction, likely complications in testing the blend effect under flotation conditions. Bubble rise velocity in blends needs to be tested to explore the origin of the large increase in gas holdup in the presence of high concentration of polyglycols in the blend compared to single frothers.

REFERENCES

Acuña, C. A., Radman, J., and Finch, J. A., 2008, "Measurement of flow visualized on surface of bubble blown in air", Colloids and Surfaces A: Physicochemical and Engineering Aspects, Vol. 330, No. 2-3, p. 112-115.

Acuna, C. and Finch, J. A., 2008, " Motion of Individual Bubbles Rising in a Swarm", International Mineral Processing Congress, D. Wang et al., Eds., Vol. 1, Beijing, China, p. 891-901.

Acuna, C., Nesset, J. E., and Finch, J. A., 2007, "impact of frother on bubble production and behaviour in the pulp zone", The 6th International Copper Conference, Aug 25-30, p. 197-210.

Albijanic, B., Ozdemir, O., Nguyen, A. V., and Bradshaw D., 2010, "A review of induction and attachment times of wetting thin films between air bubbles and particles and its relevance in the separation of particles by flotation", Advances in Colloid and Interface Science, Vol. 159, No. 1, p. 1-21.

Arzhavitina, A., and Steckel, H., 2010, " Foams for pharmaceutical and cosmetic application", International Journal of Pharmaceutics, Vol. 394, No. 1-2, pp. 1-17.

Ata, S., 2008, "Coalescence of bubbles covered by particles", Langmuir, Vol. 24, p. 6085-6091.

Ata, S., 2009, "The detachment of particles from coalescing bubble pairs", Journal of Colloid and Interface Science, Vol. 338, No. 2, p. 558-565.

Ata, s., and Jameson, G.J., 2005, "The formation of bubble clusters in flotation cells", International Journal of Mineral Processing, Vol. 76, No. 1-2, p. 123-139.

Azgomi, F, Gomez, C.O., Finch, J.A., 2007a, "Characterizing frothers using gas hold-up", Canadian Metallurgical Quarterly, Vol. 46 (3), p. 237-242.

Azgomi, F., Gomez, C.O., and Finch, J.A., 2007b, "Correspondence of gas holdup and bubble size in presence of different frothers", International Journal of Mineral Processing, Vol. 83, pp. 1-11.

Bascur, O.A., and Herbst, J.A., 1982, "Dynamic modeling of a flotation cell with a view toward automatic control", 14th International mineral Processing Congress. Toronto, Canada, October 17-23, pp. 1-21.

Bikerman, J. J., 1973, "Foams", Springer Verlag, New York.

Cappuccitti, F., and Finch, J. A., 2007, "Developing new frothers from 2-phase characterization tests", Cape Town, Nov 6-9.

Cappuccitti, F., and Finch, J.A., 2008, "Development of new frothers through hydrodynamic characterization", Minerals Engineering, vol. 21, pp. 944–948.

Cappuccitti, F., and Nesset, J., 2009, "Frother and collector effects of flotation cell hydrodynamics and their implication on circuit performance", In: Proceedings of the 7th UBC-McGill-UA International Symposium on Fundamentals of Mineral processing, Editors: Gomez, C. O., Nesset, J. E., and Rao, S. R., Sudbury, Ontario, p. 169-182.

Chesters, A. K., and Hofman, G., 1982, "Bubble coalescence in pure liquids", Applied Scientific Research, Vol. 38, p. 353-361.

Cho, Y. S, and Laskowski, J. S., 2002 a, “Effect of flotation frothers on bubble size and foam stability”, International Journal of Mineral Processing, Vol. 64, p. 69-80.

Cho, Y. S, and Laskowski, J. S., 2002 b, “Bubble coalescence and its effect on dynamic foam stability”, Canadian Journal of Chemical Engineering, Vol. 80, p. 299- 305.

Craig, V. S. J., 2004, "Bubble coalescence and specific-ion effects", Current Opinion in Colloid & Interface Science, Vol. 9, No. 1-2, pp. 178-184.

Cytec Mining Chemicals Handbook, Revised Edition, 2003.

Czarnecki, J., Malysa, K., and Pomianowski, A., 1982, “Dynamic frothability index”, Journal of Colloid and Interface Science, Vol. 86, No. 2, p. 570-572.

Dickinson, J. E., Laskovski, D., Stevenson, P., and Galvin, K. P., 2010, "Enhanced foam drainage using parallel inclined channels in a single-stage foam fractionation column", Chemical Engineering Science, Vol. 65, No., 8, p. 2481-2490.

Duerr-Auster, N., Gunde, R., Mäder, R., and Windhab, E. J., 2009, "Binary coalescence of gas bubbles in the presence of a non-ionic surfactant", Journal of Colloid and Interface Science, Vol. 333, No. 2, p. 579-584.

Dukhin, S.S., Miller, R., Loglio, G., 1998, "Physico-chemical hydrodynamics of rising bubbles. In: Mubius, D., Miller, R. (Eds.), Studies in Interfacial Science, Drops and Bubbles in Interfacial Research, vol. 6. Elsevier Science, pp. 367–432.

Engelbrecht, J.A. and Woodburn, E.T., 1975, “The effect of froth height, aeration rate and gas precipitation on flotation”, Journal of South African. Institute of Mining and Metallurgy, Vol. 10, p. 125–132.

Fernandez, J.P., “Installation of an Automated Laboratory Flotation Column” M.Eng Thesis, McGill University, 1995.

Finch, J. A., Gelinas, S., and Moyo, P., 2006, "Frother related research at McGill university", Minerals Engineering, Vol. 19, p. 726 – 733.

Finch, J. A., Nesset, J. E., and Acuna, C., 2008, "Role of frother on bubble production and behavior in flotation", Minerals Engineering, Vol. 21, p. 949-957.

Finch, J.A. and Dobby, G.S., 1990,“Column flotation”, Pergamon Press, Elmsford, NY.

Fruhner, H., Wantke, K. -D., and Lunkenheimer, K., 1999, “Relationship between surface dilational properties and foam stability”, Colloids and Surfaces A: Physicochemical and Engineering Aspects, Vol. 162, p. 193–202.

Frumkin, A.N., and Levich, V. G., 1947, " On the surfactants and interfacial motion", Zh. Fizicheskoi Khimii, Vol. 21, p. 1183–1204.

Gaudin, A.M., 1957. “Flotation”, Chapter 11, p. 327-368.

Gelinas, S., and Finch, J.A., 2007, "Frother analysis: procedure and plant experiences", Proceedings 39th Annual Meeting of the Canadian Mineral Processors of CIM, Jan. 23–25, 387–398.

George, P., Nguyen, A.V., and Jameson, G.J., 2004, “Assessment of true flotation and entrainment in the flotation of submicron particles by fine bubbles”, Minerals Engineering, Vol. 17, p. 847-853.

Ghosh, P., 2009, "Coalescence of bubbles in liquid", Bubble Science, Engineering and Technology, Vol. 1, No. 1-2, p. 75-87.

Gomez, C. O., and Finch, J. A., 2002, “Gas Dispersion Measurements in Flotation Machines”, *CIM Bulletin 95*, Vol. 1066, p. 73–38.

Gomez, C. O., and Finch, J. A., 2007, "Gas dispersion measurements in flotation cells", International Journal of Mineral Processing, Vol. 84, p. 51–58.

Gomez, C. O., Escudero, R., and Finch, J. A., 2000, "Determining equivalent pore diameter for rigid porous spargers", The Canadian Journal of Chemical Engineering, Vol. 78, 785-792.

Gorain, B.K., Franzidis, J.-P., Mainlapig, E.V., 1995, « Studies on impeller type, impeller speed and air flow rate in an industrial scale flotation cell-Part 1: Effect on bubble size distribution”, Minerals Engineering, Vol. 8, p. 615-635.

Grau, R. A., and Laskowski, J. S., 2006, “Role of frothers in bubble generation and coalescence in a mechanical flotation cell”, The Canadian Journal of Chemical Engineering, Vol. 84, p. 170-182.

Grau, R. A., Laskowski, J. S., and Heiskanen, K., 2005, “Effect of frothers on bubble size”, International Journal of Mineral Processing, Vol. 76, p. 225-233.

Gupta, A. K., Banerjee, P. K., Mishra, A., Satish, P., and Pradip, 2007, " Effect of alcohol and polyglycol ether frothers on foam stability, bubble size and coal flotation", nternational Journal of Mineral Processing, Vol. 82, p. 126-137.

Harris, C.C., 1976, "Flotation machines", In: M.C. Fuerstenau, Editor, A.M. Gaudin Memorial Volume, Vol. 2, SME (1976), pp. 753–815.

Harris, P. J., 1982, “Frothing phenomena and frothers”, In King, R. P. (Ed.), Principles of flotation, South African Institute of Mining and Metallurgy Monograph series, p. 237-263.

Hernandez-Aguilar J.R., and Finch J. A., 2005, "An experiment to validate bubble sizing techniques using bi-modal populations of known proportions", In: Graeme J. Jameson (Ed.), Centenary of Flotation Symposium, 6-9 June 2005, Brisbane, Queensland, Australia, pp. 465-472.

Hernandez-Aguilar, J.R., Coleman, R.G., Gomez, C.O., and Finch, J.A., 2004, "A comparison between capillary and imaging techniques for sizing bubbles in flotation systems", Minerals Engineering, Vol. 17, No. 1, p. 53-61.

Hesketh, R. P., Etchells, A. W., and Russell, T. W. F., 1991, "Bubble breakage in pipeline flow", Chemical Engineering Science**,** Vol. 46, No. 1, p. 1-9.

Hinze, J. O., 1955, "Fundamentals of the hydrodynamic mechanism of splitting in dispersion processes", AIChE Journal, Vol. 1, No. 3, p. 289-295.

Hofmeier, U., Yaminsky, V. V., and Christenson, H.K., 1995, " Observations of solute effects on bubble formation", Journal of Colloid and Interface Science, Vol. 174, No. 1, p. 199-210.

Huang, D. D. W., Nikolov, A., and Wasan, D. T., 1986, "Foams: Basic properties with application to porous media", Langmuir, Vol. 2, p. 672-677.

Hunter, T. N., Pugh, R. J., Franks, G. V., Jameson, G. J., 2008, "The role of particles in stabilising foams and emulsions", Advances in Colloid and Interface Science, Vol. 137, No.2, p. 57-81.

Ireland, P. M. and Jameson, G. J. 2007, "Liquid transport in a multi-layer froth", Journal of Colloid and Interface Science, Vol. 314, No. 1, p. 207-213.

Kirkpatrick, R. D., and Lockett, M. J., 1974, "The influence of approach velocity on bubble coalescence", Chemical Engineering Science, Vol. 29, p. 2363-2373.

Kitchener J.A., and Cooper C.F., 1959, "Current concepts in the theory of foaming", Quarterly Reviews, Vol. 123, p. 71-95.

Klassen, V. I., and Mokrousov, V. A., 1963, "An Introduction to the Theory of Flotation", English translation by J. Leja and G. W. Poling. Butterworths, London.

Knuutila, D., 2007, Master Thesis, McGill University.

Kracht, W. and J. A. Finch, 2009a, "Bubble break-up and the role of frother and salt", International Journal of Mineral Processing**,** Vol. 92, No. 3-4, p. 153-161.

Kracht, W., 2009, "Effect of frother on bubble coalescence, break-up, and initial rise velocity", PhD thesis, McGill University, Quebec, Canada.

Kracht, W., Finch, J. A., 2009b, "Using sound to study bubble coalescence", Journal of Colloid and Interface Science, Vol. 332, No. 1, p. 237-245.

Kracht, W., Finch, J. A., 2010, "Effect of frother on initial bubble shape and velocity", International Journal of Mineral Processing, Vol. 94, No. 3-4, p. 115-120.

Laskowski, J. S, 2003, “Fundamental properties of flotation frothers”, in Proceedings of 22nd International Mineral Processing Congress, Vol. 2, Lorenzen, L., Bradshaw, D. J., editors, South African Institute of Mining and Metallurgy, Cape Town, p. 788-797.

Laskowski, J. S, Tlhone, T., Williams, P., and Ding, K., 2003, “Fundamental properties of polyoxypropylene Alkyl ether flotation frothers”, International Journal of Mineral Processing, Vol. 72, p. 289-299.

Lee, C.H., Erickson, L.E., and Glasgow, L.A., 1987, "Dynamics of bubble size distribution in turbulent gas–liquid dispersions", Chemical Engineering Communications, Vol. 61, p. 181–195.

Lehr, F., Millies, M., and Mewes, D., 2002, "Bubble-Size distributions and flow fields in bubble columns", AIChE Journal, Vol. 48, No. 11, p. 2426-2443.

Levich, V.G., 1962, “Physicochemical hydrodynamics”, Chapter8, p. 395-471.

Lucassen-Reynders, E. H., and Lucassen, J., 1994, "Surface dilational viscosity and energy dissipation", Colloids and Surfaces: A, Vol. 85, p. 211-219.

Lynch A.J., Johnson N.W., Mainlapig, E.V., Thorne, C.G., 1981, “Mineral and coal flotation circuits and their simulation and control”, Elsevier Scientific Publishing.

Malysa, K, Krasowska, M and Krzan, M., 2005, "Influence of surface active substances on bubble motion and collision with various interfaces", Advances in Colloid and Interface Science., Vol. 114-115, p. 205-225.

Malysa, K., Lunkenheimer, K., Miller, R., and Hartenstein, C., 1981, “Surface elasticity and frothability of n-octanol and n-octanoic acid solutions”, Colloids and Surfaces, Vol. 3, N. 4, p. 329-338.

Marangoni, C. G., 1871, Ann. Phys. Chem., Vol. 143, p. 337-354.

Marrucci, G., (1969), "A theory of coalescence." Chemical Engineering Science, Vol. 24, N. 6, p. 975-985.

Martínez-Bazán, C., Montañés, J.L., and Lasheras, J.C.,1999, "On the breakup of an air bubble injected into a fully developed turbulent flow. Part 2. Size PDF of the resulting daughter bubbles", Journal of Fluid Mechanics, Vol. 401, p. 183–207.

Miller C. A., and Neogi, P., 1985, "Interfacial phenomena: equilibrium and dynamic effects", In: Surfact science series, Vol. 17, Chapter VI: Transport effects on interfacial phenomena, p. 240-298.

Moyo, P., Gomez, C.O. and Finch, J.A., 2007, “Characterizing frothers using water carrying rate”, Canadian Metallurgical Quarterly, Vol. 46, N. 3, p. 215-220.

Nambiar, D. K. R., Kumar, R., Das, T. R., and Gandhi, K. S., 1992, "A new model for breakup frequency of drops in turbulent stirred dispersions", Chemical Engineering Science, Vol. 47, No. 12, p. 2989-3002.

Neethling, S.J., and Cilliers, J.J., 2002, “The entrainment of gangue into a flotation froth”, International Journal Mineral Processing, Vol. 64, p.123-134.

Neethling, S.J., Cilliers, J.J., and Woodburn E.T., 2000, “Prediction of water distribution in flowing foam”, Chemical Engineering Science, Vol. 55, p. 4021-4028.

Neethling, S.J., Lee, H.T., and Cilliers J.J., 2003, “Simple relationships for predicting the recovery of liquid from flowing foams and froths”, Minerals Engineering, Vol. 16, p. 1123-1130.

Nesset, J. E., Aguilar, J. R. H., Acuna, C., Gomez, C. O., and Finch, J. A., 2006, “Some gas dispersion characteristics of mechanical flotation machines”, Minerals Engineering, Vol. 19, p. 807-815.

Nesset, J. E., Finch, J. A., and Gomez, C. O., 2007, "Operating variables affecting the bubble size in forced-air mechanical flotation machines", In: Proceedings AusIMM 9th Mill Operators Conference, Fremantle, Australia, p. 66-75.

Patwardhan, A., and Honaker, R. Q., 2000, "Development of a carrying-capacity model for column froth flotation." International Journal of Mineral Processing, Vol. 59, No. 4, p. 275-293.

Plateau, J.A.F., 1873, "Statique Experimentale et Teorique des Liquides Soumis aux Seules Forces Moleculaires", Gauthier-Villiard, Paris.

Pozrikidis, C., 1994, "Effects of surface viscosity on the finite deformation of a liquid drop and the rheology of dilute emulsions in simple shearing flow", Journal of Non-Newtonian Fluid Mechanics, Vol. 51, No. 2, p. 161-178.

Prince, M. J., and Blanch, H. W., 1990, "Bubble coalescence and break-up in air-sparged bubble columns", AIChE Journal, Vol. 36, No. 10, p. 1485-1499.

Pugh, R. J., 1996, “Foaming foam films, antifoaming and defoaming”, Advances in Colloid and Interface Science, Vol. 64, p. 67-142.

Quinn, J.J., Kracht, W., Gomez, C.O., Gagnon, C., and Finch, J.A., 2007, "Comparing the effect of salts and frother (MIBC) on gas dispersion and froth properties", Minerals Engineering, Vol. 20, No. 14, p. 1296-1302.

Rafeie, A. A., and Finch, J. A., 2009, "A comparison of bubble rise velocity profile of two surfactants to explain gas holdup data", In: Proceedings of the 7th UBC-McGill-UA International Symposium on Fundamentals of Mineral processing, Editors: Gomez, C. O., Nesset, J. E., and Rao, S. R., Sudbury, Ontario, p. 183-192.

Rao, S. R., and Leja, J., 2004, “Surface chemistry of froth flotation”, Second edition, Kluwer Academic, New York.

Ross, V. E., 2001, “Mechanisms operating in flotation froth”, Frothing in flotation II, Edited by Laskowski, J.S and Woodburn, E. T., 109-144.

Sadr-Kazemi, N., and Cilliers, J.J., 1997, " an image processing algorithm for measurement of flotation froth bubble size and shape distributions", Minerals Engineering, Vol. 10, No. 10, p. 1075-7083.

Sanada, T., Sato, A., Shirota, M., and, Watanabe, M., 2009, "Motion and coalescence of a pair of bubbles rising side by side", Chemical Engineering Science, Vol. 64, No. 11, p. 2659-2671.

Schramm, L. L., and W. H. F., Green, 1995, "The influence of Marangoni surface elasticity on gas mobility reduction by foams in porous media", Colloids and Surfaces: A, Vol. 94, p. 13-28.

Schwarz, S., and Grano, S., 2005, "Effect of particle hydrophobicity on particle and water transport across a flotation froth", Colloids and Surfaces A: Physicochemical and Engineering Aspects, Vol. 256, No. 2-3, p. 157-164.

Shink, D., Rosenblum, R., Kim, J.Y., and Stowe, K.G., 1992, "Development of Small Scale Flotation Cells and Its Application in Milling Operations", *Proc. 24th Annual Meeting of CMP*, Ottawa, p. 13.

Shockley, J., 2007, Summer student report, McGill university.

Smith, P.G. and Warren, L.J., 1989, "Entrainment of particles into flotation froths", Journal of Mineral Processing & Extractive Metallurgy Review, Vol. 5, No. 1-4, p. 123-145.

Stevenson, P., 2006, "Dimensional analysis of foam drainage", Chemical Engineering Science, Vol. 61, N. 14, p. 4503-4510.

Sun, S.C., 1952, "Frothing characteristics of pine oil in flotation", Min. Eng.4 (1), p. 65–71.

Tan, S. N., Fornasiero, D., Sedev, R., and Ralston, J., 2004, "The interfacial conformation of polypropylene glycols and foam behaviour", Colloids and Surfaces A: Physicochemical and Engineering Aspects, Vol. 250, No. 1-3, p. 307-315.

Tan, S. N., Pugh, R.J., Fornasiero, D., Sedev, R., and Ralston, J., 2005, “Foaming of polypropylene glycols and glycol/MIBC mixtures”, Minerals Engineering, Vol. 18, p. 179–188.

Thomas, R. M. (1981). "Bubble coalescence in turbulent flows." International Journal of Multiphase Flow**,** Vol. 7, No. 6, p. 709-717.

Trahar, W. J., and Warren, L. J., 1976, “The flotability of very fine particles — A review”, International Journal of Mineral Processing, Vol. 3, p. 103-131.

Trahar, W.J., 1981, “A rational interpretation of the role of particle size in flotation”, International Journal of Mineral Processing, Vol. 8, p. 289-327.

Tse, K. L., Martin, T, McFarlane, C. M., and Nienow, A. W., 2003, "Small bubble formation via a coalescence dependent break-up mechanism", Chemical Engineering Science, Vol. 58, No. 2, p. 275-286.

Tsuchiya, K. ., Miyahara, T.., and Fan, L.-S., 1989, "Visualization of bubble-wake interactions for a stream of bubbles in a two-dimensional liquid-solid fluidized bed", International Journal of Multiphase Flow, Vol. 15, No. 1, p. 35-49.

Walter, J. F., and Blanch, H. W., 1986, "Bubble break-up in gas--liquid bioreactors: Break-up in turbulent flows", The Chemical Engineering Journal, Vol. 32, No. 1, p. 7-17.

Wang, T., Wang, J., and Jin, Y., 2003, "A novel theoretical breakup kernel function for bubbles/droplets in a turbulent flow", Chemical Engineering Science, Vol. 58, No. 20, p. 4629-4637.

Warren, L.J., 1985, “Determination of the contributions of true flotation and entrainment in batch flotation tests”, International Journal of Mineral Processing, Vol. 14, p. 33-44.

Wilkinson, P. M., Van Schayk, A., Spronken, J. P. M., and Van Dierendonck, L., 1993, "The influence of gas density and liquid properties on bubble breakup", Chemical Engineering Science, vol. 48, No. 7, p. 1213-1226.

Wu, M., and Gharib, M., 2002, “Experimental studies on the shape and path of small air bubbles rising in clean water”, Physics of Fluids, Vol. 14, No. 7, p. L45-L56.

Xie, W., Neethling, S.J., and Cilliers, J.J., 2004, " Anovel approach for estimating the average bubble size for foams flowing in vertical columns", Chemical Engineering Science, Vol. 59, p. 81-86.

Xu, M., Finch, J.A., and Uribe-Salas, A., 1991, “Maximum gas and bubble surface rates in flotation columns”, International Journal of Mineral Processing, Vol. 32, p. 233-250.

Yianatos, J.B., Finch J.A., and Laplante, A.R.,1986, “Holdup profile and bubble size distribution of flotation froths”, Canadian Metallurgical Quarterly, Vol. 25 , p. 23-29.

Zhang, W., Nesset, J. E., and Finch, J. A., 2009, "Water recovery and bubble surface area flux", In: Proceedings of the 7th UBC-McGill-UA International Symposium on Fundamentals of Mineral processing, Editors: Gomez, C. O., Nesset, J. E., and Rao, S. R., Sudbury, Ontario, p. 155-168.

Zhang, W., Nesset, J. E., and Finch, J. A., 2010, "Water Recovery and Bubble Surface Area Flux in Flotation", Canadian Metallurgical Quarterly, Vol 49, No 4, p. 353-362.

Zheng, X., Franzidis, J. P., and Johnson, N. W., 2006, "An evaluation of different models of water recovery in flotation", Minerals Engineering, Vol. 19, p. 871 – 882.

Appendices

Appendix A – Reagent Structure*

Pentanol ($CH_3(CH_2)_4$ OH)

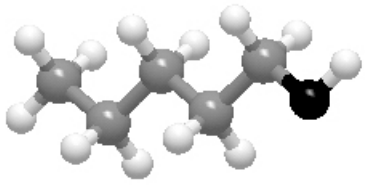

MIBC ($(CH_3)_2CHCH_2CH(OH)CH_3$)

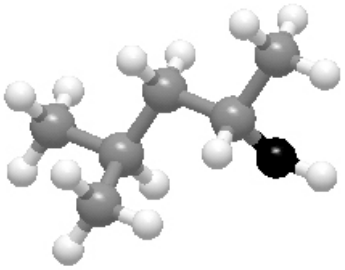

Heptanol ($CH_3(CH_2)_6$ OH)

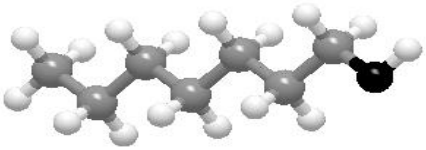

Octanol ($CH_3(CH_2)_7$ OH)

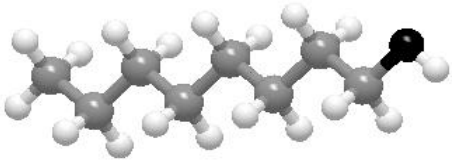

PPG425 & F150: $(H(PO)_7OH)$**

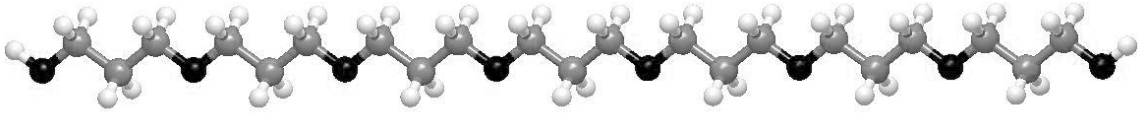

DF250 $(H(PO)_4OH)$**

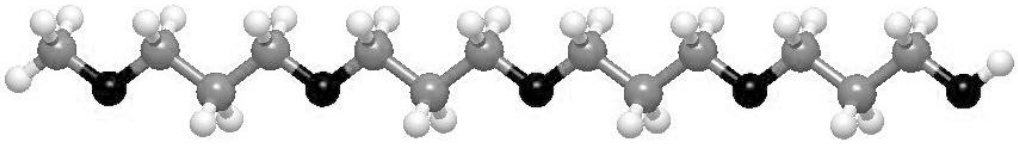

* Carbon atoms are represented in grey, oxygen atoms in black, and hydrogen atoms in white.
** PO is propylene oxide (propoxy) [-O-CH_2-CH_2-CH_2-]

Appendix B - High speed camera specifications

Model: TroubleShooter HR.

Sensor: CMOS array up to 1280 x 1024 pixels, 8 bit resolution (monochrome).

Shutter speed1 :x, 2x, 3x, 4x, 5x, 10x and 20x the recording rate.

Recording rate (fps): 16,000; 8,000; 4,000; 2,000; 1,000; 500; 250; 125.

Playback rates: 1 to 1,000 frames per second forward and reverse.

Display: Built-in 5 ’’LCD color digital display.

I/O Connectors: USB 2.0 port, compact flash memory.

Mounts: Standard C-mount lens mount 20-¼ ,tripod mount.

Power supply: Four (4) D-cell batteries or 110/220 VAC adapter.

Size & weight: 6 ’’W x 5 ’’H x 4 ’’D, 2.2 lbs. without batteries.

Table B – 1: Recording rate (fps) and image size configurations.

Frames per second	**Sensor**	**Standard memory – 1 gb**	
Recording rate	**Resolution**	**Total frames**	**Record time (sec)**
125	1280 x 1024	1,022	8.2
250	1280 x 1024	1,022	4.1
500	1280 x 1024	1,022	2.0
1000	1280 x 512	2,044	2.0
2000	1280 x 256	4,088	2.0
4000	1280 x 128	8,176	2.0
8000	1280x 64	16,352	2.0
16000	1280 x 32	32,704	2.0
125	640 x 480	4,368	34.9
250	640 x 480	4,368	17.5
500	640 x 480	4,368	8.7
1000	640 x 480	4,368	4.4
125	320 x 240	17,472	139.8
250	320 x 240	17,472	69.9
500	320 x 240	17,472	34.9
1000	320 x 240	17,472	17.5

2000	320 x 240	17,472	8.7

Appendix C – Macro Code for Image J

The following code allows processing bubble size for multiple tests with ImageJ:

```
macro "Bubble Size Analyzer" {

	Dir_r = getDirectory("Choose Source Directory ");

	//Get Folder Name
	n = lastIndexOf(Dir_r, "\\");
	dir = substring(Dir_r, 0, n-1);
	m = lastIndexOf(dir, "\\");
	TestName = substring(Dir_r, m+1, n);
	Dir_w = getDirectory("Choose Destination for Results ");

	//Prompt for Information

	Dialog.create("Parameters");
	Dialog.addString("Test Name", TestName)
	Dialog.addNumber("Pixels per mm.", 50, 2, 10, "");
	Dialog.addNumber("Min. Circularity", 0.8, 2, 10, "");
	Dialog.addNumber("Min. Object diameter", 5, 0, 10,
"pixels");
	Dialog.addNumber("Files to skip", 0, 0, 10, "");
	Dialog.addString("File Extension", "JPG");
	Dialog.addMessage("\n");
```

```
Dialog.addCheckbox("Substract Background", false);
Dialog.show();
Test = Dialog.getString();
Cal = Dialog.getNumber();
Circ = Dialog.getNumber();
min_diam = Dialog.getNumber();
k = Dialog.getNumber();
extension = Dialog.getString();
BG = Dialog.getCheckbox();

if (k != (round(k))||(k<0)) {
exit("Files to skip must be a positive integer");
}


min_area = (min_diam/Cal)*(min_diam/Cal)/4*3.1416;

run("Clear Results");

j = 0;

list = getFileList(Dir_r);

if (k>=list.length) {
exit("Too many files to skip")
}

for (i=k; i<list.length; i++)  {
```

```
if (endsWith(list[i], extension) == 1) {
  open(Dir_r + list[i]);
run("Out");
run("Out");
run("Out");

run("8-bit");

if (BG == true) {
run("Subtract Background...", "rolling=50 white");
}

//run("Threshold...");
setAutoThreshold();

if (j==0){
run("Set Scale...", "distance=" + Cal + " known=1 pixel=1
unit=mm     global");
j = 1;
}

run("Set Measurements...", "area perimeter circularity
feret's  redirect=None decimal=3");
run("Analyze Particles...", "size=" + min_area + "-Infinity
circularity=" + Circ + "-1.00 show=Nothing display exclude
include");
```

```
        //instructions to generate one file per picture;
        //saveAs("Measurements", Dir_w + list[i] - ".JPG" + ".TXT");
        //run("Clear Results");

        close();

              }

        }


        //instructions to generate only one big txt-file per test
        saveAs("Measurements", Dir_w + Test + ".txt");
        run("Clear Results");

}
```

Appendix D – Experimental Results of Bubble Size, Gas Holdup, water overflow rate, and Froth Height

D.1. Column data

Table D – 1: Pentanol

Concentration (mmol/L)	d_{32}	d_{10}	Eg (%)	Froth Depth (cm)
0.06	3.61	3.18	3.94	1.0
0.11	2.90	2.40	4.43	2.6
0.23	0.87	0.77	9.17	3.4
0.340	0.77	0.70	10.24	3.4
0.45	0.73	0.69	10.90	-

Table D – 2: MIBC

Concentration (mmol/L)	d_{32}	d_{10}	Eg (%)
0.049	3.20	2.71	4.34
0.098	1.20	0.94	10.33
0.2	0.93	0.81	11.67
0.294	0.88	0.79	12.84
0.391	0.82	0.74	13.00

Table D – 3: Heptanol

Concentration (mmol/L)	d_{32}	d_{10}	Eg (%)
0.043	1.84	0.89	5.39
0.086	1.16	0.76	9.9
0.172	0.88	0.69	12.59
0.258	0.83	0.68	14.68

Table D – 4: F150

Concentration (mmol/L)	d_{32}	d_{10}	Eg (%)	Froth Depth (cm)
1.18×10^{-3}	4.28	3.28	5.26	0.5
2.35×10^{-3}	3.76	2.99	6.15	1.03
4.71×10^{-3}	2.93	2.38	6.6	1.93
0.012	1.64	1.43	6.55	-
0.024	1.15	1.07	9.16	8.5
0.047	0.86	0.79	12.63	18
0.071	0.75	0.69	14.81	26.7
0.094	0.73	0.66	15.71	35.3
0.235	0.75	0.68	> 25	33.3
0.471	0.73	0.66	> 25	34.2

Table D – 5: DF250

Concentration (mmol/L)	d_{32}	d_{10}	Eg (%)
2×10^{-3}	3.91	3.56	5.68
8×10^{-3}	3.26	3.08	6.31
0.02	2.22	2.08	7.84
0.04	1.56	1.41	10.9
0.06	1.25	1.08	13.64
0.08	1.12	0.92	14.76
0.16	0.94	0.74	16.46
0.4	0.79	0.63	> 25

Table D – 6: PPG425

Concentration (mmol/L)	**d_{32}**	**d_{10}**	**Eg (%)**
4.71×10^{-3}	2.67	2.46	6.89
0.012	1.61	1.42	7.21
0.024	1.09	0.91	9.18
0.047	0.92	0.73	13.77
0.094	0.86	0.67	16.69

Table D – 7: Octanol

Concentration (mmol/L)	**d_{32}**	**d_{10}**	**Eg (%)**
3.84×10^{-3}	3.84	3.59	5.26
0.015	2.97	2.81	5.45
0.038	1.39	1.28	10.81
0.077	1.02	0.98	11.91
0.154	0.90	0.69	13.61
0.307	0.81	0.62	16.86

Table D – 8: F150 – MIBC blends

Concentration (mmol/L)		d_{32}	Eg (%)
F150	**MIBC**		
1.18×10^{-3}	0	4.21	5.26
	0.049	2.27	8.19
	0.098	1.49	9.48
	0.2	1.41	9.75
	0.294	1.39	10.06
2.35×10^{-3}	0	3.76	6.15
	0.049	2.00	8.59
	0.098	1.43	9.90
	0.2	1.39	10.47
	0.294	1.28	10.72
4.71×10^{-3}	0	2.93	6.60
	0.049	1.73	8.30
	0.098	1.40	10.15
	0.2	1.30	11.22
	0.294	1.19	11.00
7.1×10^{-3}	0.2	0.87	16.19
1.18×10^{-2}	0.2	0.85	19.6
4.71×10^{-2}	0.2	0.85	22.23

Table D – 9: F150 – pentanol blends

Concentration (mmol/L)		d_{32}	Eg (%)	Froth Depth (cm)
F150	**Pentanol**			
1.18×10^{-3}	0	4.29	5.26	0.5
	0.06	2.83	6.605	2.4
	0.11	1.65	7.975	7.4
	0.17	1.34	8.435	10.6
	0.23	1.26	10.395	15.7
	0.45	1.28	10.965	-
2.35×10^{-3}	0	3.76	6.15	1
	0.06	2.52	7.52	4.3
	0.11	1.69	9.16	13.1
	0.17	1.40	9.645	14.93
	0.23	1.34	9.67	17.53
	0.45	1.37	11.395	-
4.71×10^{-3}	0	2.93	6.6	2
	0.06	1.99	8.335	6.3
	0.11	1.53	9.845	17.4
	0.17	1.36	11.215	19.0
	0.23	1.31	11.645	20.7
	0.45	1.30	11.665	-
7.1×10^{-3}	0.23	1.06	17.02	-
1.18×10^{-2}	0.23	0.89	19.04	-
2.35×10^{-2}	0.23	0.88	21.15	-
4.71×10^{-2}	0.23	0.87	21.22	-

Table D – 10: DF250 – MIBC blends

Concentration (mmol/L)		d_{32}	Eg (%)
DF250	**MIBC**		
2×10^{-3}	0	3.91	5.68
2×10^{-3}	0.049	1.93	10.46
2×10^{-3}	0.098	1.13	11.34
2×10^{-3}	0.2	1.08	11.82
2×10^{-3}	0.294	1.08	12.13
8×10^{-3}	0.2	1.09	12.71
2×10^{-2}	0.2	1.01	16.38
8×10^{-2}	0.2	0.93	22.33

Table D – 11: DF250 – pentanol blends

Concentration (mmol/L)		d_{32}	Eg (%)
DF250	**Pentanol**		
2×10^{-3}	0	3.91	5.68
2×10^{-3}	0.06	2.39	6.73
2×10^{-3}	0.11	1.32	8.65
2×10^{-3}	0.23	1.08	12.15
2×10^{-3}	0.340	1.02	12.48
2×10^{-3}	0.45	0.94	14.04
8×10^{-3}	0.23	1.03	13.44
2×10^{-2}	0.23	0.90	16.13
8×10^{-2}	0.23	0.87	21.2

Table D – 12: octanol – pentanol blends

Concentration (mmol/L)		d_{32}	Eg (%)
Octanol	**Pentanol**		
0	0.23	0.87	9.17
3.84×10^{-3}	0.23	0.92	11.49
1.54×10^{-2}	0.23	1.07	10.86
0.038	0.23	1.38	9.95
0.077	0.23	1.03	12.24
0.154	0.23	0.83	16.3

Table D – 13: PPG425 – pentanol blends

Concentration (mmol/L)		d_{32}	Eg (%)
PPG425	**Pentanol**		
4.71×10^{-3}	0.06	1.87	8.63
4.71×10^{-3}	0.11	1.55	10.1
4.71×10^{-3}	0.23	1.3	11.57
4.71×10^{-3}	0.340	1.24	12.23
4.71×10^{-3}	0.45	1.21	12.42

Table D – 14: water overflow rate in the presence of F150

Concentration, (mmol/L)	Froth depth, cm	Water overflow rate, g/min
1.18×10^{-2}	5	40.2
2.35×10^{-2}	5	203.2
4.71×10^{-2}	5	299.7
7.1×10^{-2}	5	383
9.41×10^{-2}	5	408.7

Table D – 15: water overflow rate for F150 – 0.23 mmol/L pentanol blends

Concentration (mmol/L) F150	Froth Depth, cm	Water overflow rate, g/min
1.18×10^{-2}	5	198
2.35×10^{-2}	5	384
4.71×10^{-2}	5	436
7.1×10^{-2}	5	452
9.41×10^{-2}	5	471

Table D – 16: 4.71×10^{-3} mmol/L F150 – pentanol blends

Concentration (mmol/L)		Froth Depth, cm	Water overflow rate, g/min
F150	Pentanol		
4.71×10^{-3}	0.17	2	117.63
4.71×10^{-3}	0.17	4	42.51
4.71×10^{-3}	0.17	6	24.76
4.71×10^{-3}	0.17	8	12.92
4.71×10^{-3}	0.23	2	157.9
4.71×10^{-3}	0.23	4	52.12
4.71×10^{-3}	0.23	6	24.31
4.71×10^{-3}	0.23	8	13.34

D.2. Mini-mechanical cell data

Table D – 17: pentanol

Concentration (mmol/L)	Water overflow rate, g/min
5.67×10^{-2}	0
0.11	0
0.17	3.8
0.23	45.5
0.34	85.6
0.45	69

0.58	58

Table D – 18: MIBC

Concentration (mmol/L)	**Water overflow rate, g/min**
4.9×10^{-2}	0
9.8×10^{-2}	65.7
0.15	150.7
0.2	142.0
0.29	142.2
0.39	120.2
0.49	120.3

Table D – 19: DF250

Concentration (mmol/L)	**Water overflow rate, g/min**
2×10^{-3}	0
8×10^{-3}	0
2×10^{-2}	51.3
4×10^{-2}	234.2
6×10^{-2}	321.5
8×10^{-2}	348
0.12	365.6
0.16	367.1
0.4	372
0.6	377

Table D – 20: PPG425

Concentration (mmol/L)	Water overflow rate, g/min
1.18×10^{-3}	0
4.71×10^{-3}	0
1.18×10^{-2}	160.7
2.35×10^{-2}	308.6
3.53×10^{-2}	377.4
4.71×10^{-2}	405.7
7.1×10^{-2}	422.9
9.41×10^{-2}	439.25
0.24	453.8
0.47	465.85

Table D – 21: DF250 – MIBC blends

Concentration (mmol/L)		Water overflow rate, g/min
DF250	MIBC	
2×10^{-3}	4.9×10^{-2}	0
	9.8×10^{-2}	133.9
	0.15	179.4
	0.2	187.2
	0.39	188.8
8×10^{-3}	4.9×10^{-2}	199.2
	9.8×10^{-2}	353.15
	0.15	343.4
	0.2	257.8
	0.39	251.55
8×10^{-2}	4.9×10^{-2}	506.15
	9.8×10^{-2}	510.95
	0.15	515.1
	0.2	486.65

	0.39	463.7

Table D – 22: PPG425 – MIBC blends

Concentration (mmol/L)		**Water overflow rate, g/min**
PPG425	**MIBC**	
1.18×10^{-3}	4.9×10^{-2}	0
	9.8×10^{-2}	151.05
	0.15	228.6
	0.2	240.1
	0.39	240.75
4.71×10^{-3}	4.9×10^{-2}	133
	9.8×10^{-2}	236.7
	0.15	292.3
	0.2	324.6
	0.39	313.95
4.71×10^{-2}	4.9×10^{-2}	543.2
	9.8×10^{-2}	545.1
	0.15	524.75
	0.2	497.15
	0.39	483.19

Table D – 23: DF250 – pentanol blends

Concentration (mmol/L)		**Water overflow rate, g/min**
DF250	**Pentanol**	
2×10^{-3}	0.06	0
	0.11	31.35
	0.17	206.85
	0.23	309.15
	0.45	308.7
8×10^{-3}	0.06	168.2
	0.11	352.95
	0.17	422.05
	0.23	426.7
	0.45	402.85
8×10^{-2}	0.06	447.4

	0.11	464.2
	0.17	466.8
	0.23	462.8
	0.45	435.55

Table D – 24: PPG425 – pentanol blends

Concentration (mmol/L)		**Water overflow rate, g/min**
PPG425	**Pentanol**	
1.18×10^{-3}	0.06	0
	0.11	81.35
	0.17	210.6
	0.23	265.2
	0.45	277.7
4.71×10^{-3}	0.06	207.95
	0.11	328.45
	0.17	392.3
	0.23	373.6
	0.45	353.95
4.71×10^{-2}	0.06	523.45
	0.11	538.4
	0.17	519.75
	0.23	495.15
	0.45	480.95

D.3. Metso cell data

Table D – 25: F150

Concentration (mmol/L)	**d_{32}**
1.18×10^{-3}	2.57
2.35×10^{-3}	2.14
4.71×10^{-3}	1.60
9.41×10^{-3}	1.07
1.18×10^{-2}	1.00

2.35×10^{-2}	0.90
3.53×10^{-2}	0.92
4.71×10^{-2}	0.83

Table D – 26: Pentanol

Concentration (mmol/L)	**d_{32}**
0	3.03
0.06	2.42
0.11	1.71
0.17	1.22
0.23	1.16
0.340	1.14
0.45	1.00
0.68	0.78

Table D – 27: F150 – pentanol blends

Concentration (mmol/L)		**d_{32}**
F150	**Pentanol**	
1.18×10^{-3}	0.06	1.99
	0.11	1.60
	0.17	1.37
	0.23	1.16
	0.340	1.19
	0.45	1.17
2.35×10^{-3}	0.06	1.64
	0.11	1.33
	0.17	1.28
	0.23	1.30
	0.340	1.36
	0.45	1.33
4.71×10^{-3}	0.06	1.18
	0.11	1.1
	0.17	1.19

	0.23	1.15
	0.340	1.15
	0.45	1.17

Appendix E – Experimental Results of Coalescence time

Table E – 1: Coalescence time in the presence of blended frothers

Concentration (mmol/L)		**Coalescence Time, (s)**	**Standard Deviation (95% CI)**
F150	**Pentanol**		
0	0	2.48	0.16
1.18×10^{-3}	0.06	7.46	0.85
	0.11	8.38	0.60
	0.17	8.21	0.71
	0.23	8.51	0.98
2.35×10^{-3}	0.06	8.49	0.56
	0.11	8.55	0.83
	0.17	8.93	1.40
	0.23	9.66	1.66
4.71×10^{-3}	0.06	9.51	0.82
	0.11	10.89	1.78
	0.17	10.21	1.66
	0.23	11.47	1.38

Table E – 2: Coalescence time in the presence of pentanol

Concentration, (mmol/L)	**Coalescence Time, (s)**	**Standard Deviation (95% CI)**
0.06	4.97	0.34
0.11	6.81	0.33

0.17	11.36	1.21
0.23	5.68	1.16
0.28	5.25	0.82

Table E – 3: Coalescence time in the presence of F150

Concentration, (mmol/L)	**Coalescence Time, (s)**	**Standard Deviation (95% CI)**
2.35×10^{-5}	4.26	0.68
1.18×10^{-4}	5.17	0.50
2.35×10^{-4}	5.63	0.58
4.71×10^{-4}	5.99	0.46
1.18×10^{-3}	6.23	0.67
1.76×10^{-3}	8.94	1.49
2.35×10^{-3}	11.56	1.14
4.71×10^{-3}	11.68	2.00
9.41×10^{-3}	11.89	1.69
2.35×10^{-2}	11.88	1.77
4.71×10^{-2}	11.96	1.12

Table E – 4: Coalescence time in the presence of DF250

Concentration, (mmol/L)	**Coalescence Time, (s)**	**Standard Deviation (95% CI)**
4×10^{-3}	4.62	0.60
0.02	9.38	1.35
0.04	9.35	1.62
0.06	9.51	1.35
0.08	9.61	1.50

0.16	9.57	1.45

Table E – 5: Coalescence time in the presence of MIBC

Concentration, (mmol/L)	**Coalescence Time, (s)**	**Standard Deviation (95% CI)**
9.79×10^{-3}	6.23	1.09
2.94×10^{-2}	7.98	0.80
4.89×10^{-2}	10.41	1.26
7.83×10^{-2}	5.55	1.10
9.79×10^{-2}	4.29	0.88
0.15	3.54	0.93
0.2	3.61	0.92

Appendix F – Experimental Results of Bubble Breakup

F.1. One-bubble-at-a-time-break-up

Table F – 1: Ratio of daughter bubble size to mother bubble size in the presence of 0.23 mmol/L pentanol

Frequency, %	**d/d_0**
5	0.00
15	0.96
25	20.46
35	29.54
45	26.75
55	12.59
65	5.67
75	2.94
85	0.64
95	0.44

Table F – 2: Ratio of daughter bubble size to mother bubble size in the presence of 4.71×10^{-3} mmol/L F150

Frequency, %	**d/d_0**
5	0.29
15	5.73
25	16.62
35	27.79
45	22.64
55	11.75
65	7.16
75	3.72
85	2.29
95	2.01

Table F – 3: Ratio of daughter bubble size to mother bubble size in the presence of 4.71×10^{-3} mmol/L F150 + 0.23 mmol/L Pentanol

Frequency, %	**d/d_0**
5	1.05
15	1.57
25	8.38
35	18.85
45	28.80
55	15.71

65	10.47
75	7.33
85	4.71
95	3.14

F.2. Break-up from an air vortex

Table F – 4: Sauter mean diameter in the presence and absence of single and blended frothers

Frother concentration, mmol/L		**d_{32}, mm**	**Standard Deviation, (95% CI)**
F150	**Pentanol**		
0	0	2.32	0.11
0	0.23	1.63	0.03
0	0.45	1.70	0.04
4.71×10^{-3}	0	1.64	0.11
4.71×10^{-3}	0.23	1.95	0.14
2.35×10^{-3}	0.23	2.10	0.16
1.18×10^{-3}	0.23	2.01	0.17

Appendix G – Surface Tension

Table G.1 – Surface tension for F150 alone

Concentration	Surface tension, mN/m
0	73.55
1.18×10^{-3}	72.29
2.35×10^{-3}	71.65
4.71×10^{-3}	70.57
1.18×10^{-2}	68.44
2.35×10^{-2}	67.23
4.71×10^{-2}	65.33
7.1×10^{-2}	64.56
9.41×10^{-2}	63.43

Table G.2 – Surface tension for pentanol alone

Concentration	Surface tension, mN/m
0.06	73.49
0.11	73.38
0.17	73.42
0.23	73.11
0.34	73.26
0.45	73.17

Table G.3 – Surface tension for F150 – pentanol blends

Frother concentration, mmol/L		**Surface tension, mN/m**
F150	**Pentanol**	
1.18×10^{-3}	0.06	72.56
	0.11	72.34
	0.17	72.36
	0.23	72.36
2.35×10^{-3}	0.06	71.60
	0.11	71.62
	0.17	71.60
	0.23	71.52
4.71×10^{-3}	0.06	70.73
	0.11	70.60
	0.17	70.47
	0.23	70.36